SVEUČILIŠTE U ZAGREBU
PRIRODOSLOVNO-MATEMATIČKI FAKULTET
GEOFIZIČKI ODSJEK

KRISTIAN HORVATH

DYNAMICAL PROCESSES IN THE UPPER-TROPOSPHERE AND LEE CYCLOGENESIS IN THE WESTERN MEDITERRANEAN

DOKTORSKA DISERTACIJA

DOCTORAL THESIS

ZAGREB, 2008.

Sveučilište u Zagrebu
Prirodoslovno-matematički fakultet
Geofizički odsjek

Kristian Horvath

Dynamical processes in the upper-troposphere and lee cyclogenesis in the western Mediterranean

Doktorska disertacija
predložena Geofizičkom odsjeku
Prirodoslovno-matematičkog fakulteta Sveučilišta u Zagrebu
radi stjecanja akademskog stupnja
doktora prirodnih znanosti fizike

Doctoral Thesis
submitted to the Department of Geophysics
Faculty of Science, University of Zagreb
for the academic degree of
Doctor of natural sciences (Physics)

Zagreb, 2008.

This Thesis is elaborated on Meteorological and Hydrological Service, Croatia, supervised by Dr. sc. Branka Ivančan-Picek.

The author is grateful to Dr. sc. Branka Ivačan-Picek for mentorship and dedicated support during the postgraduate studies. The intense collaboration with Prof. Titular Romulado Romero March from the University of Balearic Islands, Spain and Prof. Yuh-Lang Lin from the North Carolina State University, North Carolina, USA is highly appreciated.

A big thanks also goes to an international student crew for permanent discussions and assistance: Stjepan Ivatek-Šahdan, Lluis Fita, Ivana Stiperski and Lukša Kraljević.

Contents

1. Introduction

Cyclones that appear in the basin of Adriatic Sea strongly influence the climate and weather conditions in the area. In particular, apart from the usually mild climate, cyclone activity in the Adriatic and the central Mediterranean provide the main hydrological forcing as well as trigger mechanisms for a range of extreme weather phenomena, such as local downslope windstorm Bora and heavy precipitation.

Orographically initiated cyclones are the most often type of cyclone appearing in the Adriatic region. Despite of the development of sophisticated high-resolution numerical mesoscale models, weather in the broad area of Alpine lee is still characterized with a limited predictability. Therefore, the through understanding of orographical (or lee) cyclogenesis in the region is essential. Given that upper-level dynamical factors are the strongest precursors of lee cyclogenesis events, the numerical studies on the influence of the upper-tropospheric system to the initiation of this type of cyclone in the western Mediterranean are essential to deeper understanding of the phenomenon. Furthermore, assessing the predictability of lee cyclogenesis to the initial-analysis uncertainties in the upper-level dynamical factors is of a continuous importance for everyday weather prediction in the wider Adriatic region.

In this chapter an overview of the mechanism of orographical cyclogenesis will be given. The meso-β scale climatological analysis presented in Chapter 2 will classify the types and tracks of cyclones that appear in the Adriatic, adding additional information to the existing cyclone climatologies. A description of the methods of subsequent numerical analysis, such as factor separation and piecewise potential vorticity inversion, as well as the numerical model employed, will be given in Chapter 3. In Chapter 4, the influence of the macroscale and mesoscale upper-level dynamical factors to the generation and lifecycle of the cyclone generated in the lee of the Atlas mountains will be investigated, comparing the ingredients of the analyzed event with the typical Alpine lee cyclogenesis process. In Chapter 5, results of the global model error statistics at the upper-levels will be presented. Finally, in Chapter 6 a step towards predictability will be made through the analysis of an ensemble of simulations of the MAP IOP 15 Genoa lee cyclogenesis event, with initial conditions perturbed by the derived error statistics. The approach followed will allow for assessment of the influence of the initial-analysis uncertainties in the upper-level dynamical factors to the numerical prediction of the Genoa cyclone track and intensity as well as Bora severity in the northern Adriatic.

1.1 Phenomenology of lee cyclogenesis

Lee or orographical cyclogenesis has been since long a widely recognized phenomenon, due to the increased cyclogenesis frequency in the lee of prominent mountain ranges, such as the Alps and the Rockies, and its influence of the local and non-local weather in the region. Globally, the Gulf of Genoa was identified as one of the most frequent region of cyclogenesis worldwide already in the middle of the 20th century (see detailed review in Chapter 2).

The relevance of this phenomenon, and its applicability to other mountain areas in the world, led to a sequence of field experiments, such as the 1982 Alpine Experiment (ALPEX; see Kuettner 1986) and the 1999 Mesoscale Alpine Program (MAP; e.g. Bougeault et al. 2001) that were both designed to conduct meteorological measurements in the Alpine region, to allow for deeper understanding of lee cyclogenesis and interaction of the mountain and the troposphere as well as validation and error assessment of numerical models.

The huge step forward in phenomenological understanding of Genoa lee cyclogenesis was a separation of the lee cyclogenesis process into two distinct phases (Buzzi and Tibaldi 1978; Mc Ginley 1982). While the first stage is associated with a cold front retardation, a cold air outbreak into the Mediterranean Sea and a rapid creation of a shallow vortex in the Gulf of Genoa, the second phase resembles the traditional baroclinic interaction i.e. descriptive interpretation of balanced low-level–upper-level vortex interaction (see review by Hoskins et al. 1985). It should be mentioned that baroclinic interaction of the two vortices might be conceived as an extrapolation of baroclinic instability problem (e.g. Charney 1947; Eady 1949), but should not be directly associated with it, since the latter studies the growth of an initially small-amplitude disturbance on an unstable basic state, and the first studies growth of the surface disturbance under the influence of the high-amplitude disturbance in the upper-levels.

Following this early work and results of the ALPEX experiment, the general properties of the Alpine lee cyclogenesis can be summarized as follows (e.g. Tibaldi et al. 1990):

(1) Lee cyclogenesis often occurs in association with a preexisting synoptic-scale trough and/or surface "parent" cyclone north of the Alps (i.e. its cold front) that interacts with the orography;

(2) Two-phase deepening process is found. In the first phase, due to frontal retardation, flow splitting and thermal anomaly creation, a cyclone deepens very rapidly, but remains shallow. In the second phase, the cyclone develops less rapidly resembling a process of a baroclinic interaction, but extends through the whole troposphere.

(3) The development of lee cyclone starts before the strong thermal contrasts associated with cold frontal penetration take place in the lee; and

(4) The scales of mature and deep lee cyclones are on the Rossby radius of deformation (NL_z / f, where L_z is the vertical scale of motion). The influence of orography takes the form of a high-low dipole.

Based on upper-level flow, two types of lee cyclogenesis over the Alps can be identified: the more common southwesterly upper-level flow ("*Vorderseiten*") type and the less common

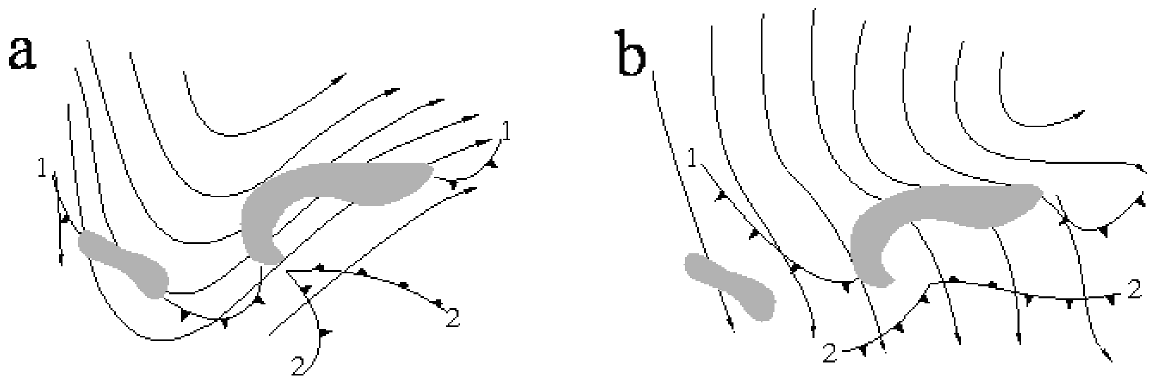

***Figure 1.1**: Two types of lee cyclogenesis over Alps: (a) Southwesterly ("Vorderseiten") type, and (b) Northwesterly ("Überströmungs") type, based on upper-level flow. The bold, solid lines indicate the upper-level flow and the surface front are plotted for two consecutive times, as denoted by 1 and 2. Pyrenees and Alps are plotted in shaded. (Adapted after Pichler and Steinacker 1987 and Lin 2007).*

northwesterly upper-level flow ("*Überströmungs"*) type (Pichler and Steinacker 1987). Both types are accompanied by blocking and splitting of low-level cold air by the Alps. The southwesterly type (Fig. 1.1a) is characterized with the advance of an eastward moving trough, where a surface low forms in the Gulf of Genoa. During the northwesterly type (Fig. 1.1b) of event, the upper-level flow blows generally from the northwest, crosses the Alps and generates a cyclone in the lee. The formation of the low occurs as well predominantly in the Gulf of Genoa, which is a favorable place of lee initiation due to complex shape of the Alpine orography.

1.2 Theories of lee cyclogenesis

For flow over mesoscale mountains with Rossby number ($R_o=U/fL$) roughly equal to unity, the effects of earth's rotation are not to be neglected. Under this situation, the advection time for an air parcel to pass over the mountain is too large to be ignored compared to the period of inertial oscillation due to earth's rotation ($2\pi/f$). Flow past many mesoscale mountain ranges, such as European Alps, US Rockies, Canadian Rockies, Andes, Scandinavian mountain range, New Zealand Alps, and the Central Mountain Range of Taiwan, belong to this category (e.g. see Holton et al. 2003, Lin 2007). Flow over a very large-scale broad mountain (e.g. Antarctica), which often gives a very small Rossby number, can be approximated by the quasi-geostrophic theory. In general, for flow over mesoscale mountains the influence of the Coriolis force is too large to be ignored, but too small to be approximated by the quasi-geostrophic theory.

The fruitful period of data acquisition and analysis during the ALPEX, resulted in creation of two mature theories of orographical cyclogenesis:

(1) baroclinic lee waves (Smith 1984)
(2) orographic modification of baroclinic instability i.e. normal mode theory of orographical cyclogenesis (Speranza et al. 1985)

In addition, the approach based on the analysis of the upper-level potential vorticity, though not useful for establishing a theory, showed extremely useful in conceptual comprehending of the phenomenon, as well as in diagnosis and numerical sensitivity tests. The subsequent sections present both theories as well as potential vorticity approach and discuss the related differences and similarities.

1.2.1 Baroclinic lee waves

The *baroclinic lee wave theory* studies a quasi-geostrophic, idealized, linear shear flow over an isolated mountain. The basic wind represents an incoming cold front or baroclinic zone (with cold air to the west), similar to the southwesterly upper-level flow type (cf. Fig. 1.1a). This basic wind profile allows for the growth of a standing baroclinic wave in the lee (south) of the mountain. Although a *baroclinic wave* is often used to imply a growing, baroclinically unstable wave, here it is defined more generally as a surface-trapped wave in a baroclinic current whose restoring force is associated with temperature advection at the boundary. Based on the quasi-geostrophic approximation, the geostrophic, Boussinesq (quasi-incompressible) potential vorticity equation on an f-plane can be written as (e.g. Gill 1982; Smith 1984, Davies and Wernli 2003):

$$\frac{D_g}{Dt}\left(\nabla^2 p + \frac{f^2}{N^2}\frac{\partial^2 p}{\partial z^2}\right) = 0 \qquad (1.1)$$

where D_g/Dt is time derivative following the geostrophic part of the motion with $u_g = -p_y/(\rho_o f)$ and $v_g = p_x/(\rho_o f)$, p is the pressure, N buoyancy (Brunt-Väisälä) frequency and f Coriolis parameter. The term inside the brackets is the quasi-geostrophic potential vorticity. The surface temperature advection equation

$$\frac{D_g}{Dt}\theta + w\frac{\partial \theta}{\partial z} = 0 \text{ at } z = 0, \qquad (1.2)$$

where θ is potential temperature, applied at surface (z=0). Assuming that the basic flow velocity is a linear function of height, i.e. $U(z) = U_o + U_z z$ and $V(z) = V_o + V_z z$, in a thermal balance, where U_o and V_o are the basic surface wind speeds, the potential vorticity in (1.1) vanishes everywhere. In this case, any perturbation to this basic state must satisfy,

$$\nabla^2 p' + \frac{f^2}{N^2} p'_{zz} = 0. \qquad (1.3)$$

The linearized form of (1.2) is

$$\frac{\partial\theta'}{\partial t}+U_o\frac{\partial\theta'}{\partial x}+V_o\frac{\partial\theta'}{\partial y}+u'_g\frac{\partial\bar{\theta}}{\partial x}+v'_g\frac{\partial\bar{\theta}}{\partial y}+w'\frac{\partial\bar{\theta}}{\partial z}=0, \tag{1.4}$$

and using the hydrostatic law $\theta'=(\theta_o/g\rho_o)(\partial p'/\partial z)$, geostrophic wind perturbation relations $u'_g=-(1/\rho_o f)\partial p'/\partial y$ and $v'_g=(1/\rho_o f)\partial p'/\partial x$, and thermal wind relations at $z=0$ (where $\bar{T}=\bar{\theta}$) $fU_z=-(g/\theta_o)\partial\bar{\theta}/\partial y$ and $fV_z=(g/\theta_o)\partial\bar{\theta}/\partial x$ it can be derived that (1.4) transforms to,

$$\left(\frac{\partial}{\partial t}+U_o\frac{\partial}{\partial x}+V_o\frac{\partial}{\partial y}\right)\frac{\partial p'}{\partial z}-U_z\frac{\partial p'}{\partial x}-V_z\frac{\partial p'}{\partial y}+\rho_o N^2 w'=0 \quad \text{at } z=0. \tag{1.5}$$

The equations (1.3) and (1.5) form a closed system as long as w' is known at $z = 0$, which can be specified by the linear lower boundary condition $w'(x,y,z=0)=U_o\partial h/\partial x+V_o\partial h/\partial y$, where $h(x,y)$ is the mountain height function.

Due to mathematical tractability the solution differs due to the choice of the zonal wind profile: for example $U_o>0$ requires $U_z<0$ and the basic wind vanishes at some height. Thus, the vanishing of the basic wind $U(z)$ at some height is the condition for obtaining a disturbance away from the mountain (see Smith 1984 for more details). Using this assumption and evaluating (1.3) and (1.5) for the steady state, two-dimensional ($\partial/\partial y=0$) problem gives

$$p'(x,z)=0, \quad \text{for } x<0, \tag{1.6a}$$

$$p'(x,z)=-(4\pi\rho_o Nf)\hat{h}(k^*)e^{-z/H^*}\sin k^* x \quad \text{for } x>0. \tag{1.6b}$$

where $k^*=f/(NH^*)$ is the wavenumber defined by the height H^* which denotes the height where basic wind vanishes and $\hat{h}(k^*)$ is the Fourier transform of $h(x)$ for $k=k^*$ (see Smith 1984 for more information).

Equation (1.6b) describes a train of standing baroclinic lee waves on the lee of the mountain. The amplitude of the wave can be estimated with typical flow and orographic parameters for Alpine lee cyclogenesis, such as $\rho_o=1\ \mathrm{kg\,m^{-3}}$, $N=0.01\ \mathrm{s^{-1}}$, $f=10^{-4}\mathrm{s^{-1}}$, $h=3\mathrm{x}10^3\mathrm{m}$,

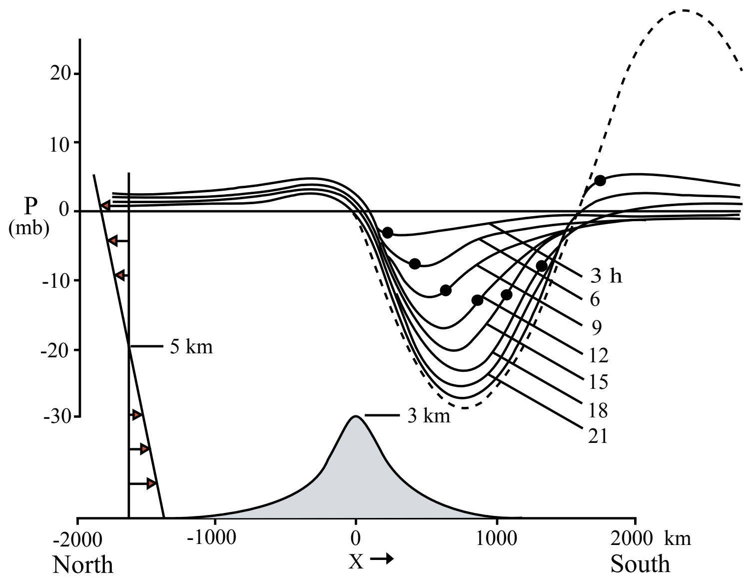

***Figure 1.2**: Steady-state and two-dimensional time-dependant solutions with the initially undisturbed flow over a bell-shaped mountain for a back-sheared flow over a $3\,km$ high mountain ridge ($\rho_o = 1\,kg\,m^{-3}$, $N = 0.01\,s^{-1}$, $f = 10^{-4} s^{-1}$, $a = 2.5\text{x}10^5 m$, $U_o = 20\,ms^{-1}$ and $H^* = 5\text{x}10^3 m$). The time-dependant solutions were obtained by applying an FFT algorithm. (Adapted after Smith 1984 and Lin 2007).*

$a = 2.5\text{x}10^5\,\text{m}$ (a is half-width of the mountain) and $H^* = 5\text{x}10^3\,\text{m}$ a pressure perturbation $p' = 28\,\text{hPa}$ can be generated. The wavelength of the baroclinic lee wave is $\lambda = 2\pi / k^* \approx 3000\ \text{km}$ which is comparable to observed baroclinic waves over the Alps.

In order to obtain the two-dimensional, time-dependant solution of (1.3), its Fourier transform should be taken applying the upper boundedness boundary condition, and then substituting the solution to (1.5) with the linear lower boundary condition. Figure 1.2 shows examples of the steady-state solution (1.6), and the time-dependant solution of an initially undisturbed flow, $p'(t = 0) = 0$, which leads to a lee cyclogenesis with pressure tendencies from 4 to 6 $hPa / 3h$. The fluid is in fact trying to form the first trough of a standing baroclinic lee wave.

1.2.2 Orographic modification of baroclinic instability

In the theory of *orographic modification of baroclinic instability* or *normal mode theory of orographical cyclogenesis* (as sometimes referred) for Alpine lee cyclogenesis, the formation of lee cyclones is primarily attributed to the baroclinically unstable modes modified by orography, though in some cases the orography can destabilize modes that are not unstable upstream (Fantini and Davolio 2001). To derive the governing equations, a small-amplitude mountain is assumed as well as and a basic flow with constant stratification and vertical shear. A zonal wind vanishes at $z = 0$, bounded between $z = 0$ and $z = H$ in vertical and by lateral walls at $y = \pm L_y / 2$. For this type of flow, the linear, nondimensional equations and boundary conditions governing the evolution of small perturbations on the mean zonal wind $\bar{u} = Uz / H$ in dimensionless units (horizontal scale is external Rossby radius of deformation (1000 km), vertical scale is *H* and velocity scale *U*) are (Speranza et al. 1985):

$$\nabla^2 \psi + \frac{\partial^2 \psi}{\partial z^2} = 0 \tag{1.7}$$

$$\frac{\partial^2 \psi}{\partial t \partial z} - \frac{\partial \psi}{\partial x} = -J(\psi, h / R_o) \quad \text{at } z = 0 \tag{1.8}$$

$$\frac{\partial^2 \psi}{\partial t \partial z} - \frac{\partial \psi}{\partial x} + \frac{\partial^2 \psi}{\partial x \partial z} = 0 \quad \text{at } z = 1 \tag{1.9}$$

$$\psi = 0 \quad \text{at } y = \pm L_y / 2 \tag{1.10}$$

where ψ is the streamfunction, *J* the Jacobian, *h* the mountain height and R_o is the Rossby number. Assuming $\psi(t, x, y, z) = \phi(x, y, z) e^{-i\omega t}$ and applying the Fourier series expansion to the above system reduces it to an eigenvalue problem, which allows one to find the most unstable baroclinic wave mode from the eigenvalues. An example of Alpine lee cyclogenesis based on the above theory is shown on Figure 1.3. The disturbance at the surface (Figs. 1.3a-b) is more localized near the mountain than that at the mid-troposphere (Figs. 1.3c-d). The total streamfunction fields (Figs. 1.3b,d) seems to capture basic structure of Alpine lee cyclones in the deep and mature stage of growth. Basically, lee cyclogenesis is explained as the intensification of the incident wave taking place on the southern (warm) side of the mountain, together with a weakening of the wave amplitude on the northern (cold) side.

1.2.3 Evaluation of the theories

The above two theories for Alpine lee cyclogenesis are related because both of them are built upon the baroclinic wave theory of Eady (1949). Eady studied baroclinic generation of eddies

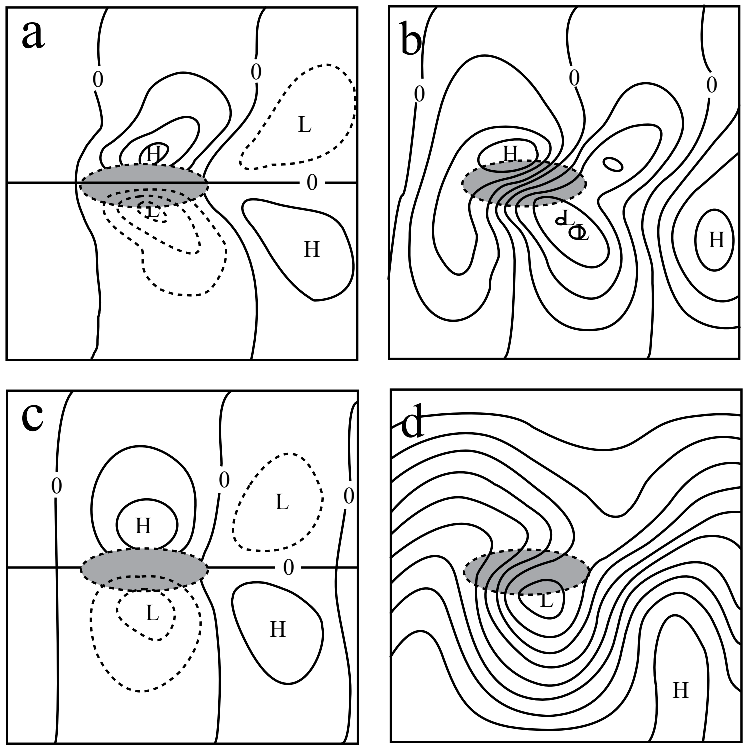

***Figure 1.3**: An example of cyclogenesis generated by a baroclinic wave in the continuous Eady model, in a long periodic channel with isolated orography. A portion of the channel of 8 x 8 nondimensional length units is shown. The shaded oval denotes the orographic contour of* $h_{max} * e^{-1}$ *(* h_{max} *is the maximum mountain height. (a) Streamfunction of orographic perturbation only at* $z = 0$*; (b) total streamfunction of modified baroclinic wave at* $z = 0$*; (c) and (d) are as in (a) and (b), respectively, but at the middle level,* $z = 0.5$*. The basic zonal wind is added in (d). (Adapted after Speranza et al. 1985 and Lin 2007).*

in a geostrophic, vertically sheared flow, which implies an existence of potential energy that is available for conversion in other forms. The theory implies conservation of potential vorticity (and potential vorticity perturbation due to linear vertical shear of the wind profiles), what can be seen in (1.3) and (1.7). However, the two lee cyclogenesis theories use different initial and upper boundary conditions, in addition to basic wind profiles. In the baroclinic lee wave theory, an undisturbed (or a localized) baroclinic wave is used to initiate the process, while a fully-developed baroclinic wave is used as the initial condition in the theory of orographic modification of baroclinic instability. In other words, Speranza et al. (2001) studied the modification of a perturbation by the mountain, while in Smith (1984) the perturbation was created by the mountain. In addition, the baroclinic lee wave theory uses a boundedness upper boundary condition, while the second theory uses a rigid lid upper boundary condition, same as that used in Eady's model. Based on initial conditions imposed, it appears that the baroclinic lee wave mechanism is more applicable to the southwesterly type, while the normal mode theory of orographical cyclogenesis is more applicable to the northwesterly type (Lin 2007). In addition, the above theories can be viewed as complementary since the Smith's theory predicts rapid formation of a shallow lee cyclone on a time scale of 18 hours seeing it as the formation of the first trough of a baroclinic lee wave, not allowing for baroclinic instability and deep cyclogenesis. In turn, these issues are tackled in the normal mode theory, which is relevant to the stages of development which follow the first rapid stage of pressure fall in the lee of the mountain range.

Further verification of these quasi-geostrophic linear theories (including the one by Pierrehumbert 1985, which differs from Speranza et al. 1985 only by different treatment of

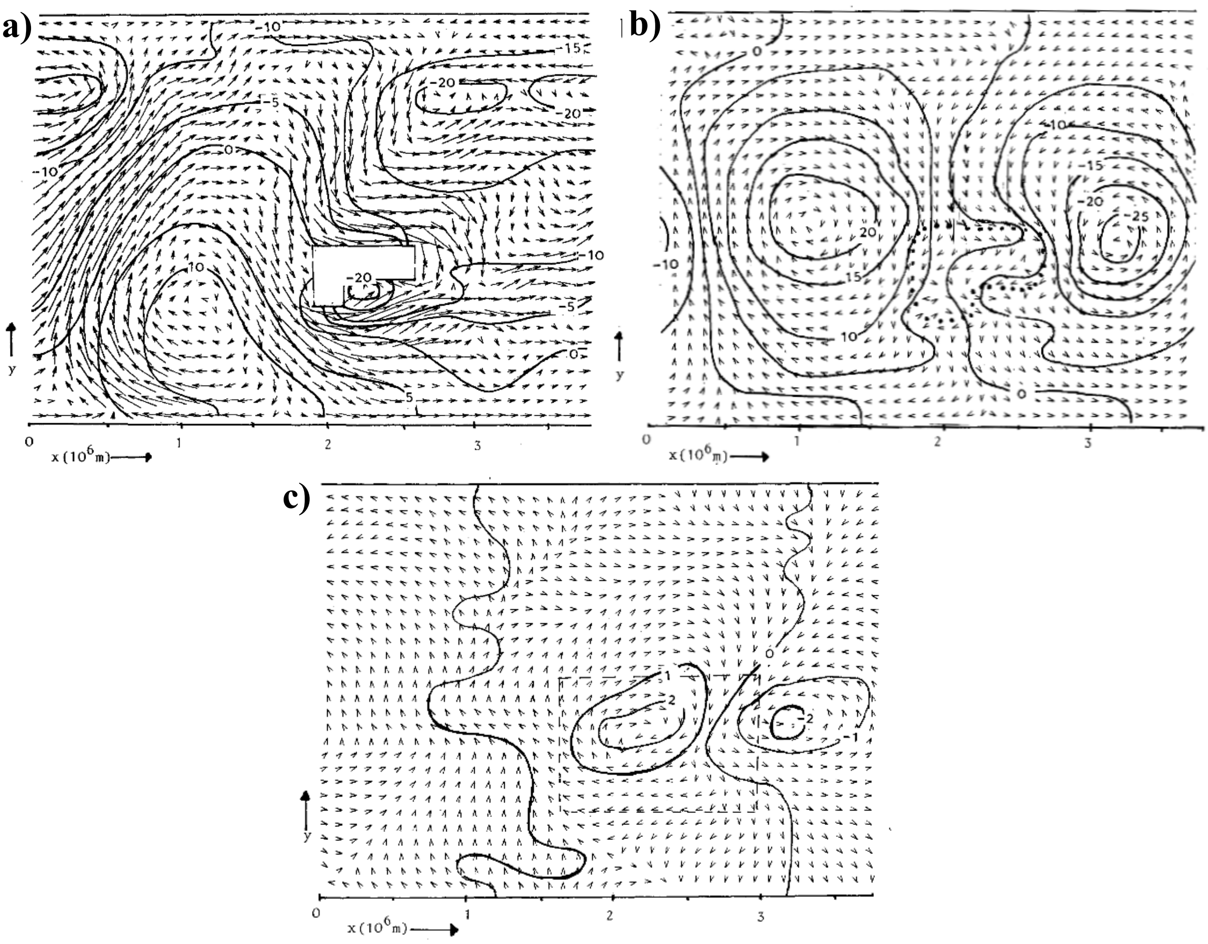

Figure 1.4: *Pressure (hPa) and wind at the lowest computational level (z=1000 m). (a) Control experiment at t=48 h. (b) Model simulation of the theoretical model by Speranza et al. (1985). (c) Model simulation of the theoretical model by Smith (1984). (Adopted after Egger 1988).*

the orography) was performed by using an "idealized" reference simulation of a lee cyclone event with a channel flow model (Egger 1988). The reference model was modified to reflect the proposed theories and tested for simulating the lee cyclogenesis in the reference experiment. The results of the numerical experiments performed showed that both theories were appreciably limited in explaining the reference lee cyclone (Fig. 1.4). In particular, it was suggested that the theories necessarily need to be non-linear in order to capture the first phase of lee cyclogenesis. The mountains need to be high enough so that realistic blocking is included in theory. Once the non-linear first phase of cyclone development is established, linear theory is sufficient to explain the subsequent deepening.

Therefore, the theoretical explanations showed constrained in explaining the lee cyclogenesis, and we will refer to potential vorticity based approach and numerical non-linear simulations in order to analyze the process in question. Nevertheless, it should be mentioned that most of the constraining assumptions in the normal model of orographical cyclogenesis (such as i.e. extension of the theory to finite amplitude, non-geostrophic, primitive set of equations, treatment of initial condition problem in place of normal mode problem, inclusion of the vertical wind shear, no restrictions of slopes etc.) were released in subsequent years, giving this theory high consistency and even closer resemblance to the observed phenomenon.

1.3 Potential vorticity and lee cyclogenesis

Since orographical cyclogenesis is essentially linked with an incoming upper-level trough i.e. increased positive potential vorticity (PV) values, several aspects originating from the "PV thinking" (see review by Hoskins et al. 1985) can be applied in conceptually comprehending the lee cyclogenesis phenomenon:

(1) Potential vorticity is conserved on an isentropic surface, which holds in adiabatic and frictionless atmosphere
(2) The invertibility principle, which holds whether or not diabatic and frictional processes are important.

The first is the familiar Lagrangian conservation principle, which in real atmosphere holds whenever the advective processes dominate over frictional and diabatic ones. Rossby (1939) was the first to realize that a form of the vertical component of the absolute vorticity:

$$\zeta_a = f + \vec{k} \cdot \left(\vec{\nabla} \times \vec{V}\right) \tag{1.11}$$

is the most important for the large-scale atmospheric flow and that many features of the flow could be modeled by assuming conservation of ζ_a in two-dimensional horizontal motion. A year later (Rossby 1940) took a step further and noticed that if h is the depth of a fluid in the barotropic model then

$$\zeta_a / h = const \tag{1.12}$$

following the fluid column. This describes the two processes that often dominate the vorticity budget, the creation of vorticity by stretching of vortex tubes and the horizontal advection of absolute vorticity. This is the simplest version of the modern concept of potential vorticity, which means there is potential for creating vorticity by changing latitude and by adiabatically changing the separation of isentropic layers.

Rossby's achievement was given a generality by an independent work of Ertel (1942), who obtained the famous result:

$$q = \frac{1}{\rho} \vec{\zeta}_a \cdot \vec{\nabla} \theta = const \tag{1.13}$$

following an air parcel in an adiabatic, frictionless motion with no approximations involved: q is conserved even for fully three-dimensional, nonhydrostatic motion. Additionally, this formula can be generalized to include both diabatic and frictional processes.

It seems that Kleinschmidt (1950 and his subsequent work, see Hoskins et al. 1985 for a through review and a full list of references) was the first to intuitively realize that not only one can use the PV as a Lagrangian tracer but that one can deduce, diagnostically, the complete dynamical fields from the spatial distribution of PV. This is called "invertibility principle" and in order to retrieve, diagnostically, dynamical fields such as wind, temperature, vertical velocity, geopotential field and static stability, it is necessary to:

(i) specify a kind of balance condition
(ii) specify a kind of reference state
(iii) solve the problem globally, with a proper attention to boundary conditions

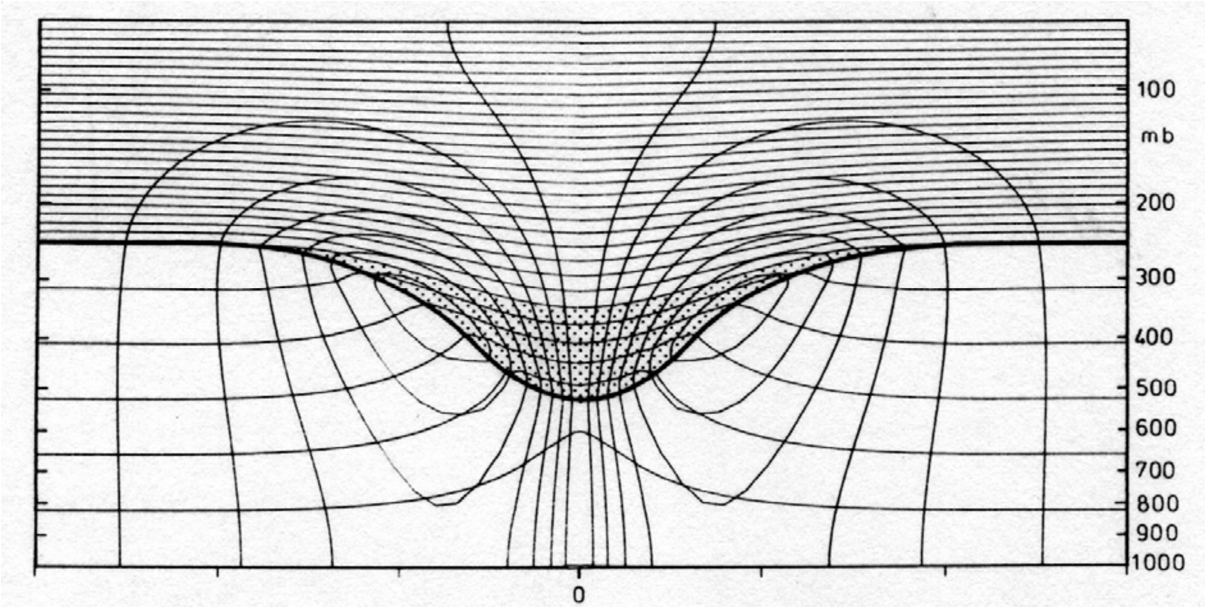

Figure 1.5: *Circularly symmetric flows induced by simple, isolated, positive PV anomaly (whose location is shown stippled), with isentropes (opened full lines) and isotachs (closed full lines) indicated. The sense of the azimuthal wind is cyclonic. The tick marks on the x-axes are drawn every 833 km, and only half of the domain is shown (the undisturbed θ distribution was imposed as a boundary condition at distance r = 5000 km from the centre of the domain. The thick line represents the tropopause and the two sets of thin lines isentropes every 5 K and transverse velocity every 3 ms^{-1} (Adopted after Thorpe 1985).*

An example of the flows induced by a simple, isolated PV anomaly (Thorpe 1985) shows that positive upper-level PV anomaly is associated with increased (decreased) static stability and warmer (colder) air in upper-levels (lower levels) compared to the reference state (Fig. 1.5). This is in accordance with phenomenological evidence of Alpine lee cyclogenesis, discussed in Section 1.1.

Dynamically, the influence of the upper-level potential vorticity anomaly is to induce the surface thermal anomaly over a surface baroclinic zone through the cyclonic circulation induced from the upper-levels (Fig. 1.6a). The created surface thermal anomaly induces its own surface cyclonic circulation which interacts with the upper-level flow. The interaction of upper-level – low-level vortices strengthens the cyclonic circulation throughout the whole troposphere (Fig. 1.6b).

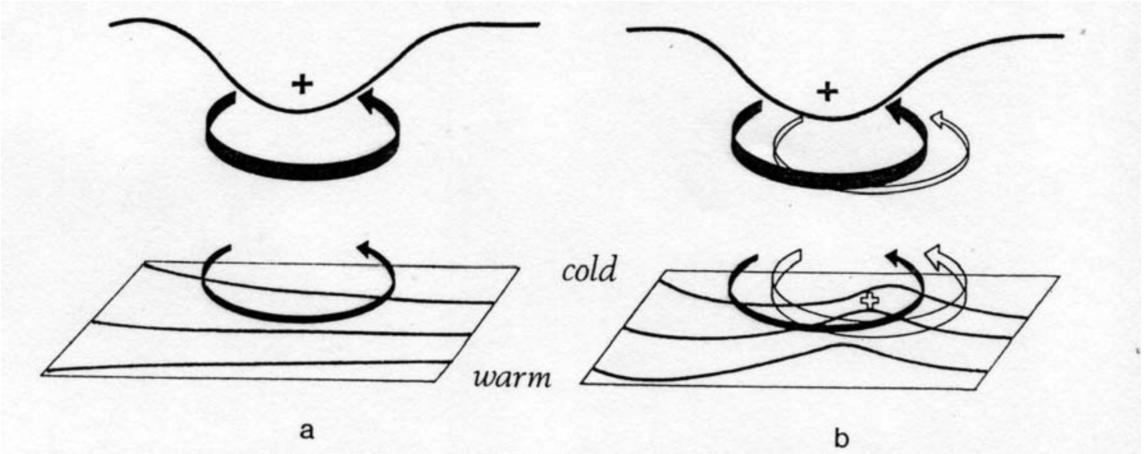

Figure 1.6: *A schematic diagram of cyclogenesis associated with an advection of the positive upper-level PV anomaly above the surface baroclinic zone. (a) Advection of the positive upper-level PV anomaly over a baroclinic zone initiates the creation of a surface thermal anomaly. (b) Induced cyclonic circulation due to creation of the surface thermal anomaly interacts with the upper-level cyclonic flow. The low-level and upper-level vortices mutually reinforce each other. (Adopted after Hoskins et al. 1985).*

The ample experimental and phenomenological evidence (e.g. such as collected in ALPEX (Kuettner 1986) and MAP (Bougeault et al. 2001) as discussed in Section 1.1.) of the co-existence of Alpine lee cyclogenesis, thermal anomaly in the lee of the Alps and upper-level potential vorticity anomaly moving over the Alpine range, indicates that the lee cyclogenesis might be conceptually comprehended as PV induced cyclogenesis. The process seems to be similar to the one shown on the Figure 1.6, except that the creation of the thermal anomaly is not due to deformation of the baroclinic zone due to induced circulations from the upper-levels, but to flow splitting and frontal retardation on the Alps, as discussed earlier.

However, due to the flow-splitting and frontal retardation, most orographic cyclones entail the violation of the balanced and inviscid dynamics during the first phase of their development. Thus, a dynamical interpretation may be sought by considering the first-phase unbalanced generation of low-level orographic perturbation and assuming that the subsequent development approximately follows the balanced dynamics. It then follows from the invertibility principle (Hoskins et al. 1985) that any vortex contributing to the second phase should be either a thermal anomaly or a low-level PV anomaly. In recent studies (e.g. Aebischer and Schär 1998) it was argued that beside thermal anomaly which occurs due to the frontal retardation, low-level PV anomaly created by flow deformation on the orographical obstacle (so-called primary "*PV banner*") has an influence on the initiation and localization of the lee cyclone. Namely, most of the Alpine lee cyclones tend to be bounded to the SW edge of the mountain (where often a strong primary PV banner forms), not being equally distributed in mountain-sized thermal anomaly.

More recently, a perturbation theory was derived for flows with Froude number $Fr << 1$ and Rossby number $R_o >> 1$ that showed that the influence of the Coriolis effect was to produce an asymmetry of the pressure perturbation in the lee of the mountain (Hunt et al. 2001), compared to the non-rotating cases of low-Froude number flows past the obstacle, adding value to understanding of the preference of the western part of the Alpine lee for cyclone initiation. However, unlike flows over the Alps ($R_o \sim 1$), this flow regime belongs to strongly unbalanced flow regime. Therefore, the incomplete picture of the associated scale interaction and known influence of diabatic processes and moisture due to proximity of this edge to the Mediterranean Sea (e.g. Dell'Osso and Radinović 1984; Kuo et al. 1995) did not allow the complete reduction of the existing uncertainties in the understanding of the phenomenon.

The use of the invertibility principle in studies of lee cyclogenesis has been numerically applied to a much lesser extent than for regular mid-latitude cyclogenesis, such as connected with THORPEX experiment (see e.g. Shapiro and Thorpe 2004). Bleck and Mattocks (1984) were the first ones to realize the fact that lee cyclogenesis is often accompanied with an advection of the high PV values (PV anomalies). A few years later Mattocks and Bleck (1986) associated the potential vorticity anomaly in the upper-troposphere with a baroclinic wave traversing the Alps, seemingly using the first application of the invertibility principle (within a geostrophic framework) to the lee cyclogenesis.

They have shown that the use of invertibility principle to assess balanced (geostrophic) modifications in the initial conditions of the numerical sensitivity simulations seems to be a powerful tool in estimating the influence of the upper-level potential vorticity anomaly to lee cyclogenesis. Later on, significant efforts were used to formulation of the higher-order accuracy inversion formulation, using Ertel's PV and non-linear balance operators (Davis and Emanuel 1991). However, the nonlinearity in the inversion operator for Ertel's potential vorticity (unlike the linear formulation of quasi-geostrophic potential vorticity) renders inversion of individual portions of the potential vorticity field ambiguous, which was attributed by formulation of a so-called piecewise potential vorticity inversion (Davis 1992).

The formulation of the piecewise method enabled quantitative estimates on the influence of the various aspects of the upper-level potential vorticity anomaly to the lee cyclogenesis. This approach is taken in this study, facilitated with numerical experiments that tackled macroscale and mesoscale modifications in both position and intensity of the upper-level potential vorticity anomaly, enabling further qualitative and quantitative estimates of the interaction between the upper and the lower troposphere during the lee cyclogenesis.

2. Cyclonic activity in the Adriatic region

Weather, climate and hydrology of the wider Adriatic area are strongly determined by the cyclone activity in the Adriatic Sea. In addition, extreme weather phenomena, such as local downslope windstorm Bora (known as "*Bura*" in Croatia) (e.g. Smith 1987; Klemp and Durran 1987; Bajić 1989; Jurčec 1989; Ivančan-Picek and Tutiš 1996; Enger and Grisogono 1998; Grubišić 2004; Belušić et al. 2004; Göhm and Mayr 2005), strong winds called Scirocco and Tramontana (Jurčec et al. 1996; Cavaleri et al. 1999; Pandžić and Likso 2005), heavy orographic precipitation, thunderstorms, supercells and mesoscale convective systems (Ivančan-Picek et al. 2003) are often triggered by the cyclone activity in the Adriatic and the central Mediterranean. Since many of the cyclones in the Mediterranean are of mesoscale dimensions, at least in the initial stage of their development, meso-β cyclone classification was performed to complement the early cyclone climatologies in the area (e.g. Van Bebber 1891; Pettersen 1956; Radinović 1965; see Radinović 1987 for a review).

2.1 Data and methodology

A manual subjective analysis technique was used to analyze the cyclone activity over the Apennine and Adriatic areas. In addition, the subjective analysis included objective guidance regarding the cyclone intensity and duration, while circulation criteria remained predominantly subjective. The present work is based on the 4-yr (2002-2005) T511 operational analysis data with 6-hr temporal resolution, acquired from the European Centre for Medium-range Weather Forecasts (ECMWF). Among the available model data archives, this dataset allows for the highest spatial resolution in the related mid-latitudes (~40 km).

As the first step, an occurrence of the pressure lows was identified based on the mean sea level pressure (MSLP) 2 hPa closed isobar in the target area of the Adriatic. Then, streamlines were analyzed to identify the associated circulation pattern in the pressure low area. If the pressure low was above the sea or flat land, closed circulation cyclone identification was required. However, if the cyclone was shallow or in the vicinity of the mountains, a strong surface convergence (significant streamline curvature) pattern was recognized. Namely, this type of streamline pattern is often present in the process of cyclone initiation in mountain areas as well as during its passage over the mountain range. In particular, e.g., in cases of weak cyclone initiation of the Alpine lee over northern Italy, where complex terrain strongly modifies the surface circulation, strong surface convergence was taken as sufficient criterion for cyclone detection if the system satisfied objective MSLP threshold. This choice kept the analysis somewhat subjective, but more in accordance with conceptual models as well as other climatology studies. Once a cyclone was detected in the area of interest, it was back-traced (traced) to the place of origin (deterioration or exit out of the domain).

The subjective cyclone detection and tracking criteria was aimed at isolating somewhat more significant and intense cyclones, both in terms of duration and intensity that are more important for the weather and climate in the region. In accordance, objective constraints included the 2 hPa closed isobar in duration of at least 6 hours for all the cyclones that appear in the Adriatic. However, very few cyclones were added to the classification, even if it did not fully satisfy the above MSLP closed isobar criteria. These exceptions belong to the “twin” cyclone type, as will be discussed in the next section, where the secondary center was sometimes well-defined in vorticity field but not in pressure field. In several such cases, at least 1 hPa closed secondary pressure low was required.

Finally, the above criteria were designed in accordance with the spatial and temporal dimensions of the cyclones identified in the operational practice, conceptual models, and Adriatic cyclone case studies (e.g. Radinović 1987; Ivančan-Picek 1998; Brzović 1999). In particular, this type of MSLP and circulation thresholds aims at improving the identification of cyclone initiation and tracking in the lee areas of the Alps and Apennines, in a dedicated regional cyclone analysis.

2.2 Classification of Adriatic cyclones

Based on the mean sea level pressure and closed circulation criteria described in Section 2.1,

Table 2.1: *Seasonal variability of the cyclone types in the Adriatic region detected in period 2002-2005*

	A-I	A-II	B	AB	C-I	C-II	**TOTAL**
DJF	14	4	10	3	14	3	**48**
MAM	6	2	6	2	11	2	**29**
JJA	7	0	11	1	1	1	**21**
SON	8	4	7	2	10	1	**32**
TOTAL	**35**	**10**	**34**	**8**	**36**	**7**	**130**

four categories of cyclones that appear in the Adriatic basin and their associated tracks are detected and classified as the following types (Horvath et al. 2008a):

(1) A – Genoa cyclones (the Gulf of Genoa and northern Italy)
  a. A-I – continuous Genoa cyclones
  b. A-II – discontinuous Genoa cyclones
(2) B – Adriatic cyclones
  a. B-I – northern Adriatic cyclones
  b. B-II – middle Adriatic cyclones
(3) AB – co-existing Genoa and Adriatic cyclones ("twin" or "eyeglass" cyclones)
(4) C – non-Genoa and non-Adriatic cyclones
  a. C-I – continuous cyclones
  b. C-II – discontinuous cyclones

Cyclones initiated in the Gulf of Genoa or northern Italy (Type A) constitute almost 35% of the cyclones that enter the Adriatic basin and most often occur in the winter (Figs. 2.1a-b, Table 2.1). This type of cyclone usually traverses to the northern Adriatic over the northern Italy and Po Valley, without a significant disturbance of vorticity pattern above the peninsula (Type A-I). Once in the northern Adriatic, the cyclone tracks diverge: whilst the main path slides down the basin, a subset of cyclones follow the secondary tracks by crossing the northern Dinaric Alps and advecting either eastward or northeastward. In contrast, a subset of the Genoa cyclones after initiation slides along the western Italian coast to the Tyrrhenian Sea and traverse the middle Apennines on the way to the Adriatic. Due to the height of the middle Apennines range (2912 m), a subset of these cyclones becomes discontinuous over the mountain (Type A-II). This process is accompanied by the simultaneous presence of two cyclone centers on the upstream and downstream parts of the mountain (more information

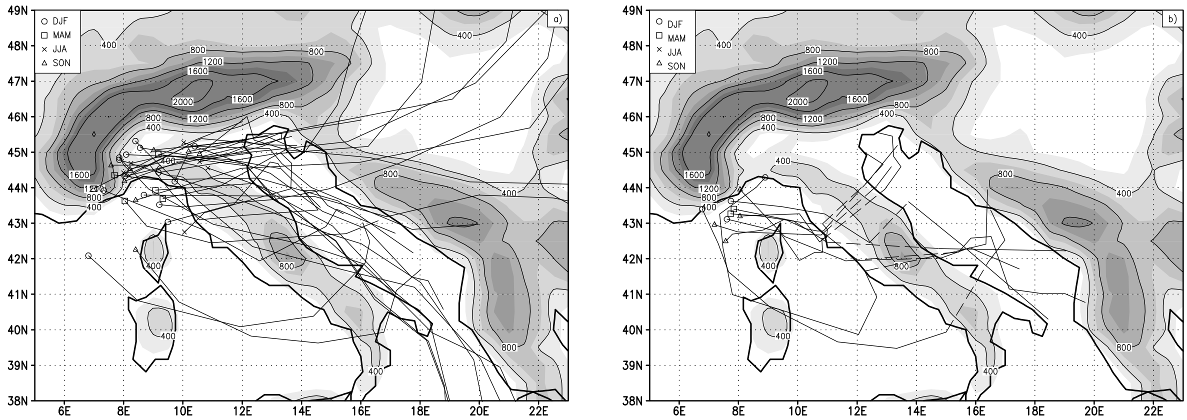

Figure 2.1: *Track plots of Genoa (a) Type A-I continuous and (b) Type A-II discontinuous cyclones, as inferred from the ECMWF T511 analysis (2002-2005). Most of the A-I cyclones cross the Apennine peninsula in the north, whilst most of the A-II cyclones traverse to Adriatic over the middle Apennines.*

about the streamline patterns of discontinuous cyclones can be found in Horvath et al. 2008a). Type A cyclones cause a chain of related weather conditions on the eastern Adriatic coast, where strong “Jugo” (mountain channeled Scirocco wind, see Jurčec et al. 1996) and mountain induced precipitation (on western slopes of the Dinaric Alps) precede strong Bora wind, that starts at the northern Adriatic and gradually spreads towards the southern Adriatic as the cyclone moves down the basin. These cyclones are moderately well predicted, although Bora wind speed and gustiness as well as precipitation site-specific forecasts over the eastern Adriatic coast are sometimes rather poorly forecasted, e.g. due to erroneous forecast of the exact cyclone location.

Adriatic cyclones (Type B) are the smallest scale cyclones analyzed, often with horizontal dimensions of the basin width (≤200 km). These cyclones are initiated in localized areas of the northern Adriatic (Type B-I) and western part of the middle Adriatic (Type B-II) and comprise 26% of the total number of cyclones detected in the basin (Fig. 2.2). Type B-I cyclones typically initiate in the northern Adriatic and move southeastward over the basin. The initiation process of this type of cyclone seems to be phenomenologically similar to the Genoa lee cyclogenesis process. These cyclones form mostly in the cold part of the year and can deepen considerably. Type B-II initiates in the lee of the middle Apennines and quickly traverses the Adriatic Sea perpendicular to the main axis. The cyclones tend to form more often in the warmer part of the year and usually do not deepen more than 5 hPa in the

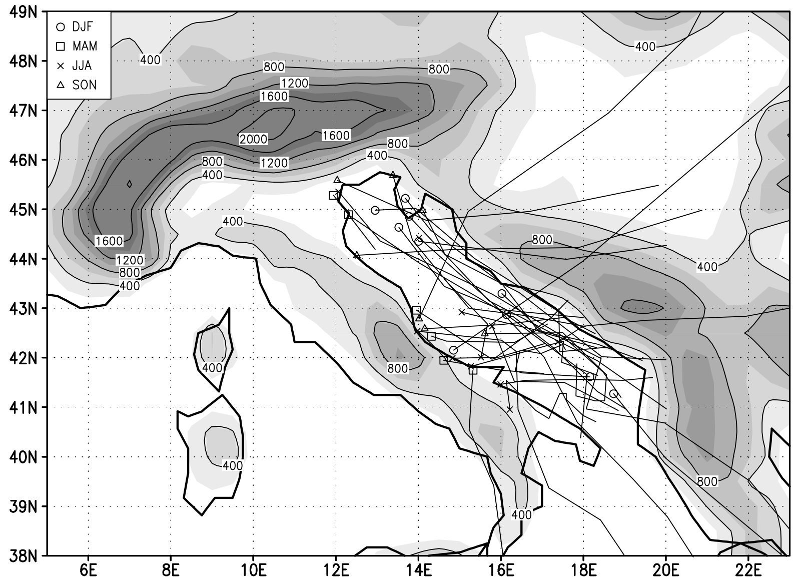

***Figure 2.2**: Track plots of Adriatic cyclone types, as inferred from the ECMWF T511 analysis (2002-2005): Type B-I continuous cyclones move from north to south along the Adriatic Sea and Type B-II discontinuous cyclones initiate in the lee of Middle Apennines and traverse the Adriatic perpendicular to the main basin axes.*

Adriatic area. This type of rather shallow cyclone often gets blocked by the Dinaric Alps and decoupled from the short-wave upper-level disturbance simultaneously. As a whole, the northern and the middle Adriatic regions have similar frequency of cyclone appearances.

While the weather conditions of Type B-I cyclones appear similar to those of Type A cyclones, Type B-II cyclones, due to their shallowness cause high impact weather only in summer (e.g. summer storms), when their seasonal distribution has a maximum. However, probably due to their scale and weak intensity, these cyclones are the least predictable of all cyclone types identified in the study. Therefore, knowledge about their climatology and physical mechanisms might have a potential use in everyday operational forecast practice.

Another type of cyclone initiated in the region is the twin or eyeglass cyclone type (Type AB). These cyclones are characterized with the simultaneous presence and evolution of two cyclones, one in the Adriatic and one in the Gulf of Genoa (Fig. 2.3). This rather rare type of cyclone (comprising 6% of the total number of cyclones in the region) usually slides down along the western and eastern part the Apennine peninsula, and occasionally an Adriatic twin member crosses the Dinaric Alps to the east.

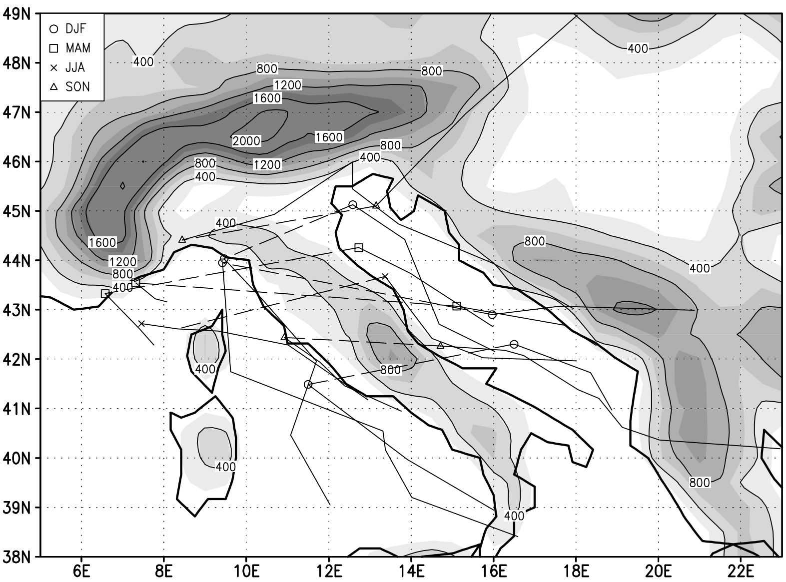

Figure 2.3*: Track plots of Type AB twin or eyeglass cyclones with two coexisting cyclonic centers, as inferred from the ECMWF T511 analysis (2002-2005): the first in the Adriatic Sea and the second in the Gulf of Genoa (or Tyrrhenian Sea). The centers usually move along the main peninsula axes.*

Type C cyclones traverse to the Adriatic over Apennine peninsula, but have initiation areas other than the Gulf of Genoa and constitute 33% of the total number of cyclones detected in the Adriatic (Figs. 2.4a-b). Similar to the Type A cyclones, they can be continuous (Type C-I) or discontinuous (Type C-II) over the Apennine mountain range. The migration areas include the Atlantic Ocean, Atlas, the Pyrenees, Iberian peninsula, Alboran Sea and others. Due to their dimension and remote location of initiation, these cyclones and related weather (that highly depends on the location of the cyclone entrance in the Adriatic basin) are usually well forecasted. These cyclones occur most often in winter and the least during the summer. Since the main summer cyclogenetic area in the western Mediterranean is the Iberian peninsula (Trigo et al. 1999), it is noteworthy that their tracks diminish as they approach the Genoa Bay and the Adriatic along their northeastward track. This seems to be a consequence of the lack of upper-level forcing (which is a characteristic of thermally induced Iberian summer cyclones) and the existence of predominant etesian circulation that disable the farther cyclone northeastward protrusion to the Adriatic. In addition, Type C cyclones occasionally experience a chain-like series of redevelopments along the Mediterranean. This amplifies the complexity of the analysis and might longitudinally increase the uncertainty of the Mediterranean cyclone climatology.

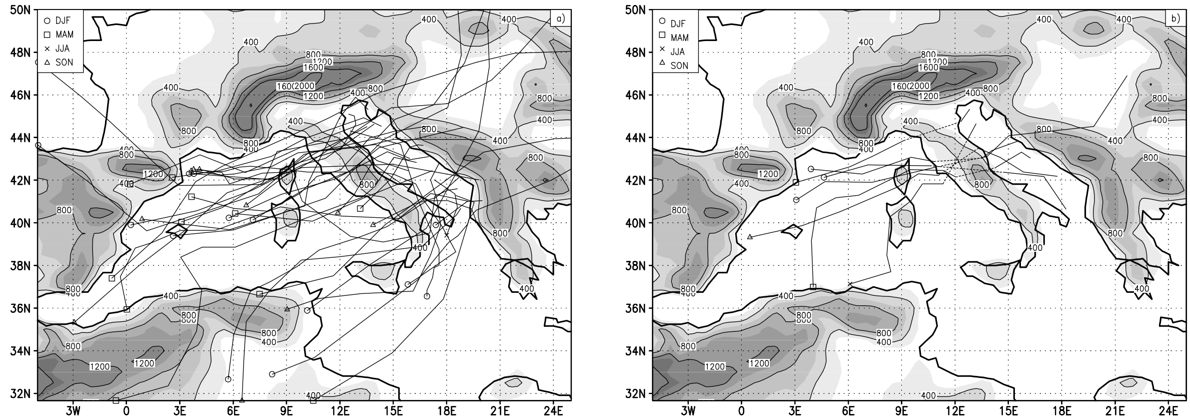

Figure 2.4: *Track plots of non-Adriatic and non-Genoa (a) Type C-I continuous and (b) Type C-II discontinuous cyclones, as inferred from the ECMWF T511 analysis (2002-2005). This type of cyclone is initiated in the areas of the Pyrenees, Iberia, Atlas, Alboran Sea and Atlantic as well as over the Mediterranean.*

Therefore, we have seen that the most of the cyclones that appear in the Adriatic are induced in the lee sides of mountain ranges in the western Mediterranean (such as the Alps, the Atlas, the Pyrenees and the Apennines), often with the presence of an upper-level trough moving over the mountain (Horvath et al. 2008a). Since mountain range and upper-level dynamical factors are the strongest precursors of lee cyclogenesis events, study on the influence of the upper-tropospheric systems to the initiation of the lee cyclones as well as their sensitivity to uncertainties in the initial-analysis of the upper-level dynamical precursor is of great importance for everyday weather prediction in the wider Adriatic area, as well as analysis of extreme weather in the region.

3. Methods and model description

3.1 Factor separation method

Factor Separation (FS) method is used in the analysis presented in Chapter 4, allowing us to quantify not only the contributions of the sole investigated factors (e.g. such as upper-level potential vorticity (PV) anomaly or orography), but also their mutual interaction. It is a useful approach if the analyzed system is nonlinear i.e. if interactions among investigated factors are expected. In order to evaluate the influence of n factors and their mutual synergies it is necessary to run 2^n model simulations. So as to illustrate the method fully described in Stein and Alpert (1993), a single pure factor, double and triple interaction effects are listed for reference bellow:

$$F_i = f_i - f_0 \tag{3.1}$$

$$F_{ij} = f_{ij} - (f_i + f_j) + f_0 \tag{3.2}$$

$$F_{ijk} = f_{ijk} - (f_{ij} + f_{ik} + f_{jk}) + (f_i + f_j + f_k) - f_0 \tag{3.3}$$

where f_{ijk} (f_{ij} i.e. f_i) denotes a value of the predicted field in simulation when factors i, j and k (i, j i.e. i) are switched on. F_i is a part of predicted field due to sole contribution of a factor i and F_{ijk} (F_{ij}) is a part of predicted field only due to interaction of factors i, j and k (i, j); f_0 denotes so-called background simulation when all analyzed factors were withheld (switched off) from the simulation.

3.2 Potential vorticity inversion principle

The application of the piecewise PV inversion (formulated by Davis and Emanuel 1991 and Davis 2002) first requires a choice among the PV formulations. Here, the equation for the

Ertel's PV will be used, defined as (Rossby 1940; Ertel 1942):

$$q = \frac{1}{\rho} \vec{\eta} \cdot \vec{\nabla} \theta \tag{3.4}$$

where ρ is the density, $\vec{\eta}$ is the absolute vorticity vector, and θ is the potential temperature. Subsequently, PV anomaly needs to be defined, and it is a common practice that it is defined as a deviation of the instantaneous state and a time average of PV through the 7-10-day period, although other options (comparing instantaneous state with PV climatology, or time-space average over a defined period, level and domain) could be used as well. The PV perturbation equation is:

$$q' = q - \overline{q} \tag{3.5}$$

The inversion of the equation (3.4) i.e. calculation of the balanced flow is performed with the use of Charney's (1955) balance equation, since it is non-linear and accurate even for meteorological systems characterized by large Rossby numbers (Romero 2008):

$$\nabla^2 \phi = \nabla \cdot f \nabla \psi + 2m^2 \left[\frac{\partial^2 \psi}{\partial x^2} \frac{\partial^2 \psi}{\partial y^2} - \left(\frac{\partial^2 \psi}{\partial x \partial y} \right)^2 \right] \tag{3.6}$$

where f is the Coriolis parameter, ϕ geopotential, ψ streamfunction and m map factor of the projection[1].

The additional diagnostic equation used for solutions in ϕ and ψ is an approximate form of equation (3.4), assuming a hydrostatic balance and scale analysis result that the rotational component of the flow is much greater then the irrotational wind component:

$$q = \frac{g \kappa \pi}{p} \left[\left(f + m^2 \nabla^2 \psi \right) \frac{\partial^2 \phi}{\partial \pi^2} - m^2 \left(\frac{\partial^2 \psi}{\partial x \partial \pi} \frac{\partial^2 \phi}{\partial x \partial \pi} + \frac{\partial^2 \psi}{\partial y \partial \pi} \frac{\partial^2 \phi}{\partial y \partial \pi} \right) \right] \tag{3.7}$$

[1] Typical values of map factor m in mid-latitudes range from 1.00 (~30N) to 1.08 (~70N)

where p is the pressure, g is the acceleration due to gravity, $\kappa = R_d / C_p$ is the ratio of the gas constant to the isobaric heat capacity for dry air, and the vertical coordinate π is the Exner function $C_p(p/p_o)^\kappa$, with p_o = 1000 hPa.

The closed system of equations (3.6) and (3.7) is solved given the q by successive overrelaxation method, iterating until convergence is achieved. The solution is reached using Neumann-type conditions ($\partial\phi/\partial\pi = f\partial\psi/\partial\pi = -\theta$) applied on the top and bottom boundaries, and Dirichlet conditions applied on the lateral boundaries.

Next, a balanced time-mean flow $(\overline{\phi},\overline{\psi})$ is inverted from the previously defined reference state $\overline{q}$, using equations identical to (3.6) and (3.7) except that all dependent variables are mean values and the mean potential temperature $\overline{\theta}$ is used for the top and bottom boundary conditions. The perturbation flow (ϕ',ψ') is given by:

$$(\phi',\psi') = (\phi,\psi) - (\overline{\phi},\overline{\psi}) \tag{3.8}$$

The "piecewise" inversion follows the same procedure, except that a number of PV anomalies could be arbitrarily defined from q':

$$q' = \sum q_n' \tag{3.9}$$

Then following this decomposition one can obtain the part of the flow associated with each PV anomaly q_n , using additional assumptions on the linear decomposition of ϕ' and ψ' (Davis 1992; Romero 2008).

3.3 Numerical model description

The analysis is based on extensive use of numerical simulations performed with the non-hydrostatic version of the fifth generation of the Pennsylvania State University - National Center for Atmospheric Research (NCAR) mesoscale model MM5 (Dudhia 1993, Grell et al. 1994). The model uses terrain influenced vertical co-ordinate with enhanced vertical resolution near the surface to better represent turbulent processes in the atmospheric boundary layer. The horizontal grid has an Arakawa-Lamb B-staggering of the velocity variables with respect to the scalars. For this study and numerical experiments discussed in Chapters 4 and 6, the following model details were used:

1) Atlas lee cyclogenesis (Chapter 4):

(i) A single domain of 160x160 points was chosen centered at 5.0E and 37.0N, with 23 vertical levels and 24 km horizontal resolution.

(ii) Macroscale sensitivity simulations were initialized on 00 UTC 11 Nov 2004 and run for the 72 hour period, while mesoscale sensitivity simulations were initiated on 00 UTC 12 Nov 2004 and run for the same forecast period.

(iii) Initial and boundary conditions were provided from the global National Centers for Environmental Prediction (NCEP) Final Analysis, at ~1deg resolution, with a 6-hourly coupling interval, including sea surface temperature. They were horizontally interpolated to the model resolution and enhanced by assimilation of surface and upper-air observatios.

(iv) The planetary boundary layer description used a modified version of Blackadar (1979) scheme (Zhang and Anthes 1982; Zhang and Fritsch 1986) parameterization. Other physical parameterizations included Betts and Miller (1993) cumulus parameterization, simple-ice explicit moisture scheme and cloud-radiation scheme, while for soil parameterization a multi-layer soil temperature model was used (Dudhia 1996).

2) Genoa lee cyclogenesis (Chapter 6):

(i) A triple-nested domains of 190x190/181x181/181x181 points were chosen, with the primary domain centered at 10.0E and 50.0N, with 35 vertical levels and 22.5/7.5/2.5 km horizontal resolution.

(ii) Simulations were initialized on 00 UTC 06 Nov 1999 and run for the 72 hour period.

(iii) Initial and boundary conditions were provided from the MAP reanalysis project of ECMWF, at T511 horizontal resolution (~40 km), with a 6-hourly coupling interval, including sea surface temperature. They were horizontally interpolated to the model resolution.

(iv) The planetary boundary layer description used Hong-Pan scheme (Hong and Pan 1996) parameterization. Other physical parameterizations included "Kain-Fritsch 2" cumulus parameterization (Kain and Fritsch 1993; Kain 2002), a modified version of mixed-phase explicit moisture scheme "Raisner 2" (after Reisner et al. 1998) and a cloud-radiation scheme, while for soil parameterization choice of options included a multi-layer soil temperature model (Dudhia 1996).

4. Sensitivity of cyclogenesis in the lee of the Atlas mountains to the upper-level dynamical factors

In Chapter 2, it was shown that most of the cyclones that appear over the Adriatic are cyclones initiated in the lee of the western Mediterranean mountain ranges, such as the Alps, the Atlas, the Pyrenees and the Apennines. A detailed review of the efforts in understanding the Alpine lee cyclogenesis, including theoretical, phenomenological and numerical approaches (Chapter 1), showed that a positive upper-level potential vorticity (PV) anomaly (i.e. trough or large scale baroclinic wave) is a crucial ingredient of the Alpine lee cyclogenesis.

In order to assess the similarities and differences with the Alpine lee cyclogenesis, the second

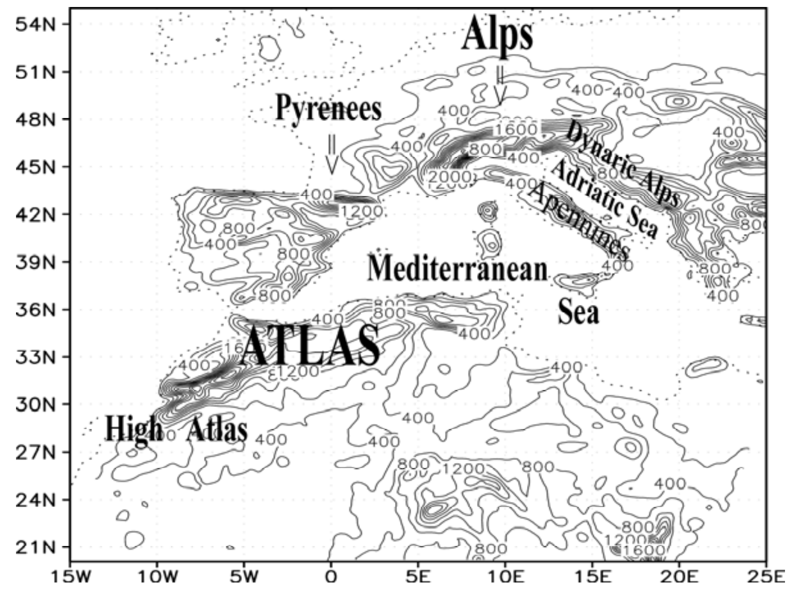

Figure 4.1*: The western Mediterranean and northwest African region with sites mentioned in the text. The area corresponds to a 24-km resolution MM5 model orography in the domain, with contours every 300 meters, starting from 300 meters.*

highest impact region of the Mediterranean lee cyclogenesis, the one in the lee of the Atlas mountains (Fig. 4.1), will be numerically analyzed. In addition to the climatological study presented in Chapter 2, it should be mentioned that cyclones originating in northwest Africa (henceforth NWA) or Saharan cyclones are well known to influence the weather in the whole Mediterranean, since half of the cyclones that enter the Mediterranean are initiated in NWA (Radinović 1987). Although some of them originate in the southern Sahara, most of them are initiated in the lee of Atlas Mountains (Pedgley 1972). Upon arrival above the Mediterranean Sea, an Atlas lee cyclone can be subjected to a strong deepening and experience considerable growth-rates values, reaching the ones associated with explosive cyclogenesis. In this way, possibly two of the most severe impact Mediterranean cyclones in the last few years were initiated in the Atlas lee (10-12 Nov 2001, 12-15 Nov 2004), this being one of the reasons for increased interest in modeling of NWA cyclogenesis (Horvath et al. 2006).

4.1 Synoptic overview and observations

Since the observational data in Sahara region is rather sparse, usually reliance is made on the ability of the model to forecast the regional weather events. For the purpose of analysis and model verification, surface analysis of the European Centre for Medium-Range Weather Forecast (ECMWF) will be used to investigate the low-level evolution of the cyclone. On the other hand, satellite pictures will be used to address the relevant upper-tropospheric circulation features.

The synoptic setting, within which the range of severe weather events over the Mediterranean area developed from 12-15 Nov 2004, followed a deep cyclogenesis initiated in the lee of Atlas mountain. The synoptic pattern at low levels was determined by a stationary Azore anticyclone producing a strong northerly winds over the eastern Atlantic and Portugal area (Fig. 4.2a). At the same time, a moderate, zonally-oriented quasi-stationary baroclinic zone over the North-African coast started to deform, creating an Atlas-sized thermal anomaly. In subsequent hours, the Azore high and associated winds near the SW Atlas edge intensified and created an orographic pressure perturbation above the target area (Fig. 4.2b). Near the SW mountain edge, a strong shear line extended deep into the lee, indicating the region of an enhanced low-level PV anomaly and an increased surface baroclinicity. In subsequent hours, a

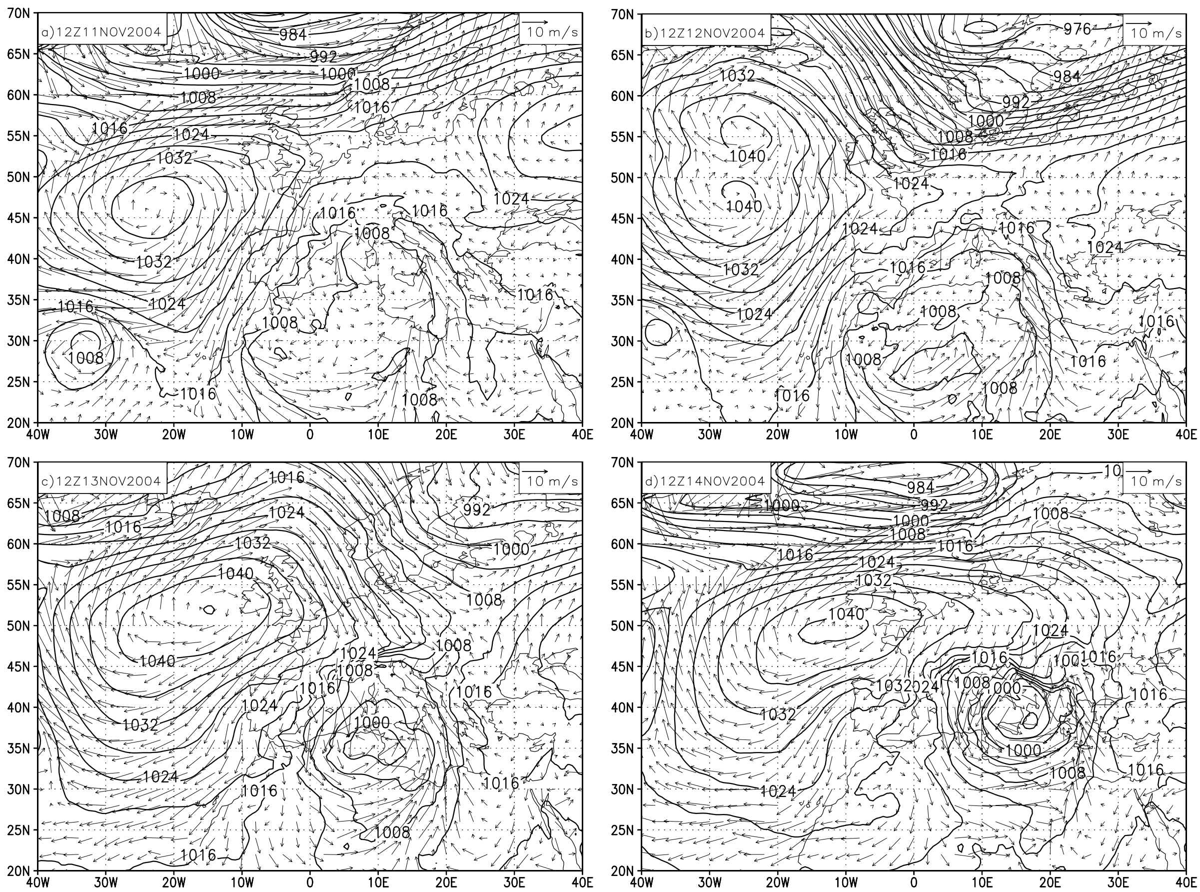

***Figure 4.2**: Surface synoptic situation, as inferred from the ECMWF analysis, showing mean sea level pressure and 10 m wind vectors over Europe and the eastern Atlantic on (a) 12 UTC 11 Nov 2004, (b) 12 UTC 12 Nov 2004, (c) 12 UTC 13 2004 and (d) 12 UTC 14 Nov 2004.*

shallow low-level vortex gradually built up moving to the north-east. On 12 UTC 13 Nov2004 (Fig. 4.2c), cyclone centre already approached the Mediterranean, where it was quickly advected eastward, continued to deepen and caused a range of severe weather events. This low-pressure centre, combined with the anticyclone, created a strong north-south pressure gradient over the Alpine and Dinaric Alpine region (Fig. 4.2d). These synoptic conditions are generally conducive for the development of Mistral and flow deflection around the eastern end of the Alps leading to severe mesoscale Bora phenomenon along the eastern Adriatic coast. Measurements showed the existence of sustained wind of 35 ms^{-1}, over 24 hour interval over a wide area of the eastern Adriatic and gusts occasionally reaching 60 ms^{-1}, what were one of the highest Bora gust values ever recorded.

The synoptic situation at upper levels is shown on the EUMETSAT water vapor imagery (Fig. 4.3), which is strongly linked to the upper-level PV distribution (e.g. Lagouvardos and

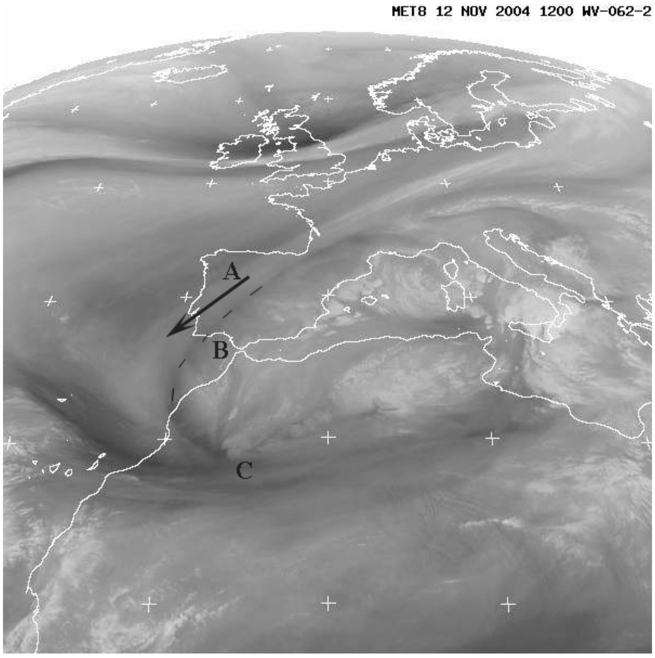

Figure 4.3*: Water-vapor 6.2 level 1.5 Meteosat MSG image on 12 UTC 12 Nov 2004 showing an upper level trough over Western Europe and North Africa. Arrow (A) denotes the upper-level jet stream, dashed line (B) the associated dark stripe and point C denotes the cyclone initiation point.*

Kotroni 1990; Mansfield 2001). Strong upper-level trough extended over the Mediterranean and Western Europe. Dark stripe on the figure indicated the subsidence area on the cyclonic part of the jet stream, identifying the area of very low water vapor content and the highest upper-level PV values. Later on, as inferred from the satellite imagery (not shown), following a southward advection to the area above Atlas Mountains, the trough was advected northeastward towards the Mediterranean region. On 14 Nov 2004, in the maturing stage of the cyclone development, a strong frontal activity can be identified over the southern Italy on the high-resolution visible spectra satellite image (not shown), indicating the existence of a heavy flood-raising precipitation that reached over 200mm/24h.

4.2 The control run

The synoptic evolution of the lee cyclone in the control simulation is shown on Figure 4.4. A deep, positively tilted trough extended over the Western and Central Europe and advected southward (Figs. 4.4a-b). The positive upper-level PV anomaly at 300 hPa level reached 14

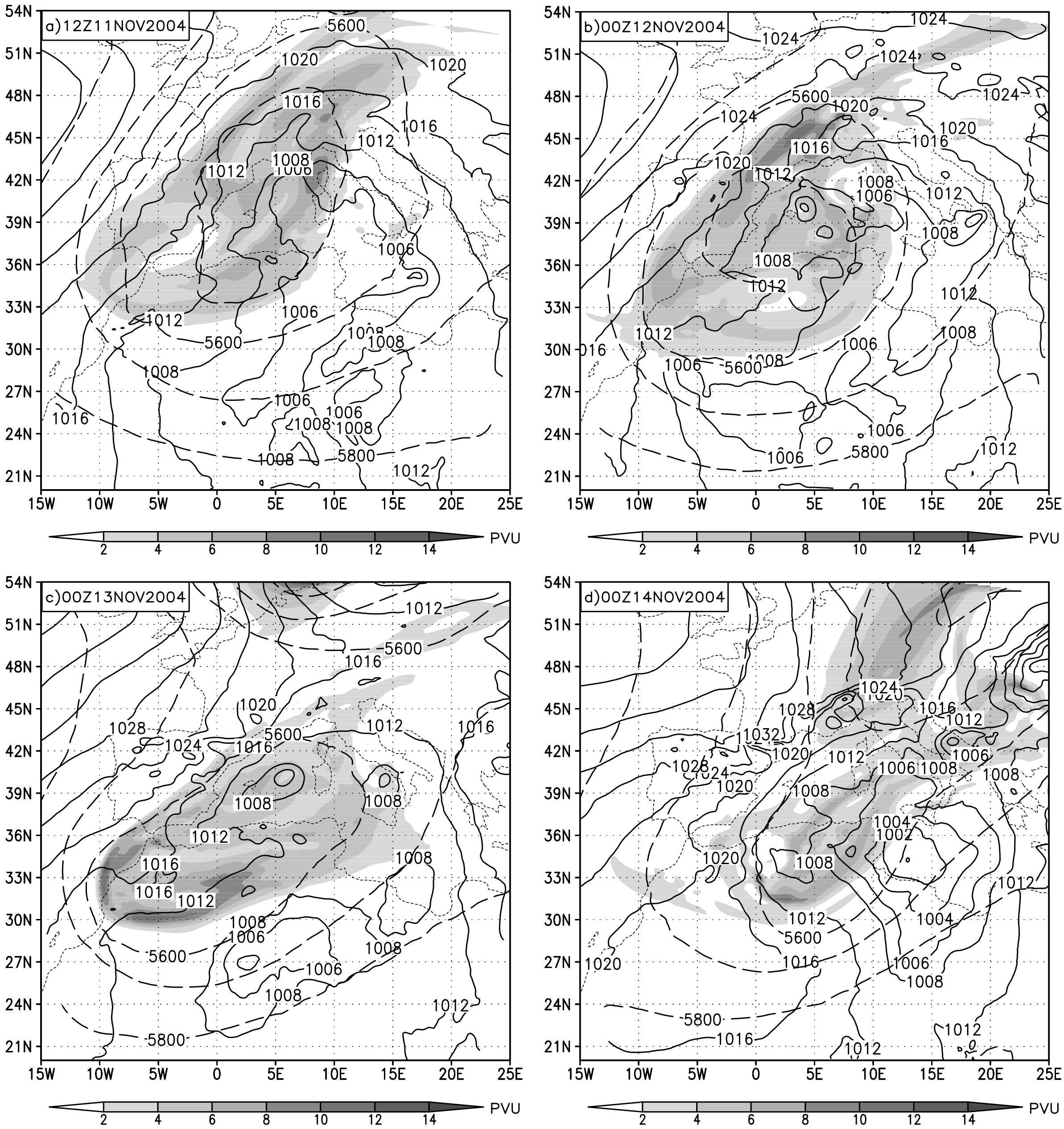

Figure 4.4: *MM5 model forecast of synoptic scale evolution on (a) 12 UTC 11 Nov 2004, (b) 00 UTC 12 Nov 2004, (c) 00 UTC 13 Nov 2004 and (d) 00 UTC 14 Nov 2004. Mean seal level pressure contours are plotted in continuous line with 4 hPa above 1008 hPa and 2 hPa below 1008 hPa values. Upper-level PV values at 300 hPa are shaded (white under 2 PVU black over 14 PVU), while geopotential at 500 hPa is plotted in dashed (every 100 gpm).*

PVU at the time it was advected over the Atlas region (Fig. 4.4c). This cut-off low induced a closed upper-air circulation ("cut-off") as indicated by geopotential height distribution. While the trough approached the mountain range, a surface cyclone was initiated in the lee. In subsequent hours, the system coupled and advected towards the Mediterranean. The intensity of the cyclone in this phase of the lifecycle was somewhat underestimated, as inferred from the ECMWF analysis (cf. Fig. 4.2). Towards the mature stage of cyclone development in the end of the analysed period (Fig. 4.4d), which is approximately the time when cyclone left the lee and entered the Mediterranean (00 UTC 14 Nov 2004), the upper-level PV anomaly weakened, probably at the expense of interaction with the low-level vortex as well as upper-level dissipation processes, due to strong diabatic effects associated with cloudiness and developing convection. The axis of the lee cyclone had a slightly negative tilt that tended to get more neutral with time. All of the aforementioned facts agree with the Pettersen and Smebye (1979) cyclone type B, and are in close resemblance with the typical lee cyclogenesis synoptic features.

The mesoscale analysis of the lower troposphere conditions in the control simulation reveals that strong northerly winds together with thermal properties of the north-African land created an Atlas-sized thermal anomaly already on 10 Nov 2004, far prior to the cyclogenesis. However, soon upon its creation, cold air crossed the lower NE part of the Atlas range and reduced the thermal anomaly to the lee of High Atlas Mountains (Fig. 4.5a). Alongside with high surface heat flux impact in the arid mountain lee (model simulation value reaching 400 Wm^{-2}), this situation led to a creation of a more localized warm thermal anomaly and associated depression in the lee of High Atlas Mountains. A strong shear line existed on 00 UTC 12 Nov 2004 as primary orographic PV banner of a considerable horizontal distance starting over the SW Atlas edge and overcoming 2.5 PVU in intensity (Fig. 4.5b). At the same time, two frontal low-level PV sources were present: the first one corresponding to the front that crossed the central and northern parts of Atlas and the second one more to the east. In this period and subsequent hours, the very cyclone centre was located in a small quasi-barotropic zone and an area of enhanced low-level PV.

During the 12 Nov 2004, the cyclone moved northward towards the Mediterranean area and low-level PV banners weakened. On 00 UTC 13 Nov 2004 (Fig. 4.5c), primary orographic PV banner merged with the frontal one and formed a continuous source of enhanced low-level PV away from the mountain. At the time, cyclone centre attached to the frontal baroclinic zone and remained so until the end of the analysed period. Orographically induced PV banner seemed to feed the low-level cyclone, resembling some of the documented cases of Alpine lee cyclogenesis (Aebischer and Schär 1998). On 00 UTC 14 Nov 2004, the last time-sequence of the analysis, roughly corresponding to the time the cyclone left the lee and entered the maritime area, the cyclone centre reached 1000 hPa depth, characterised with a well defined frontal structure (Fig. 4.5d). Despite of the fact that differences between model simulations and ECMWF analysis reveal that model simulation of the investigated process was of somewhat limited quality, its features were captured well enough to make the case appropriate for the sensitivity study and deduction of factor contributions to the event.

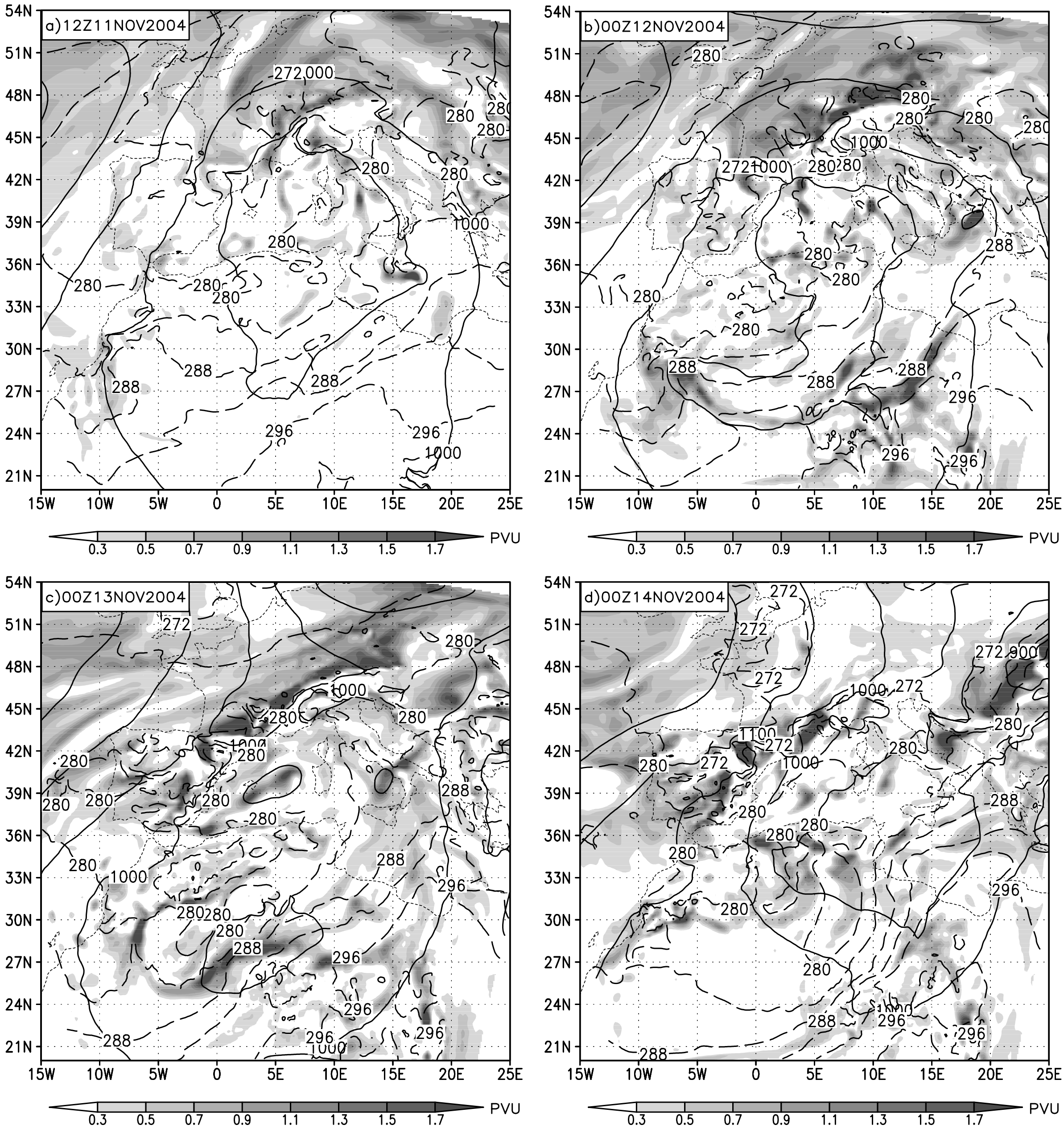

***Figure 4.5**: MM5 model forecast of low-level conditions at 925 hPa on (a) 12 UTC 11 Nov 2004, (b) 00 UTC 12 Nov 2004, (c) 00 UTC 13 Nov 2004 and (d) 00 UTC 14 Nov 2004. Low-level PV is shaded (white under 0.3 PVU and black over 1.7 PVU). Geopotential is in continuous line (every 50 gmp), while temperature is in dashed (every 4 K).*

4.3 Sensitivity experiments

4.3.1 Macroscale sensitivity

Previously, a positive upper-level PV anomaly, orography and surface sensible heat flux (SSHF) were identified as main factors affecting the 12-15 Nov 2004 cyclogenesis event. Here, the contributions of the investigated factors to the mean sea level pressure and cyclone centre position will be addressed qualitatively, with a special emphasis on the influence of the upper-level trough and its interactions with other factors.

As mentioned in Section 3.2, for the purpose of separating mutual interactions among the three investigated factors, 8 simulations had to be done (simulations reflecting the influence of SSHF and its interaction with orography will be discussed here only briefly, refer to Horvath et al. 2006 for more details). Thus, to address the orographic contribution to the process, Atlas Mountain was subtracted from the terrain field. Secondly, the surface sensible heat flux (SSHF) was withheld in a series of simulations, allowing for determination of the

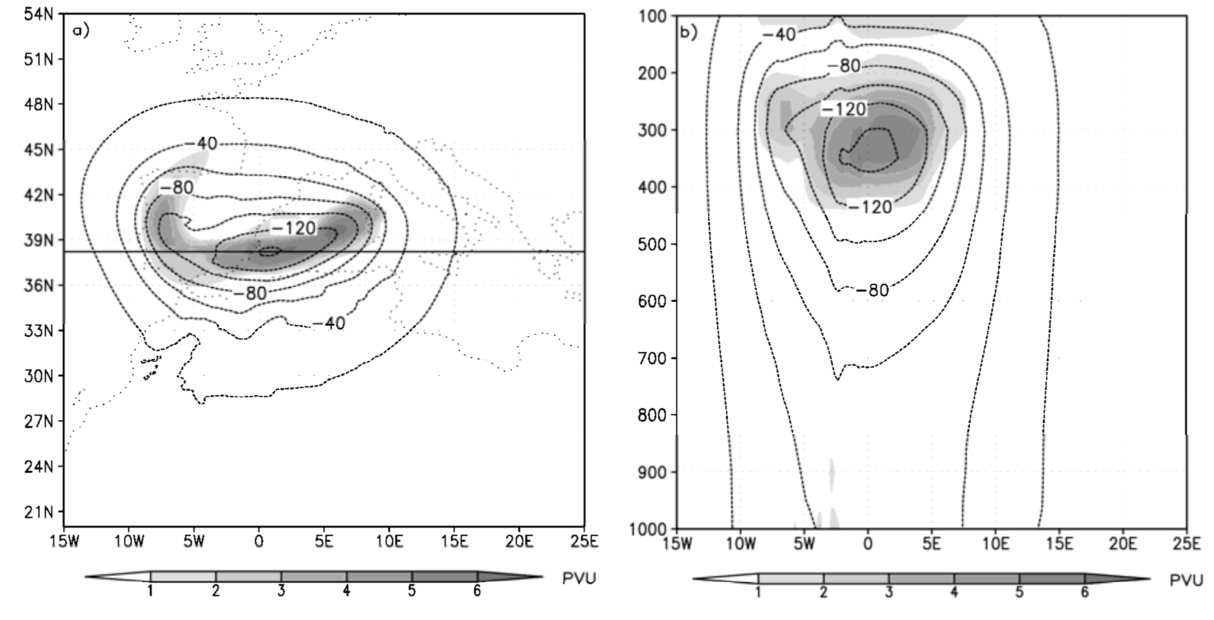

Figure 4.6: *Upper-level PV perturbation at 300 hPa subtracted from the initial conditions on 00 UTC 11 Nov 2004, the model simulations starting time (a) in horizontal (solid line denotes the position of the vertical cross-section through the perturbation) (b) in vertical. The associated geopotential perturbations at the 300 hPa level and in vertical cross-section are superimposed (dashed).*

influence of associated surface forcing. Finally, the upper-level PV anomaly was subtracted from the initial conditions to address the role of upper-level dynamical processes in the cyclogenesis. The PV inversion was performed at the control simulation starting time using the initial conditions in isobaric co-ordinates on the outermost model domain resolution and domain. The PV anomaly was defined as the departure from the 10-day time average (centred on 00 UTC 12 Nov 2004) PV field between 500 hPa and 100 hPa levels. However, in simulation with upper-level PV anomaly subtracted from the initial conditions, cyclone was excessively changed, both in intensity and in path. Thus, in order to keep the similarity with the real case, the PV perturbation used for the sensitivity study addressed only part of the total PV anomaly (Figs. 4.6a-b). This resulted in the upper-level PV anomaly that e.g. on 06 UTC 12 Nov 2004 reached 8 PVU, compared to the almost 14 PVU associated with of the original upper-level PV anomaly. This should be kept in mind when considering the quantitative contributions of the upper-level PV perturbation as well as its interactions with other investigated factors.

4.3.1.1 Contributions to cyclone deepening

Figure 4.7 presents the time evolution of the factor contributions to the mean sea level pressure value illustrating the dominance of different processes at different stages of cyclone development. The analysis focused on the period starting from 00 UTC 12 Nov 2004 (24 hours after the simulation started) what is the approximate time of cyclogenesis commencement in the simulation.

The first pronounced cyclogenetic influence was an orographic one, starting around 00 UTC 12 Nov 2004, cumulatively exerting 5 hPa deepening on the cyclone. This influence was associated with a frontal retardation and creation of the thermal and low-level PV anomalies in the lee of High Atlas that were not present in the simulations without orography. At that time and in subsequent hours, the cyclone centre was mostly attached to the quasi-barotropic lee area, marking the first phase of lee cyclogenesis. On 06 UTC 13 Nov 2004, orographic influence first diminished, and then became strongly cyclolytic (destruction of cyclone). This type of duality of orographic influence was already noticed in a study of Alpine cyclogenesis by Alpert et al. (1996) and was probably due to cyclone movement out the favorable lee area. Similar results were achieved in Tsidulko and Alpert (2001), although cyclogenetic influence

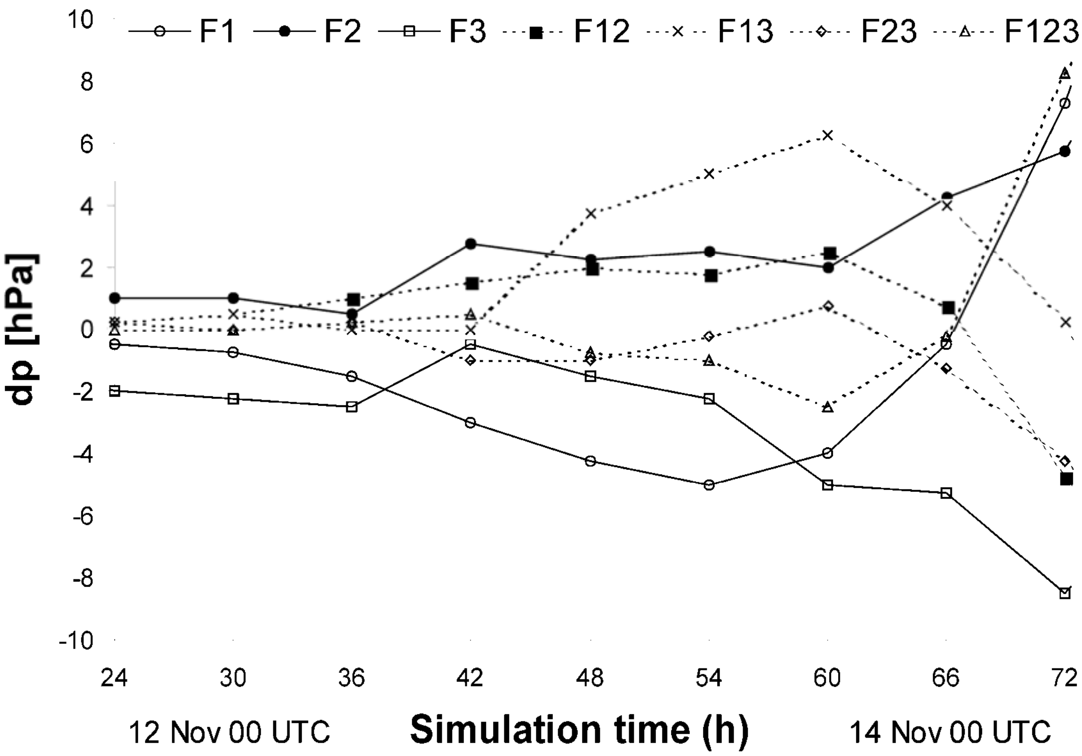

Figure 4.7: *The 48-hour time evolution for 7 local contributions to the cyclone deepening (hPa), after 24 hours of simulation. F1, F2 and F3 are influences of orography, surface sensible heat flux and upper-level PV perturbation (half of total PV anomaly, cf. Fig. 4.6), respectively and are plotted in continuous line. Other interactions are plotted in dashed line (e.g. F13 denotes the influence of the interaction between orography and upper-level PV perturbation).*

of orography in their analysis does not seem to be as intensive as in this study.

The upper-level PV perturbation started to contribute to cyclogenesis at the time its strongest core advected over the Atlas lee (cf. Fig. 4.4) on 18 UTC 12 Nov 2004. Its influence in subsequent period was associated with a reduced stability of the troposphere and a creation of a slightly stronger thermal anomaly at the surface (inclusion of the upper-level PV cooled the surface air impinging on the Atlas). Furthermore, stronger PV advection at upper levels induced greater low-level vertical velocities (e.g. in accordance with quasi-geostrophic omega equation, see e.g. Holton 1972) and stronger low-level convergence, resulting in a more intense low-level vortex development. In other words, cyclonic circulation of the upper-level PV perturbation propagated vertically (downward) to the middle and lower troposphere.

However, as later analysis is going to show, the difference between speed of advection in simulations that define the upper-level PV perturbation influence (f_0 and f_3, refer to Section 3.1) indicated that the part of its strong cyclogenetic influence in the end of the analysed period was partially related to moist processes over the Mediterranean Sea.

The influence of the interaction between orography and upper-level dynamical factors was clearly cyclolytic during the 18-hour period, starting from 18 UTC 12 Nov 2004. It will be shown later in the analysis of cyclone paths (cf. Fig. 4.8), that it seems to be connected to cyclone destruction on the orographical obstacle on the way to the Tunisia area. Afterwards, on 12 UTC 13 Nov 2004 and subsequent hours, the interaction contributed to the cyclone recovery. At that time lower and upper-level vortices were tilted to the favorable western direction with height. Rough estimates of geopotential at 300 hPa and mean sea level fields on 12 UTC 13 Nov 2004 yielded a horizontal dimension of the upper-level trough wave of L=60° (~666 km), and a separation of the centers close to 0.15*L (~100 km). If these numbers were applied to the idealized conceptual models of low-level–upper-level vortex interaction or linear instability theory (Bretherton 1966; Hoskins et al. 1985), the surface and upper-level waves would tend to hold themselves against the zonal flow (i.e. against differential advection), growing and reinforcing each other. This qualitative consideration seems to be roughly applicable at the end of the analyzed period, when the low-level and upper-level centers tended to be almost locked in phase (cf. Fig. 4.4).

The most prominent influence of the SSHF is the afternoon cyclolysis, which primarily appears to be due to increased mixing of the baroclinic zone (for the influence of latent heat flux and its interaction with the orography as well as additional numerical experiments reflecting the influence of the surface lee side thermal anomaly see Horvath et al. 2006). Furthermore, it has been observed that inclusion of the SSHF in simulations strengthens the upper-level PV perturbation. This is in qualitative agreement with the cyclogenetic interaction that SSHF and upper-level PV perturbation seemed to show in the afternoons. An interaction between SSHF and orography as well as the triple-interaction among the investigated factors did not exert a significant impact on the cyclone centre deepening, except in the very end of the analyzed period. The corresponding results at that time instant should be interpreted with care, because of the cyclone centre spread in the end of simulations. Namely, in some simulations cyclone centers entered the Mediterranean, while in others still stayed on the continent. In this way, it is possible that moisture processes could have influenced the results

Table 4.1: *Comparison of prominent features of the 12-15 Nov 2004 cyclogenesis to the lee of the Atlas mountain with the common features of Alpine lee cyclogenesis.*

	Alps	**Atlas Nov 2004 event**
Necessary existence of a primary cyclone	Yes	No
Thermal anomaly creation	Transient	Quasi-permanent + Transient
2 phases of dynamical development	Yes	Yes
Necessary existence of an upper-level trough	Yes	Yes
The highest deepening rates	Initiation phase	Mature phase (a probable influence of moisture from the Med. sea)

significantly in the mature stage of cyclone development at the very end of the analyzed period.

The differences and similarities in the synoptic features and deepening process in cases of cyclogenesis to the Alpine (with the use of references, e.g. see Chapter 1) and Atlas lee (inferred from the analysis of the investigated 12-15 Nov 2004 event) are summarized in Table 4.1. Since any generalization is incomplete if done on the basis of analysis of a single case, the related list (Table 4.1) should not be interpreted as a general rule. The clear existence of an orographic influence in the first stage and an upper-level trough influence in the latter stage of cyclone deepening suggested the dynamical resemblance of Alpine and Atlas lee cyclogenesis, though the deepening rates in the first phase of cyclone initiation to the lee of Atlas were lower then in a typical case of Alpine lee cyclogenesis. Besides this issue, the main difference seems to be the creation of the thermal anomaly in the lee of the mountain ranges. In the Alpine lee, thermal anomaly is a transient feature arising primarily due to existence of the “parent” cyclone and cold front retardation on the mountain. In the Atlas lee, thermal anomaly was not associated with a “parent” cyclone, but rather with Azores high, which was responsible for the sustained northwesterly winds over the Atlas mountains and creation of the localized thermal anomaly in the lee of the High Atlas mountains. In addition, the north

Saharan thermal properties supported the creation of the thermal anomaly which extended over the broad Atlas lee.

4.3.1.2 The analysis of cyclone paths

Analysis of cyclone centre paths in the simulations is shown on Figure 4.8. A cyclone centre path for simulation with total the upper-level PV anomaly subtracted from the initial conditions is added to the picture. Considering the latter first, it can be seen that without the upper-level PV anomaly in the initial conditions the cyclone initiation point and movement were excessively changed. The shallow cyclone was indeed formed in the vicinity of Ahaggar mountain (cf. Fig. 4.1), due to a weak advection of the upper-level PV from the boundary conditions over that area. Thus, the analysis suggests that a strong positive upper-level PV advection is crucial for the cyclogenesis to occur in the lee of the Atlas. The influence of orography on cyclone paths was clearly resolved - four of the closest cyclone paths to the Atlas range corresponded to four simulations with orography included. Therefore, in the first

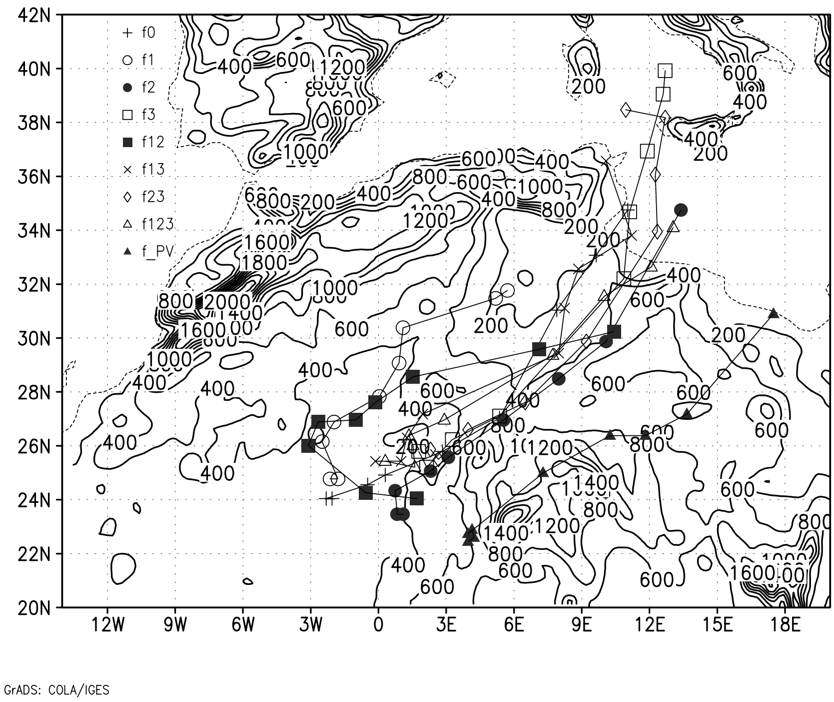

Figure 4.8*: Time evolution of the cyclone centers in nine simulations, starting from 00 UTC 12 Nov 2004, plotted every 6 hours. f_0 is the simulation with all three investigated factors withheld, and f_PV is the simulation with total upper-level PV anomaly subtracted from the IC (refer to text). Other simulation denotations are described in text (Section 3.1).*

place orography tended to move the location of cyclone initiation to the favourable lee area where orographically induced low-level PV and thermal anomalies were the strongest. The preference of movement closer to the mountain is kept until the cyclones reached the Mediterranean Sea. In contrast, the inclusion of upper-level PV perturbation moved the position of the cyclone formation away from the mountain. It seems that stability of the lower atmosphere on the windward side of the Atlas played an important role in localising the formation place. Namely, in simulations with the upper-level PV perturbation included, the lower atmosphere was less stable underneath. A closer look reveals that in those simulations cold air parcels on the windward side were able to cross the mountain slightly more efficiently and moved the thermal anomaly southeastward. Adversely, in simulations without the upper-level PV perturbation, low-level stability was stronger and the air was forced to go around the obstacle, creating a thermal anomaly deeper inside the mountain lee. Considerable differences of cyclone paths in simulations with variable intensity of upper-level PV anomaly indicated that upper-level dynamical factors have a potential to control the tracks of cyclones initiated in the Atlas lee on their way towards the Mediterranean Sea.

Inspection of the cyclone path in the simulation with the orography and the upper-level PV perturbation included showed that the cyclone ran into the orographical obstacle on the way to Mediterranean Sea. The associated effective landrise cyclone traversed was almost 500 m, and has not been experienced in the other simulations of interest (F_0, F_1 and F_3, refer to Section 3.1) to such an extent. Hence, this unique cyclone path and cyclone destruction over the hill could have been the reasons for the strong cyclolytic influence the analysed interaction tended to produce. This idea qualitatively resembles the studies on tropical cyclones passing over island terrain (e.g. Bender et al. 1987) that reported a strong cyclone filling as the cyclone passes the land disturbance. However, cyclolytic influence lasted for 18 hours and it is not clear whether this type of orographic influence could be held responsible for the cyclolysis during the whole period.

Significant differences were noted in time instances when the cyclone reached the Mediterranean Sea. The two slowest cyclones were attached to orographically dominated simulations (F_1, F_{12}), while the two fastest, to the upper-level PV perturbation (F_3, F_{23}). As expected, the sensible heat flux did not have a significant impact on the cyclone track variability. The aforementioned strong dependency indicates that orographic influence was to keep the cyclone in the mountain lee, while the upper-level PV perturbation induced a faster advection of the low-level pressure system to the Mediterranean Sea.

4.3.2 Mesoscale sensitivity

In this section, the numerical analysis on the sensitivity of the deep and severe impact 12-15 Nov 2004 Mediterranean cyclone initiated in the lee side of the Atlas Mountains to the exact details of the upper-level PV anomaly will be presented. Namely, though the apparent predictability of some cases of cyclones on the lee side of the Atlas Mountains suggested a controlling role by large-scale forcing, closer examination revealed that significant mesoscale development led to actual weather pattern (Tripoli et al. 2005). Therefore, it might be possible that a part of the predictability of the 12-15 Nov 2004 cyclone in the lee side of Atlas Mountains is determined by the exact mesoscale details of the upper-level circulations, rather then large-scale features of the trough itself. In addition, it was recently shown that small

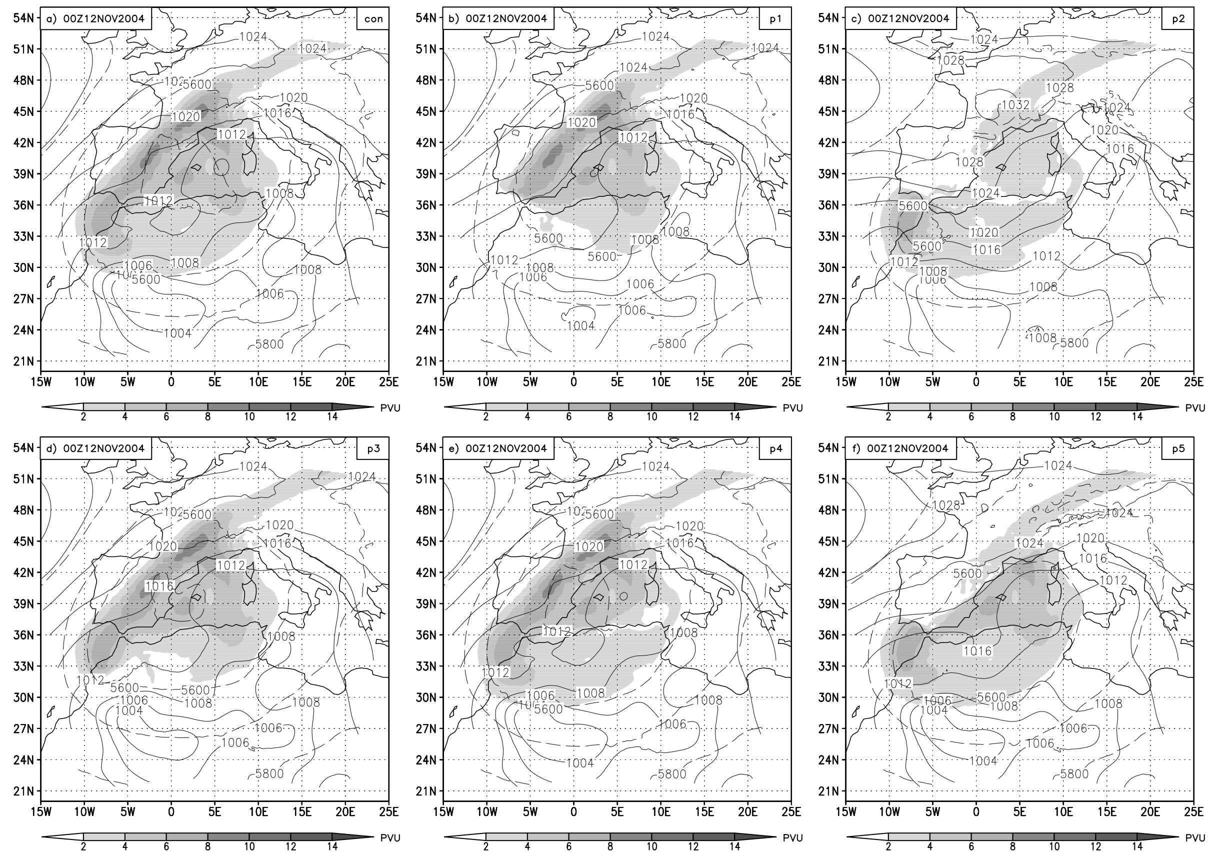

Figure 4.9*: Ensemble of initial conditions on 00 UTC 12 Nov 2004 showing mean sea level pressure (solid), 300 hPa PV (shaded) and 500 hPa geopotential (dashed) in (a) Control simulation. (b-f) Experiments p1, p2, p3, p4 and p5, respectively.*

(<200 km) and medium (<2000 km) scales of motion (Tan et al. 2004; Zhang et al. 2007) are more sensitive to initialization errors and can strongly influence forecast error growth. Motivated by these facts, this study is designed in order to assess the sensitivity of the mesoscale forecast to the intensity of mesoscale PV anomalies.

The subtraction of the upper-level mesoscale PV anomalies from initial conditions was performed with the same technique as for macroscale sensitivity (see Sections 3.2 and 4.3.1 or Horvath and Ivančan-Picek 2008), except that inversion was done on 00 UTC 12 Nov 2004, which was the starting time of mesoscale simulations in order to increase the model accuracy in the mature dissipation of the event (14 Nov 2004). Within the total PV anomaly, individual PV cores of interest (mesoscale regions of local PV maximum within the trough, also referred to as mesoscale PV anomalies or mesoscale upper-level circulations), arbitrary in a sense that neither their magnitude nor scale necessarily fit the initial-analysis errors, were selected and inverted at the simulation starting time. After the initialization (including removal of the integrated mean divergence), this procedure resulted in the formation of an arbitrary six-member ensemble of initial conditions (Figs. 4.9a-f).

4.3.2.1 Contributions to cyclone deepening

It was shown earlier that the initial phase of the cyclone formation was associated with moderate deepening rates, reaching no more than 5 hPa over the land of the NWA, due to a mixture of both cyclogenetic and cyclolytic effects. The cyclogenetic influence primarily included orographic influence on the cyclone formation as well as positive upper-level PV advection, while the cyclolytic influence appeared to be due to weakening of the cyclone by deflection on the local orography (Section 4.3.1). Among the mesoscale simulations, the cyclone was the deepest in the control run, while there appears to be no cyclone deepening in the experiment with the greatest upper- level PV modification p2 (Fig. 4.10). However, the horizontal scale of this modification is much greater than in the other sensitivity simulations, and it might be considered excessive.

The overall strength of the jet streak is well correlated with the low pressure intensity in the baroclinic phase of cyclone development over the land. As discussed above, this phase of development resembled qualitative considerations of quasi-adiabatic low-level-upper-level

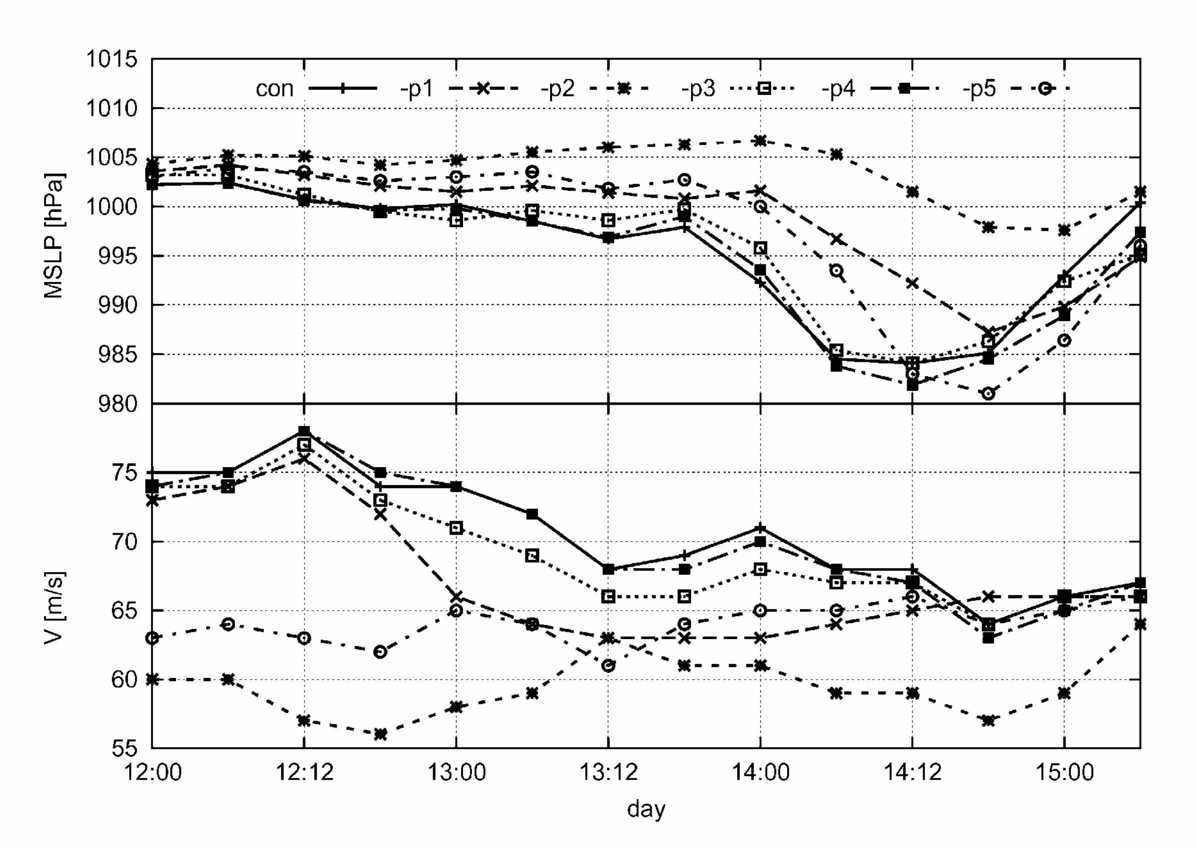

Figure 4.10*: Time-series of the mean sea level pressure values in the cyclone centers (upper row) and jet streak intensities (lower row) in the whole ensemble of simulations. See Fig. 4.9 for experiment denotations.*

vortex interaction (with vortices almost locked in phase) and linear instability theory. During this stage, the spread of cyclone intensities is the greatest just prior to the moment when the deeper cyclones (p3, p4), moving closer to the Atlas lee, impinged, deflected and weakened on the NE part of the range (18 UTC 13 Nov 2004). It should be noted that the cyclone was highly sensitive to the strongest mesoscale PV anomalies (excluding experiment p2), isolated in experiments p1 and p5. The cyclone intensity in these simulations (approx. 25% of the cyclone in the control simulation), implied the high cyclone sensitivity to the most active mesoscale circulations of the upper-level precursor. Upon reaching the Mediterranean Sea, the cyclones strongly deepened and moved towards the Ionian and southern Adriatic seas. At this stage of development, the absolute spread of cyclone depths was the greatest in the whole lifecycle, most likely due to the different advection speeds towards the Mediterranean (cf. Fig. 4.11). On 12 UTC 14 Nov 2004 the weakest cyclone is the one with the greatest jet stream modification (p2), reaching 1002 hPa, while the rest of the ensemble members reached 982-992 hPa, with no significant spread in jet streak (or PV) intensity. It will be shown that for the least intensive cyclone, besides the weaker influence of upper-level dynamical factors, this appears to be due to different cyclone tracks and slower cyclone advection towards the Mediterranean. Related with the above, it should be noted that at the stage of cyclone development over the sea, cyclogenesis might be strongly enhanced by latent heat flux from the sea, which can synergistically couple with the upper-level dynamical factors. This being beyond the current stage of analysis, nevertheless might have reflected through a hidden interaction in this non-linear system. Finally, in the dissipation phase the cyclone intensities become more uniform, what appears to be associated with the cyclolysis in the final stage of the cyclone lifecycle.

4.3.2.2 The analysis of cyclone paths

In the initial phase of the cyclone development, the cyclone track diffluence in the ensemble of simulations showed quasi-linear propagation with time (Fig. 4.11). The farthermost tracks (from the control run) were the ones with the greatest upper-level PV modifications (p2, p5). This appears to be due to the fact that in those simulations the low-level vortex was

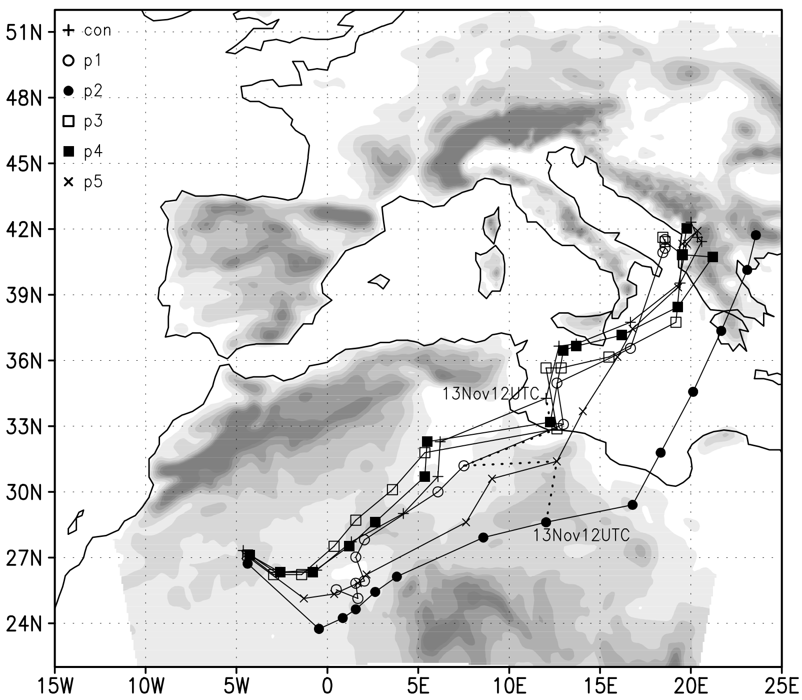

***Figure 4.11**: The spread of cyclone tracks in the ensemble of simulations during 00 UTC 12 Nov 2004 – 00 UTC 15 Nov 2004 (solid) and position of cyclone centers on 12 UTC 13 Nov 2004 (dashed).*

developing not in the very lee, but rather farther to southeast and away from the mountain, in the broad scale warm anomaly of Saharan origin. This resembles the earlier experiment with the total PV anomaly subtracted from the initial conditions, suggesting the crucial role of the mesoscale dynamical circulations in determination of the exact cyclone track.

As the cyclone moved towards the Mediterranean Sea, the cyclone track diffluence reached its overall maximum. In addition, at that time the cyclone tracks closer to the Atlas Mountains were deflected to the northeast near the NE tip of the range, apparently reducing the spread of cyclone centre positions. This type of orographic influence was recently studied through identification of the control parameters (e.g. vortex Froude number) for diagnosing track deflections and continuity for tropical cyclones traversing Taiwan (Lin et al. 2005). Though these were not tested here, it might be possible that similar control parameters exist for extra-tropical cyclones impinging on mid-latitude mountain ranges.

Once cyclones reached the Mediterranean and strongly deepened, the cyclone tracks became confluent. This appears to be associated with the orography of the southern Italy (Sicily and Calabria) and southwestern part of the Balkan peninsula, that seem to encompassed a marine zone of track confluence for cyclones that moved towards the southern Adriatic area. In addition to the track deflection on the aforementioned mountain ranges, surface fluxes from the sea, documented to have a partial control of the lee cyclone tracks over the sea (e.g. Alpert et al. 1996), might have contributed to the selection of the preferred cyclone track during the mature phase of cyclone development. Finally, a cyclone dissipation phase was characterized with quasi-stationary cyclone positions over the Balkan peninsula in most of the ensemble members. However, in some simulations cyclones were deflected towards the northern Adriatic by the Dinaric Alps, thus increasing the spread of the cyclone centre positions.

Therefore, it seems that besides steering from the upper-levels, the Mediterranean mountain ranges played a crucial role in determining the cyclone track and movement. Therefore, the strong orographic control of Mediterranean cyclones appears obvious throughout their lifecycles.

5. Statistics of the initial-analysis potential vorticity error

In Chapters 2 and 4, it was shown that the upper-level dynamical factors are a crucial ingredient for both Alpine and Atlas lee cyclogenesis and that these phenomena are strongly sensitive to the arbitrary macroscale and mesoscale modifications in the upper-level trough intensity. However, the issue of predictability can not be assessed with such arbitrarily defined perturbations to the initial conditions. In order tackle this matter, such modifications to the initial conditions need to be defined, which reflect, at least statistically, the realistic initial-analysis error.

In this chapter, it is aimed at assessing the initial-analysis errors in the upper-level dynamical factors with the use of the operational analysis of European Centre for Medium-Range Weather Forecast (ECMWF) and National Centers for Environmental Prediction (NCEP). The overall idea is that the differences between Ertel's potential vorticity (PV) fields in the two global reanalysis can serve as a proxy for estimating the model errors in the upper-level precursor, both in amplitude (intensity) and in phase (displacement). The strategy to calculate the error statistics is as follows:

1. select 21 case of the deepest Mediterranean storms using the results of the Mediterranean Experiment – MedEx (http://medex.inm.uib.es/) project
2. interpolate both reanalysis sources (ECMWF, NCEP) to the same grid resolution of 22.5 km in horizontal and 11 vertical levels throughout the troposphere
3. calculate Ertel's PV for each analysis in each time instant available during the lifecycle of each event
4. in each time instant and at each level, compare the fields and deduce the phase error by maximizing the correlation between fields in a given area; the calculation was not done on the whole domain, but on a grid subset of 20x20 points (which is an estimate

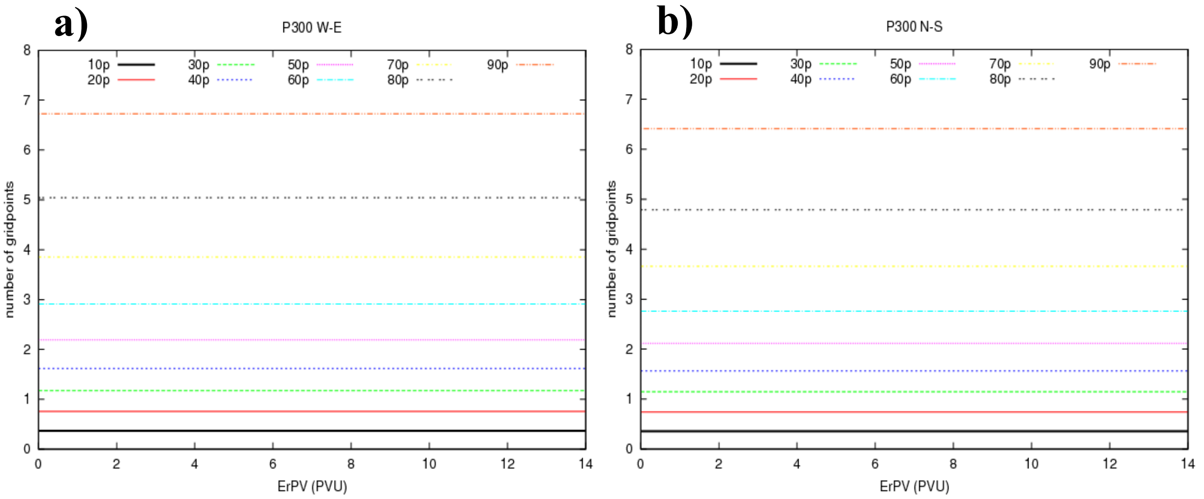

Figure 5.1*: Phase (displacement) errors at 300 hPa, shown in percentiles for errors in (a) west-east direction and (b) north-south direction.*

of the dimensions of mesoscale cores of Ertel's PV within the trough), surrounding each grid point of the calculation domain

5. calculate the phase error statistics by using phase errors for all grid points
6. remove the phase error for each point by moving one field (20x20 grid points) with respect to the other so that the maximal correlation is achieved
7. compare the new fields after removal of the phase errors and calculate the amplitude error statistics from the pairs of Ertel's PV (ECMWF, NCEP) values for each grid point.

Therefore, due to the procedure, the statistics might be viewed as the error statistics on the mesoscale i.e. for mesoscale Ertel's PV dynamical cores. The results of the error statistics in phase (displacement) and amplitude (intensity), calculated at 11 levels throughout the troposphere, are presented at 300 hPa, the level representative for upper-level dynamical factors. Phase error statistics, calculated as insensitive to the PV intensity, was similar in west-east and north-south directions (Figs. 5.1a-b). Average phase errors (i.e. 50th percentile) yielded somewhat less than 50 km, while the extreme errors (as indicated by 90th percentile) equaled close to 150 km. On the other hand, amplitude errors were calculated depending on the Ertel's PV values and classified in bins (Figs. 5.2a-b), expressed in terms of the percentage of average value of the Ertel's PV from both operational analysis centers. For the 50th percentile at 300 hPa level, values of amplitude errors range from 21% for Ertel's PV equaling 1 PVU to 9% for Ertel's PV equaling 7 PVU. On the extreme case of the 90th

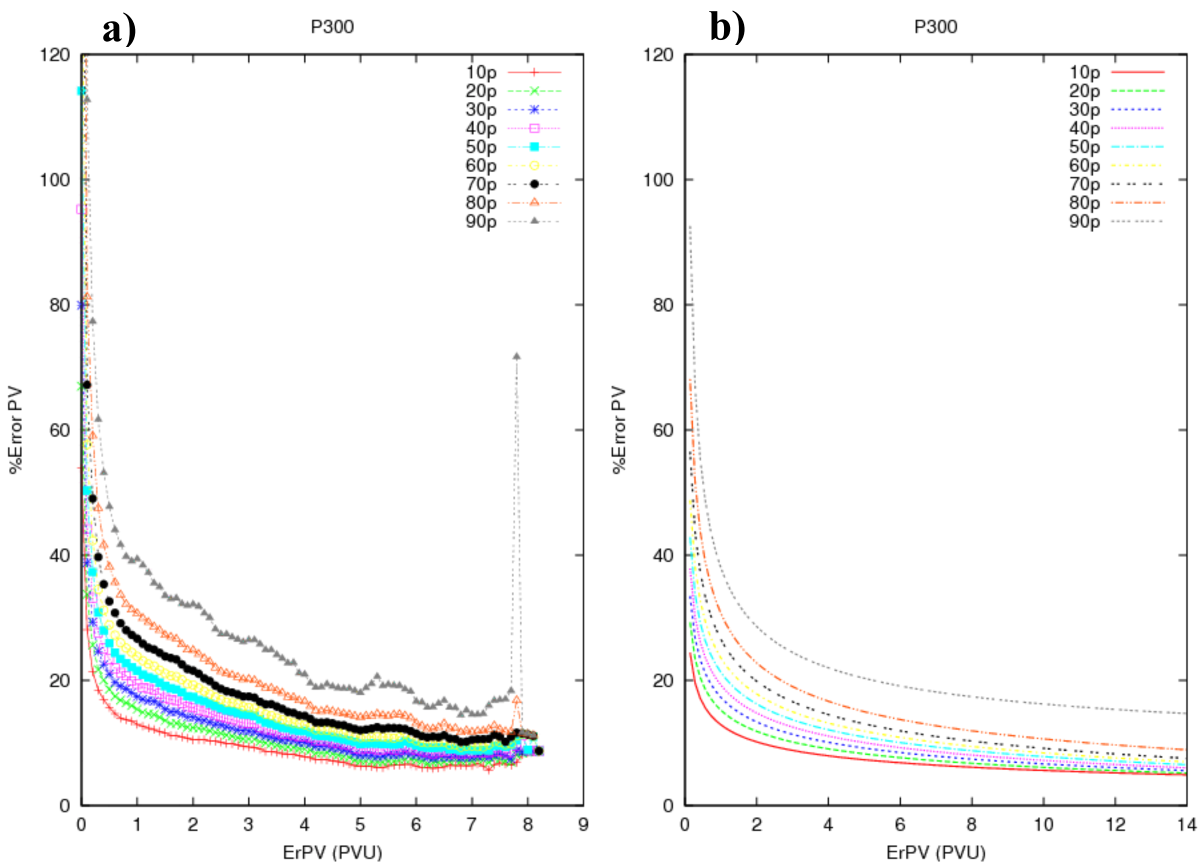

Figure 5.2: *Amplitude (intensity) errors at 300 hPa, shown in percentiles for (a) real data and (b) least squares fit. The single-peak value at 7.8 PVU on real data dependency (left) results from a small number of members in the associated bin, which affected the percentile calculation.*

percentile, values range from 40% and 15% respectively.

The fitted observed relationships might be used for point-to-point modification of the initial Ertel's PV values depending on their intensity. In this way, an ensemble of initial conditions could be made with an estimate of uncertainty in Ertel's PV field throughout the troposphere and tested for ensemble numerical weather prediction system. Here, however, the analysis will study the influence of initial uncertainties in the upper-level trough only, thus exploring the sensitivity of the lee cyclogenesis to the initial-analysis uncertainties in the upper-level dynamical factors.

6. Sensitivity of the Genoa lee cyclone to initial-analysis errors in the upper-level dynamical factors

It was shown that prediction of the intensity and track of western Mediterranean lee cyclones (the most prominent being the Alpine and Atlas lee cyclones) highly depends on both macroscale and mesoscale characteristics of the upper-level trough. Therefore, the following questions arise: what is the sensitivity of the lee cyclones in the region to the initial errors in the upper-level trough? To what extent are the lee cyclones and the associated phenomena (e.g. cyclonic Bora) sensitive to initial-analysis errors in the upper-level potential vorticity (PV) field? In other words, what is the predictability of Mediterranean lee cyclones and cyclonic Bora in the Adriatic with respect to initial uncertainties in the intensity and position of the upper-level dynamical factors?

The lee cyclogenesis event chosen for the study was a typical example of a deep and rapid Alpine lee cyclogenesis event, well documented during the Mesoscale Alpine Programme – MAP (Bougeault et al. 2001). Observational evidence from the MAP field campaign (e.g. Hoinka et al. 2003), including in-situ aircraft data, wind profiler data and Differential Absorption Lidar (DIAL) collected during the Intensive Observation Period (IOP) reveal the advection of the strong PV streamer (very narrow elongated upper-level PV anomaly, see Massacand et al. 1998) advection over the Alps, as well as its rich mesoscale structure. Numerical experiments confirm the sensitivity of the lee cyclone to both orography and upper-level anomaly (e.g. Hoinka et al. 2003; Buzzi et al. 2003) as well as to the strong mutual interaction. Furthermore, a strong influence of the orography on the evolution of the streamer was found due to vertically propagating gravity waves and gravity-wave enhanced convection. Finally, the assimilation of the additional non-GTS data showed that the Alpine lee cyclogenesis and the related extreme events are sensitive to assimilation of additional measured data. In other words, the accuracy of the model simulations increased with the use of additional data collected during the campaign, suggesting that there is an existing uncertainty in the operational global model analysis regarding the specification of initial-analysis state of atmosphere. Therefore, the goal of the subsequent analysis is to use the statistics of the initial-analysis error in the upper-level PV (presented in Chapter 5) to evaluate the sensitivity and predictability of Genoa lee cyclone to its main precursor, the upper-level dynamical factors.

6.1 Synoptic overview and observations

The synoptic setting, within which the occurrence of a deep lee cyclogenesis (MAP IOP 15) took place, followed a passage of the primary cyclone north of the Alps. On 00 UTC 06 Nov 1999, as inferred by analysis of the European Centre for Medium-Range Weather Forecast (ECMWF), a strong primary cyclone was present in the North Sea north-west of the Alps (Fig. 6.1a). At the upper troposphere, a deep upper-level trough advected over the Alps, in a starting phase of a cut-off (Fig. 6.1b). The upper-level jet reached over 50 ms^{-1} on the western flank of the upper-level system. A rapid creation of a shallow vortex in the Gulf of Genoa took place from 00 - 12 UTC 06 Nov 1999, with the mean sea level pressure dropping to 1004 hPa (cf. Fig. 6.3). At the same time, the western branch of the cold front impinging on the Alps resulted in a strong Mistral breakthrough, as recorded over the Gulf of Lion, while local southeasterly “Jugo” wind still blew over the Adriatic. Upon its initiation, the cyclone moved along the western part of the Apennine peninsula and deepened, reaching 997 hPa just east of Corsica (Fig. 6.1c). Concurrently, the PV streamer, elongated in the N-S direction as it appears in the ECMWF analysis (Fig. 6.1d), was composed of two main inner nuclei, the southernmost being directly associated with the incipient cut-off process. In the early hours of 07 Nov 1999, heavy rain occurred over the northern Italy and the Apennines reaching more then 60 mm / 12 hr (Buzzi et al. 2003). Around midday of 07 Nov 1999, the eastern branch of the cold front resulted in Bora breakthrough in the northern Adriatic area. Later that day and on 08 Nov 1999, strong pressure gradients developed over the northern Dinaric Alps (Fig. 6.1e) and sustained wind speeds overcame 25 ms^{-1}, reaching gusts over 40 ms^{-1} at Maslenica Bridge (Ivatek-Šahdan and Ivančan-Picek 2006). The separation of the two upper-level PV nuclei resulted in formation of two separate closed upper-level circulation systems (Fig. 6.1f). Eventually, upon crossing over Sardinia, the cyclone slowly started to dissipate while moving farther to the eastern Mediterranean.

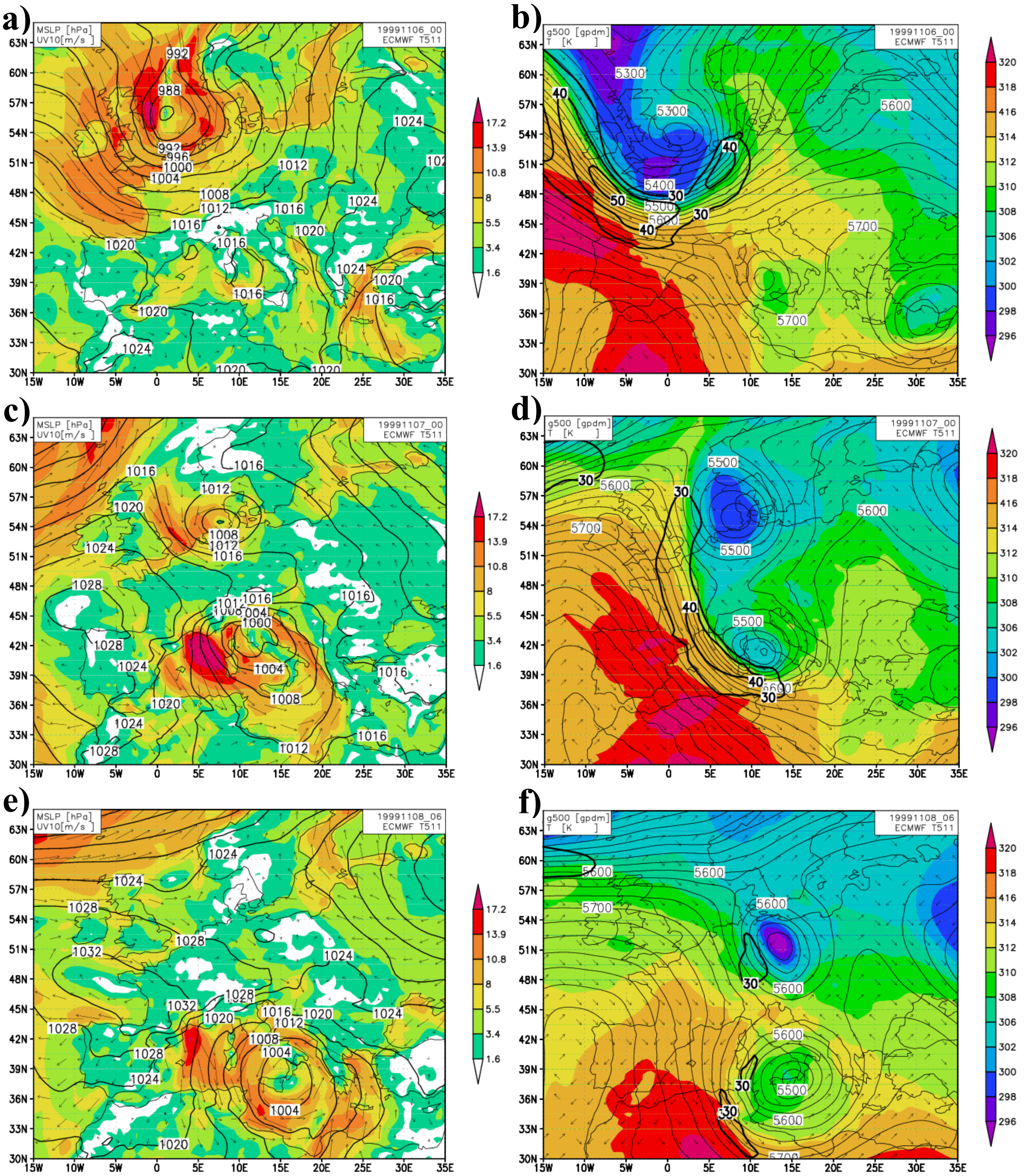

Figure 6.1: *Mean sea level pressure, 10-m wind vectors and 10-m wind speed (left) and potential temperature, geopotential and wind speed (with the upper-level jet denoted in bold lines with a 10 ms*$^{-1}$ *interval starting from 30 ms*$^{-1}$*) at 500 hPa (right) at (a-b) 00 UTC 06 Nov 1999, (c-d) 00 UTC 07 Nov 1999 and (e-f) 06 UTC 08 Nov 1999, as inferred from the ECMWF analysis.*

6.2 The control run

Model setup employed for the numerical analysis is specified in Section 3.3 and the results of the control run of the outermost domain are presented on Figure 6.2. The upper-tropospheric southwesterly flow during the commencement of cyclogenesis (00 UTC 06 Nov 1999 – 12 UTC 06 Nov 1999) suggested this case resembled more to the southwesterly ("*Vorderseiten"*) type of Alpine lee cyclogenesis (Figs. 6.2a-b). In other words, the backshear of the wind with height corresponded to conditions imposed in baroclinic wave theory (Smith 1984), described in Section 1.2, for the largest portion of the Alps. On 12 UTC 06 Nov 1999, the southeastern tip of the upper-level streamer traversed the Alps and the surface cyclone in the Gulf of Genoa rapidly deepened reaching 1008 hPa (Figs. 6.2c-d). The surface thermal structure indicated the breakthrough of the western part of the primary cold front between the Alps and the Pyrenees and creation of a thermal anomaly in the Alpine lee. A warm "Jugo" was present over the whole Adriatic, since the eastern branch of the cold front has not yet surrounded the Alps. On 12 UTC 07 Nov 1999, the simulated cyclone was well developed over the southern Italy, while Bora breakthrough took place over the northern Adriatic (Fig. 6.2e). The upper-level cut-off separated into two nuclei, which were connected with a PV thinning region over the Alps (Fig. 6.2f). The intensity of the main southernmost cut-off nuclei reached 11 PVU. After 18 UTC that day, the deepening has attenuated and the mature cyclone maintained its intensity towards the end of the simulation.

Verification of the mean sea level pressure in the centre of the cyclone is shown on Figure 6.3. According to the deepening rates, the first most rapid phase of development ended approximately at 18 UTC 06 Nov 1999, while the end of the second phase of deepening was indicated with a vanishing deepening rates at around 12 (18) UTC 07 Nov 1999 in the ECMWF analysis (MM5 simulation). Compared to the ECMWF analysis, the intensity of the cyclone was simulated with a satisfactory accuracy in the deepening phase of the cyclone lifecycle, and somewhat less accurately in the mature stage of well developed cyclone in the end of 07 Nov 1999 and subsequently. The latter might be associated with several issues, related with the quality of ECMWF analysis in the very cyclone centre, the accuracy of the MM5 model formulation of the (upper-level) dissipation, surface fluxes and planetary boundary layer parameterizations. Despite the somewhat poorer model accuracy in the latter phase of the cyclone lifecycle, the case seems to be modelled satisfactorily enough in order to investigate the predictability of the system in a number of subsequently presented sensitivity simulations.

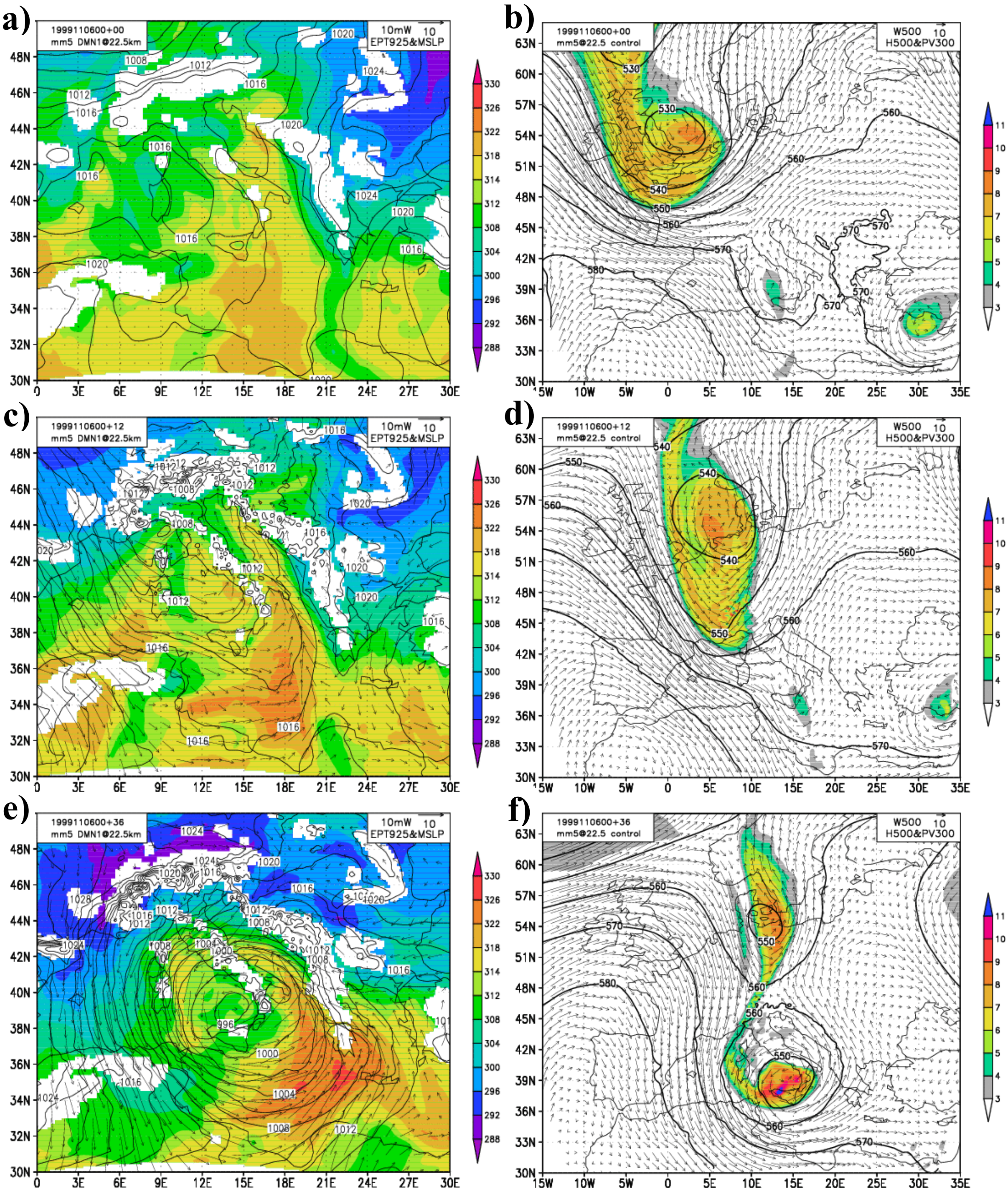

Figure 6.2*: Simulated mean sea level pressure (solid), equivalent potential temperature at 925 hPa (shaded) and 10-m wind vectors (left) and PV at 300 hPa (PVU, shaded), geopotential height at 500 hPa (dag, solid) and wind vectors at 500 hPa (right) at (a-b) 00 UTC 06 Nov 1999, (c-d) 12 UTC 06 Nov 1999 and (e-f) 12 UTC 07 Nov 1999.*

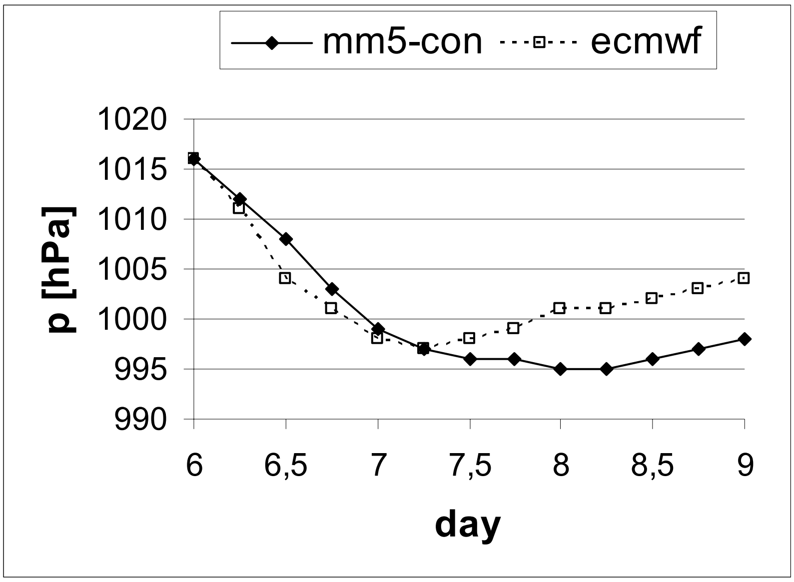

Figure 6.3: *Mean sea level pressure at the centre of the lifecycle from the control run and ECMWF analysis throughout the cyclone lifecycle.*

6.3 Sensitivity experiments

6.3.1 Description of sensitivity experiments

The initial conditions in the analysis were modified by using the PV error statistics described in Chapter 5. The modifications were performed using the 90th percentile of the PV error statistics, averaged over the 500 – 200 hPa layer and values of Ertel's PV > 1. Thus, the upper-level dynamical factors were subjected to macroscale (averaged) modifications in both

Table 6.1: *Description of sensitivity simulations showing the experiment denotations and related modifications in the initial conditions.*

EXP	Description of the experiment
7E	Trough moved to east for 157.5 km (7 grid points in outermost mm5 domain)
7N	Trough moved to north for 157.5 km (7 grid points in outermost mm5 domain)
7S	Trough moved to south for 157.5 km (7 grid points in outermost mm5 domain)
7W	Trough moved to west for 157.5 km (7 grid points in outermost mm5 domain)
+p1	Trough intensity increased for 23 %
-p1	Trough intensity decreased for 23 %

position as well as intensity, with respect to trough in the initial conditions. More specifically, the initial trough was moved to the east, north, south and west for 157.5 km (experiments 7E, 7N, 7S, 7W position unchanged (experiments +p1 and -p1 respectively) compared to the trough in the initial conditions (Table 6.1, Figs. 6.4a-f). Therefore, the ensemble of six

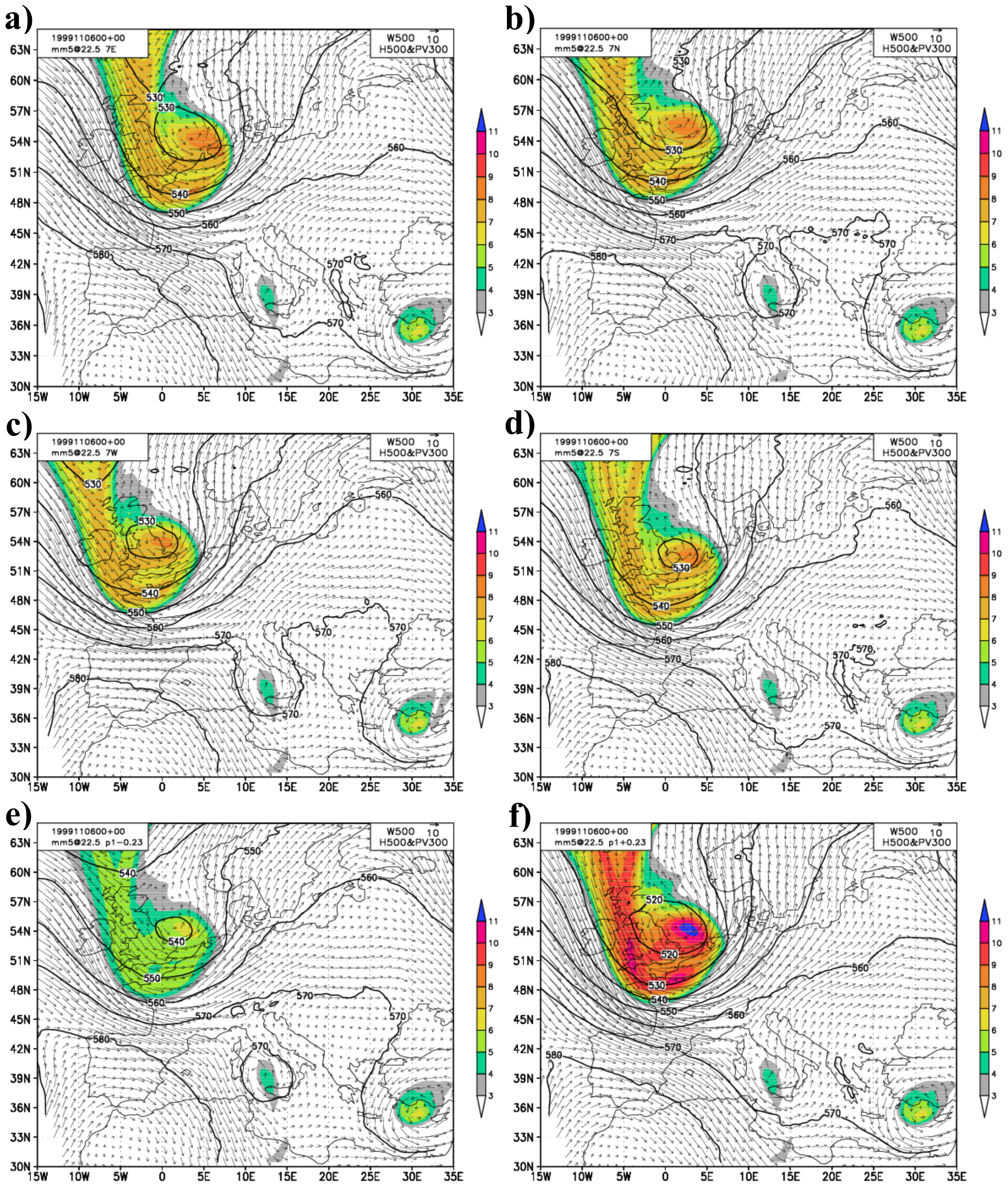

***Figure 6.4**: Geopotential height (dag) and wind vectors at 500 hPa and PV at 300 hPa (shaded) in the ensemble of initial conditions at 00 UTC 06 Nov 1999: (a) 7E, (b) 7N, (c) 7W, (d) 7S, (e) –p1 and (f) +p1.*

sensitivity simulations was created using deterministically scaled modifications in the upper-level dynamical factors. Since these modifications were made with the 90th percentile of the error statistics, in 90% of the deepest Mediterranean cyclones (i.e. strongest PV streamers), realistic initial-analysis PV errors are estimated to be less then specified here. Therefore, these experiments might be viewed to give a reasonable estimate on the impact of the greatest possible initial-analysis uncertainties in the upper-level dynamical factors to the formation and development of the MAP IOP 15 Genoa lee cyclone.

6.3.2 Sensitivity of cyclone intensity

The spread of cyclone centre intensities throughout the cyclone lifetime is shown on Figure 6.5. The initial spread of intensities reflects the 3D nature of the Ertel's PV modifications and equals 8 hPa. The spread of intensities increased towards the maximum in the end of the first and beginning of the second phase of development (18 UTC 06 Nov 1999 – 06 UTC 07 Nov 1999). The maximal spread of intensities reached 18 hPa during the 12-hr period starting at 18 UTC 06 Nov 1999. The most (least) intensive cyclone in the deepening phase was the one in the experiment with increased (decreased) intensity of the upper-level streamer. Moving the upper-level trough to the west and to the east did not change the intensity of the lee cyclone. Nevertheless, the lee cyclone intensified in 7S and attenuated in 7N experiments (4 hPa

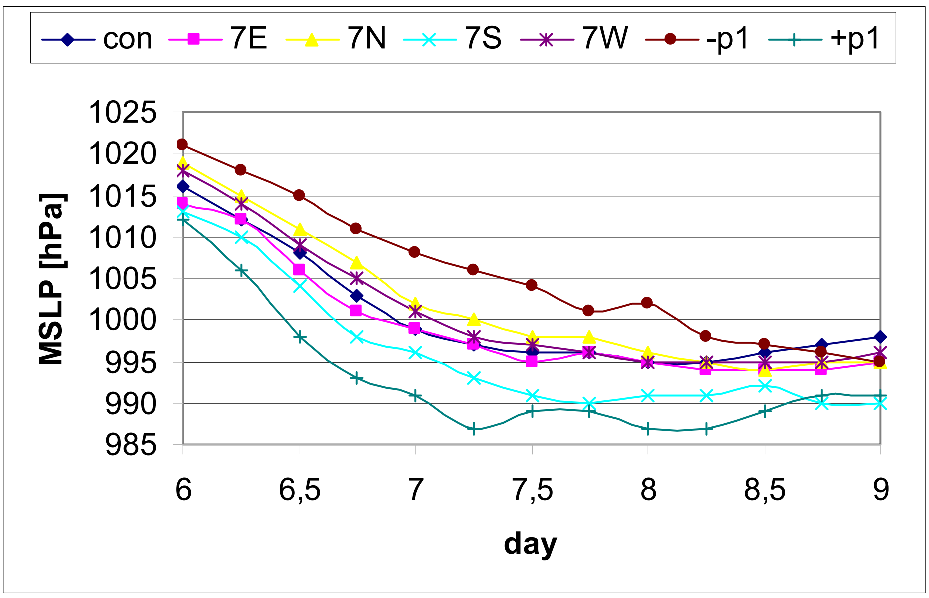

Figure 6.5*: The spread of mean sea level pressure in the cyclone centre during 00 UTC 06 Nov 1999 – 00 UTC 06 Nov 1999 in the ensemble of simulations.*

difference between maximum cyclone depths), despite the differences in timing of cyclogenesis commencement (estimated to be a maximum of 6 hours in the whole ensemble), resulting in up to 9 hPa difference of the mean sea level pressures in the cyclone centers. Since the Alps strongly modify the streamer and the cut-off process (e.g. Hoinka et al. 2003), considerably different upper-level trough evolution and resulting interaction with the surface cyclone could be found throughout the ensemble members. More details on the simulated cut-off process in the ensemble of simulations will be further discussed later on. Geographically, the time period of maximal spread in cyclone centre intensities belonged to the area of the northern and middle Apennines.

After 12 UTC 07 Nov 1999 the spread of cyclone intensities started to decrease. In this and subsequent part of the cyclone lifecycle, though the PV streamer has already started to dissipate, the cyclone still maintained its intensity. The resulting decrease in the spread of intensities equaled 8 hPa towards the cyclone dissipation phase in the end of the simulations. This indicated a weak influence of the initial uncertainty in the upper-level conditions on the cyclone intensity in the late mature and dissipating phases of the cyclone lifecycle, probably due to weak dependence of the cyclone depth to the upper-level streamer intensity.

6.3.3 Sensitivity of cyclone centre position

The influence of the initial uncertainty on the cyclone position is analyzed by tracking the cyclone centre throughout its lifecycle in the ensemble of simulations (Fig. 6.6). The tracking was done using streamlines at 900 hPa to reduce the uncertainties related with the estimation of the cyclone centers from the mean sea level pressure charts over the complex Apennine orography.

In the initial phase of cyclogenesis commencement (00 UTC 06 Nov 1999 - 12 UTC 06 Nov 1999), the spread of cyclone centre positions was considerably smaller than the modification introduced in the upper-levels, indicating that a SW edge of the Alpine range is a strong precursor to the location of cyclone initiation. Several issues seem to account for this preference for the asymmetry of pressure perturbation in the lee of the mountain, as discussed in Chapter (1), such as the influence of (1) baroclinicity (2) Coriolis force, (3) creation of the primary low-level PV banner and (4) proximity of the sea. Nevertheless, at these early hours

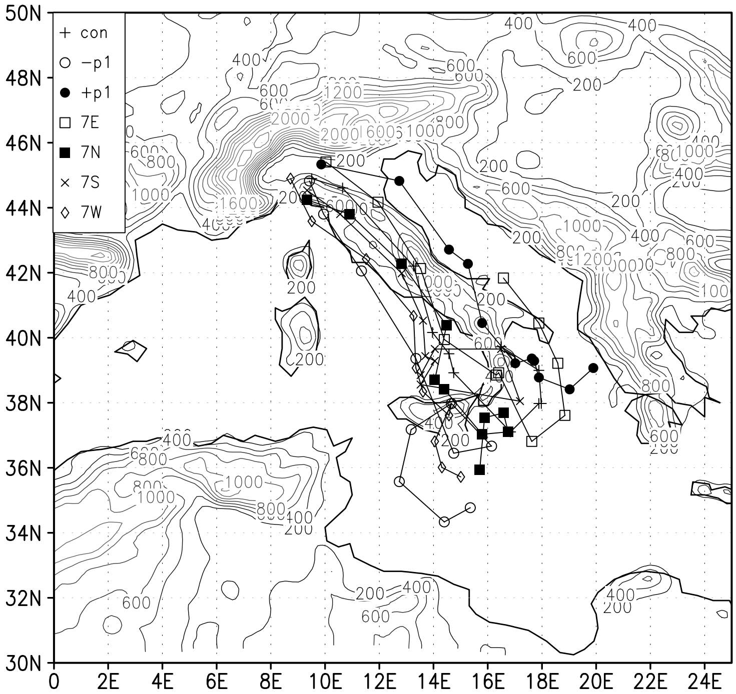

***Figure 6.6**: Time evolution of the cyclone centers in the ensemble of simulations, starting from 12 UTC 06 Nov 1999, plotted every 6 hours. Prior to the starting time instant, very strong deepening (cf. Fig. 6.5) was present, but without closed surface circulation.*

of cyclone initiation, the positions seem to reflect the initial upper-level modifications: the most eastern cyclone position was present in the 7E experiment, while the most western cyclone centre position was simulated in the 7W experiment. However, already on 18 UTC 06 Nov 1999, cyclones diverged: while most of the cyclones moved west of the control run, the strongest cyclone (+p1) slid along the eastern part of the Apennine peninsula entering the western part of the northern Adriatic Sea.

It is not completely clear why the stronger upper-level trough forced the deepening cyclone to move over to the Adriatic, since the generation of cyclones in the Adriatic has not been extensively studied within the framework of numerical analysis. However, it seems that in the experiment (+p1) thermal anomaly and the frontal structure of the lee cyclone formed more to the east compared with the control run, while the opposite effect was noticed in the simulation with the decreased intensity of the incoming trough (Figs. 6.7a-b). Namely, in the +p1 simulation, the stability of the flow impinging on the Alps was decreased (not shown) while the background wind speed was increased, effectively reducing the Scorer parameter upstream of the SW edge of the Alps. Both effects are conceptually related with the modification of the

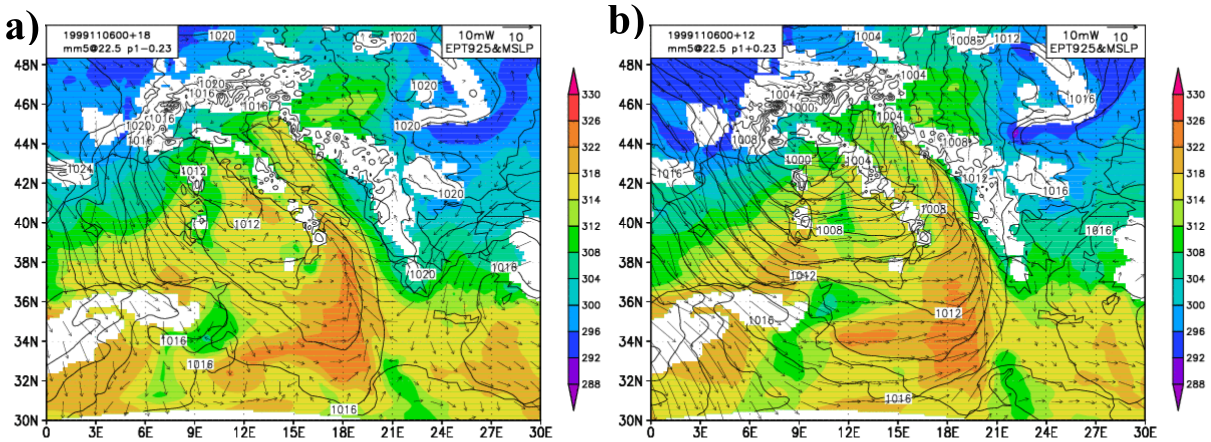

Figure 6.7: *Mean sea level pressure, equivalent potential temperature at 925 hPa and 10-m wind vectors in (a) –p1 experiment at 12 UTC 06 Nov 1999 (b) +p1 experiment at 18 UTC 06 Nov 1999. The times chosen correspond to nearly the same stage of the cold front breakthrough to the Mediterranean.*

upper-level trough intensity (e.g. Hoskins et al. 1985) and contribute to the linearization of the low-level flow over the (western) Alps. Since the impinging winds were the strongest over the western part of the range and the amount of blocking was increasing from the western to the central part of the Alps, linearization of the flow resulted in a weaker blocking and more intensive "flow over" regime over the western part of the range. Therefore, the resulting Mistral front extended farther to the east, resulting in an eastward shift of the surface thermal anomaly and developing frontal system.

After the initial increase, the spread of cyclone tracks was fairly constant until the end of the second phase of deepening (approx. 18 UTC 07 Nov 1999), while the cyclones quickly advected southeast along the Apennines. Once the cyclones reached the southern part of Apennines and Sicily, in the mature stage of the lifecycle, the spread of cyclone positions strongly increased. For example, on 00 UTC 09 Nov 1999, the last time instant of the analysis, differences in positions of cyclone centers reached more than 750 km. At that time, the farthest cyclones belonged to experiments with increased and decreased upper-level trough intensity (+p1 and -p1 respectively), as well as the trough moved to the east (7E). The inspection of the upper-level flow (Figs. 6.8a-f) suggests that this increase appears to be related with different upper-level dynamics in the mature stage of vortex rollup (e.g. Saffman and Baker 1979, Hoskins et al. 1985). Namely, it seems that the Alpine range might have played a role in determining the upper-level dynamics. Namely, a numerical analysis of the

MAP IOP 15 streamer indicated the strong role of the impinging southerly flows over the eastern part of the Alpine orography on the PV thinning and the cut-off process (Hoinka et al. 2003). In addition, it was demonstrated that active upper-tropospheric diabatic processes due to convection caused by gravity waves above the mountain, account for a significant

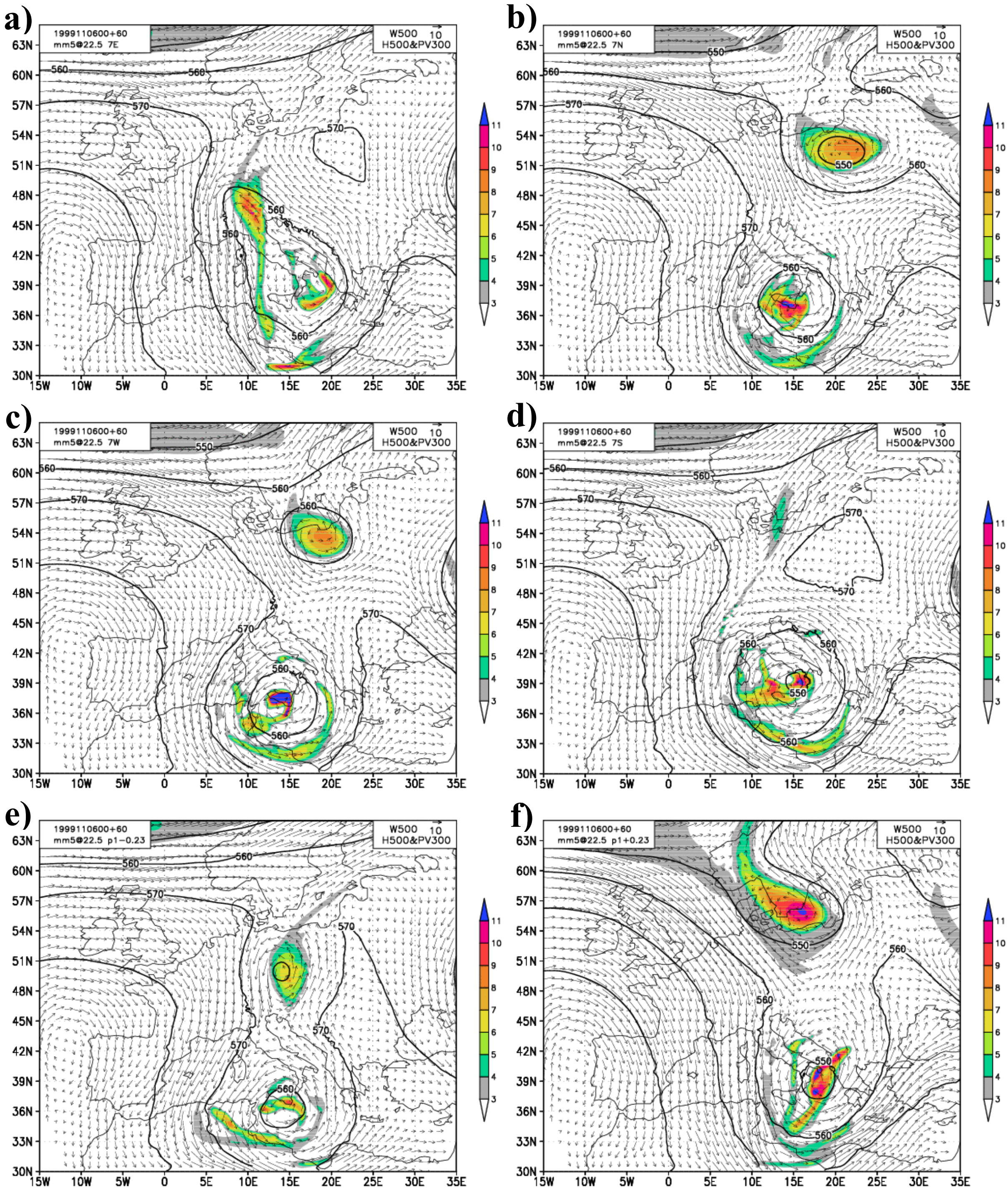

Figure 6.8: *Geopotential height (dag) and wind vectors at 500 hPa and PV at 300 hPa (shaded) in the ensemble of sensitivity simulations at 12 UTC 08 Nov 1999: (a) 7E, (b) 7N, (c) 7W, (d) 7S, (e) -p1 and (f) +p1.*

reduction in the streamer intensity. While the influence of orography on the streamer intensity reduction and cut-off process was not equal, it is suggested that modifications in the initial conditions changed the conditions for vertically propagating mountain waves, and the resulting upper-level conditions influencing the cut-off. In favor to this hypothesis, it seems that the cut-off was the weakest in the 7E experiment (Fig. 6.8a), since in this very simulation a mid-tropospheric critical level (suppressing vertical wave energy propagation) for the impinging southerly flow was extended farther to the east due to eastward shift of the northwesterly upper-level flow, resulting in a smaller portion of the (eastern) Alps interacting with the traversing upper-level streamer. In addition, to some extent a possible contribution, resulting from the errors of the PV inversion should not be completely neglected.

Therefore, in the initial phase of cyclone development the spread of cyclone centers appears to be affected by the variability of the (non)linearity of the low-level flow impinging to the Alps and partly associated with the upper-level streamer intensity. In the mature and dissipating phase, the large spread of cyclone centers seems to be due to different scenarios of upper-level vortex rollup, influenced by the Alpine orography depending on the exact position of the trough. In a chain of events that contributed not only to different cyclone evolutions, but also to strong differences in the properties of cyclonic Bora that took place along the eastern Adriatic coast.

6.3.4 Sensitivity of Bora intensity in the northern Adriatic

It was demonstrated in the preceding sections that the effect of the initial-analysis uncertainty in the upper-level trough reflected on the intensity of the impinging flow over the Alps, amount of blocking as well as lee cyclone intensity and position. This has a strong potential to affect cyclonic Bora flow over the Dinaric Alps. In the first place, cyclonic Bora strongly depends on the cyclone presence in the Adriatic, Tyrrhenian or Ionian Seas (Jurčec 1989; Večenaj 2005; Horvath et al. 2008b). The influence of the cyclone position and intensity due to arbitrary mesoscale modifications of the upper-level PV anomaly has been studied in a number of numerical experiments of the 12-15 deep Mediterranean cyclone (Horvath and Ivančan-Picek 2008). The results indicated that macroscale (mesoscale) PV modifications in the upper-level circulations, accounted for 50% (25%) of Bora severity in the southern Adriatic. In the second place, Bora (whether cyclonic or anticyclonic) is strongly sensitive to the properties of the background flow (henceforward "background" is with respect to the Dinaric Alps) which has been widely studied (e.g. Smith 1987; Klemp and Durran 1987; Bajić 1989; Ivančan-Picek and Tutiš 1996; Enger and Grisogono 1998; Grubišić 2004; Belušić et al. 2004; Göhm and Mayr 2005; Göhm et al. 2008). It is known that the background flow is closely related with the amount of blocking over the Alps and properties of the eastern branch of the flow surrounding the Alps. Therefore, the initial-analysis uncertainty in the upper-levels might reflect on the properties of background flow through its influence on the blocking over the Alps, having a potential to modify Bora response over the Adriatic.

Due to the above reasons, the analysis will assess the sensitivity of Bora, taking place during the MAP IOP 15 event, to initial-analysis PV errors. During the event, a strong Bora outbreak was recorded along the northern Adriatic coast, while at the same time Bora in the southern Adriatic was of a moderate intensity. The observed wind speeds reached locally up to 28 m/s at Maslenica Bridge in the northern Adriatic and 10 m/s at Makarska station (a southern

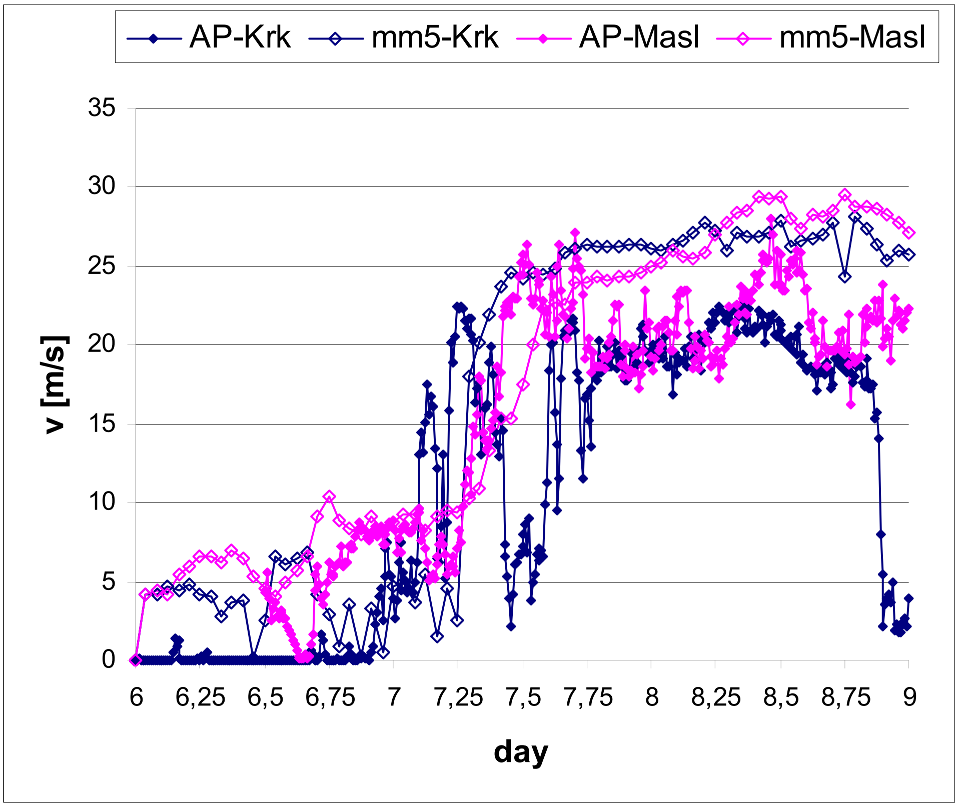

Figure 6.9: *A comparison of modeled (triangles) and observed (squares) 10-m wind speeds at Krk bridge in the northern Adriatic (unfilled marks) and Maslenica bridge (filled marks) during 06-09 Nov 1999.*

Adriatic station prone to strong Bora). The intensity of simulated and measured Bora wind speeds indicated that, although the modeled Bora was somewhat overestimated in the mature phase of the cyclone lifecycle, the control run successfully captured the onset and severity of this Bora event (Fig. 6.9). Since this event was characterized with a much stronger Bora outbreak in the northern Adriatic, the analysis will be devoted to the northern Adriatic Bora only, with a special attention to the lee side of the Velebit mountain range.

Bora in the northern Adriatic started in the morning of 07 Nov 1999, following a strong "Jugo" (Fig. 6.10a). The outbreak first took place over the Trieste region and the Bora front quickly extended towards the southeast. By 08 Nov 1999, the mature stage of Bora took place along the entire northern Adriatic (Fig. 6.10b). The greatest wind speeds were simulated in the lee of the central and the highest part of the Velebit range, where the lee side point of the analysis was chosen. Offshore, the greatest wind speeds occurred in the lee of Vratnik pass, in the northern part of the Velebit mountain.

The spread of Bora intensities equaled approximately ±30% of the wind speed in the control run. This partially reflects the gross features of the analyzed spreads of cyclone intensity and track (Fig. 6.11). The strongest outbreak of Bora was simulated in experiment with the strongest cyclone intensity and position closest to the target region (+p1) for the most of the simulation period. However, the deepest cyclone and the strongest Bora in the end of the

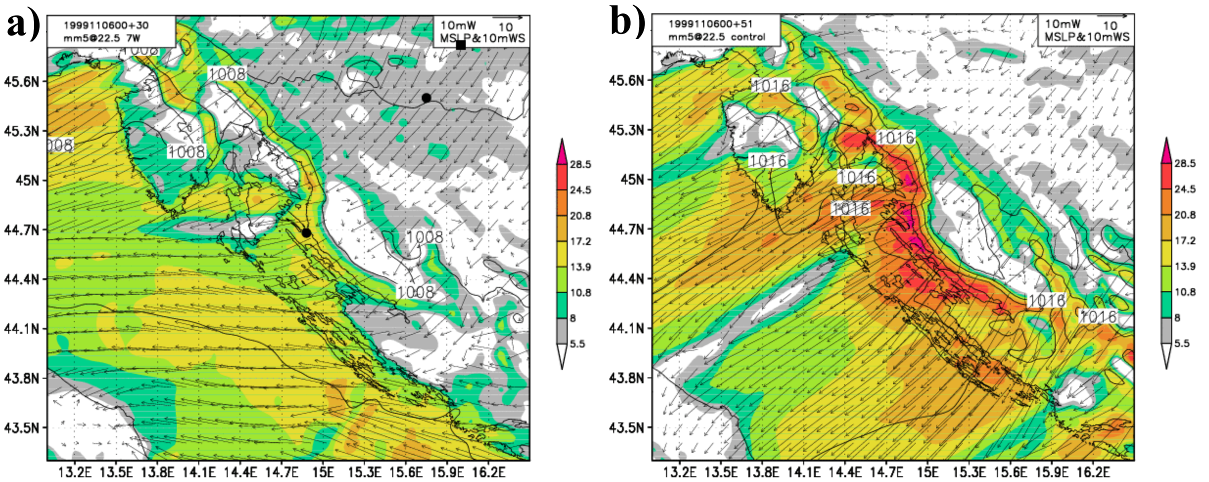

Figure 6.10: *Mean sea level pressure, 10-m wind vectors and 10-m wind speed (shaded) at (a) 06 UTC 07 Nov 1999 and (b) 03 UTC 08 Nov 1999. Points of analysis mentioned in the text are denoted on the left panel: Zagreb, background and lee points of analysis (from NE to SW).*

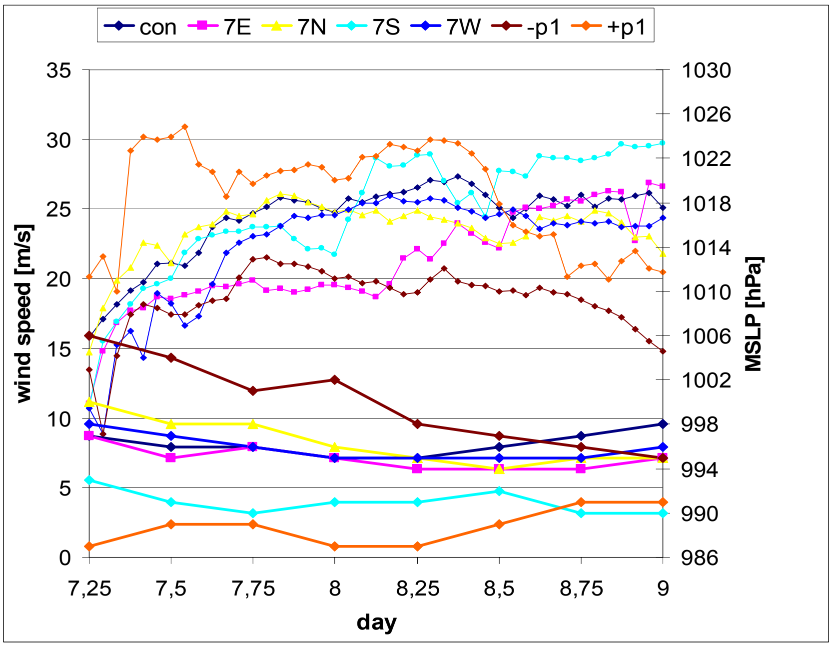

Figure 6.11: *Mean sea level pressure in the cyclone centre during 06 UTC 07 Nov 1999 – 00 UTC 09 Nov 1999 in the ensemble of simulations in the lee of the Velebit mountain (cf. Fig. 6.10).*

forecast range were simulated in the 7S experiment. In addition, the weakest winds in the mature phase of Bora (08 Nov 1999) were simulated in the experiment with generally the weakest cyclone and farthest cyclone centre (-p1). Therefore, the synoptic setting proves to be a strong predictor of the cyclonic Bora flows, in accordance with aforementioned studies. However, other variations do not conform to this macroscale reasoning. For example, during 07 Nov 1999, stronger cyclone closer to target region in experiment 7E was associated with weaker Bora winds than the less intensive cyclone farther away from the northern Adriatic in experiment –p1. Additionally, though in the final time sequence of the simulations (00 UTC 09 Nov 1999) cyclones in experiments 7W, 7N and -p1 were at similar positions in the central Mediterranean (cf. Fig. 6.6) and of similar intensities, resulting Bora strength strongly differed (15 ms^{-1} in -p1, 22 ms^{-1} in 7N and 24 ms^{-1} in 7W experiments). Therefore, macroscale forcing reflected through the cyclone intensity and position was not the only contributing factor to Bora variability.

As mentioned earlier, due to the influence of initial perturbations on the eastern branch of the air surrounding the Alps, it is expected that the initial modifications reflected on properties of both synoptically induced critical level and the background low-level jet flow. Therefore, the flow properties will be investigated by the analysis in terms of the vertical profile of the Scorer parameter and Froude number. The Scorer parameter is approximated as:

$$l^2(z) = N^2(z)/U^2(z) \tag{6.1}$$

where $N(z)$ is Brunt-Väisälä frequency and $U(z)$ is cross-mountain wind speed component (Scorer, 1949). The point of analysis is just SW of Zagreb (cf. Fig. 6.10) and is considered to reflect well the properties of the background flow impinging on the northern part of Dinaric Alps.

Vertical profiles of the Scorer parameter in each of the ensemble members are shown in the mature phase of Bora, 03 UTC 08 Nov 1999 (Fig. 6.12a) and 12 UTC 08 Nov 1999 (Fig. 6.12b). In the control run and most of the other ensemble members, Scorer parameter was nearly constant with height indicating a deep layer of impinging flow. However, on 03 UTC 08 Nov 1999, in experiments -p1 and 7E (with far the weakest Bora simulated, cf. Fig. 6.11) synoptic critical levels[2] existed at 700 hPa and 600-650 hPa respectively, indicating a strong layering of the troposphere. The existence of synoptic critical levels was inherently associated

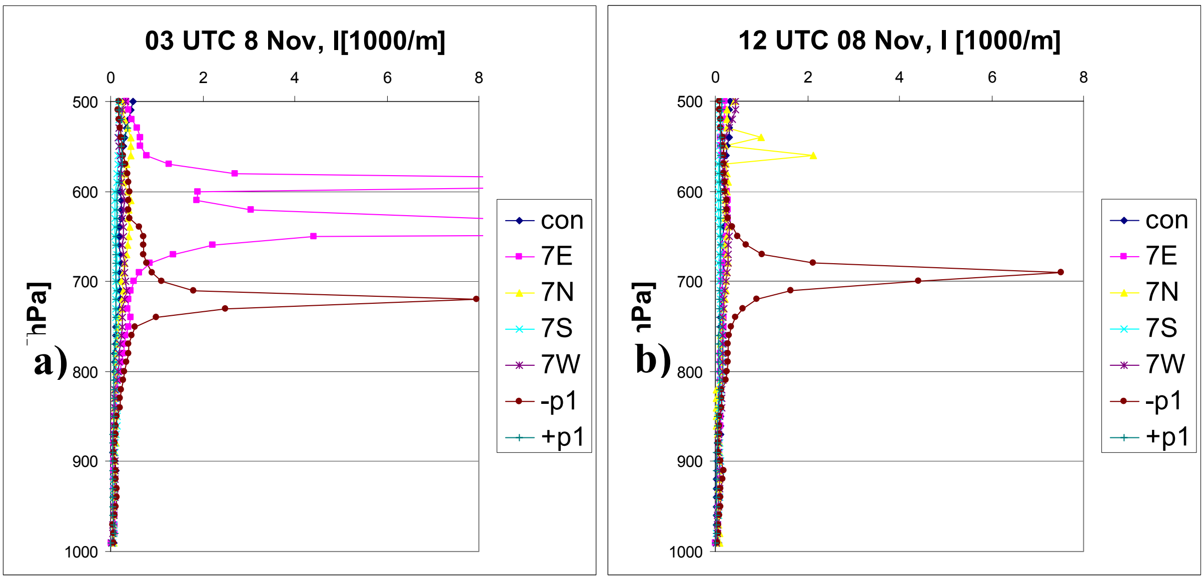

***Figure 6.12**: Vertical profiles of the Scorer parameter at the background point of analysis (cf. Fig. 6.10) in the ensemble of simulations on (a) 03 UTC 08 Nov 1999 and (b) 12 UTC 08 Nov 1999.*

[2] Critical level is the altitude at which relative horizontal phase speed of internal gravity waves equals the wind speed, resulting in vanishing of the cross-mountain component of wind speed.

with the different cut-off dynamics in different members of the ensemble as discussed earlier and the presence of the southerly upper-tropospheric flows above the Dinaric Alps. Though these results seem to be in contrast with theoretical considerations about energy trapping and positive feedback of critical levels on the downslope windstorms, other parameters, such as model ability to simulate background inversions and the amount of linearity of the background flow need to be considered in order to draw relevant conclusions on this issue. Nevertheless, the existence of prominent differences in the synoptically induced vertical structure of the atmosphere indicates that initial uncertainties in the upper-levels might be responsible for the (non)existence of layering in the atmosphere and qualitative changes of Bora response in the lee.

Furthermore, the linearity of the low-level flow is examined thorough the non-dimensional mountain height $\hat{h}$ (the inverse of the integral background Froude number). In general, with respect to linearity of the flow, several regimes exist in three-dimensional, stratified, uniform, hydrostatic flow over an isolated mountain (e.g. see Durran, 1990; Epifanio, 2003; Lin, 2008), controlled by the non-dimensional mountain height (or inverse Froude number) $\hat{h}$ and horizontal mountain aspect ratio b/a, where a and b are mountain scales in x and y directions, respectively (Table 6.2). The non-dimensional mountain height was calculated as:

$$\hat{\mathrm{h}} = Nh/U \tag{6.2}$$

where N is a Brunt- Väisälä frequency, vertically integrated between the height of the planetary boundary layer and the tropopause, h is the mountain height, and U is cross-mountain wind speed component. For the calculation, U was vertically integrated between the

Table 6.2 *Flow regimes for three-dimensional, stratified, uniform, hydrostatic flow over an isolated mountain of the horizontal mountain aspect ratio (b/a)=3, where a and b are mountain scales in x and y directions and* $\hat{h}$ *is the non-dimensional mountain height (adopted after Lin 2008).*

1	$\hat{h} < 0.83$	Liner flow
2	$0.83 < \hat{h} < 1.09$	Non-linear flow – gravity wave breaking
3	$1.09 < \hat{h} < 2.92$	Non-linear flow – gravity wave breaking, upstream blocking, lee vortices
4	$\hat{h} > 2.92$	Non-linear flow – very strong upstream blocking, lee vortices

height of the mixed layer and the critical level or the tropopause. Height of the planetary boundary layer was determined at 12 UTC and also used for calculations at 03 UTC (similar to Göhm and Mayr 2005).

Inverse Froude number was calculated with mountain height h=1300 m, which reflects the height of the mountain range just upstream of the lee side point of analysis. During the nighttime, on 03 UTC 08 Nov 1999, in the simulations with the weakest Bora strength (-p1, 7E), non-dimensional mountain height (greater than 3 and 2.5 respectively) indicated the existence of excessive blocking that might have unfavorably influenced Bora severity (Fig. 6.13). The least non-linear background flows were present in simulations +p1 and 7S ($\hat{h}$ ~ 1.2-1.3), which had the strongest Bora at the time of analysis.

During the daytime, at 12 UTC 08 Nov 1999, flows were generally more linear and the strongest decrease of non-linearity was modeled in 7E experiment, in which Bora significantly increased since 03 UTC 08 Nov 1999. However, this increase can not be uniquely associated with the change in flow linearity, since other parameters, such as critical level existence and cyclone proximity considerably changed. Nevertheless, the analysis suggests that flow regimes responsible for the qualitatively different downslope wind

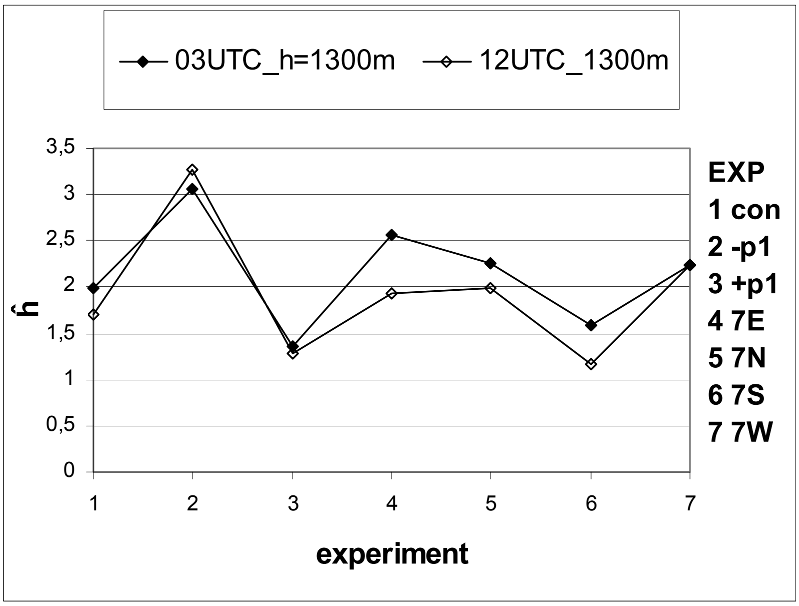

Figure 6.13*: Integral background Froude number at 03 UTC 08 Nov 1999 and 12 UTC 08 Nov 1999 in the ensemble of simulations at the background point of analysis (cf. Fig. 6.10).*

response can significantly change due to the initial uncertainties in the upper-level dynamical factors. In addition, strong spatial variability of the flow regimes might be expected in a real Bora environment due to unequal height of the mountain range and existence of individual peaks and mountain passes ranging from 700-1600 m a.s.l in area favorable for the northern Adriatic Bora. Finally, due to co-existence of several discussed factors influencing the flow regime, further numerical experiments are needed in order to identify contribution of each of the factors involved to this severe Bora event.

Thus, it was demonstrated that initial-analysis upper-level uncertainties affect Bora response in the lee of Dinaric Alps in a two-fold manner: (1) through the influence on Genoa cyclone intensity and position and (2) though the influence on the property of the background flow. Therefore, the uncertainties in the initial-analysis of the macroscale dynamics propagate to a range of smaller-scale phenomena in a chain of dynamically related mesoscale events, which is a climatologically the dominant characteristic of weather in the region. Furthermore, since the high sensitivity of the numerical weather forecast to the initial conditions often yields a deterministic forecast of limited quality, the improvement of the numerical weather prediction in the area is very likely to be reached through the establishment of the limited area model ensemble prediction system. One of the feasible approaches would be to use the PV errors statistics to derive ensemble perturbations throughout the troposphere. In addition, the perturbations could be scaled with the results of adjoint[3] simulations, which is the ensemble forecasting approach currently being tested at the University of Balearic Islands (Romero 2008, personal communication). Another approach is currently being developed within the "mesoscale" community in Europe, which aims to produce limited area multi-model ensemble prediction system in the region.

---

[3] Adjoint model is a model composed of adjoint equations that maps a sensitivity gradient vector $\nabla x\, J(t_0) = T\, \nabla x\, J(t_1)$, from a forecast time, t_1, to an earlier time, t_0, which can be the initial time of a forecast trajectory. In essence, the results of the adjoint model identify sensitivity zones for a particular forecast.

7. Conclusions

The classification of cyclone tracks in the Adriatic was carried out based on the European Centre for Medium-Range Weather Forecast (ECMWF) T511 long cut-off analysis during 4-yr period (2002-2005). The manual analysis performed used objective criteria on the mean sea level pressure and a closed circulation thresholds. The related classification of cyclone tracks and types indicated the existence of four types of cyclogenesis over the Adriatic Sea.

The first type of cyclone present in the Adriatic (Type A) is Genoa cyclones which is the most frequent cyclone type in the Adriatic (35%). Two subcategories are found: (I) continuous track Genoa cyclones (Type A-I) that cross over the Apennines to the Adriatic Sea and (II) discontinuous track cyclones (Type A-II) where new surface cyclones is generated over the Adriatic Sea under the influence of a parent cyclone generated in the Gulf of Genoa (Genoa cyclones) and moving towards the Adriatic but blocked by the Apennines. This type of cyclones is most often in the winter season.

The second type (Type B) is cyclones developed in situ over the Adriatic Sea without any apparent connections with other pre-existing cyclones in the surrounding area. This latter type of cyclone comprises 26% of the cyclones present in the Adriatic. Two isolated cyclogenetic centers are found: (I) the northern Adriatic (Type B-I) that are deeper cyclones similar to Type A, and (II) the middle Adriatic (Type B-II) that are shallow cyclones more frequent in warmer part of the year.

The rarest type of cyclone is “twin” or “eyeglass” cyclones (Type AB) which are a mix of cyclones types A and B (6% of the total number of detected cyclones). In this type of cyclone, two cyclones co-exist and stride along the Apennines.

The forth cyclone type identified (Type C) are cyclones moving from the Mediterranean Sea, but not from the Gulf of Genoa (non-Genoa cyclones). This type of cyclones originates from cyclogenetic areas of Atlas, Pyrenees, Alboran Sea, Iberia and Atlantic Sea and comprises almost 33% of total cyclones detected. In this type two subcategories are found: (I) continuous track cyclone (Type C-I) that is able to cross over the Apennines to the Adriatic Sea continuously and (II) discontinuous track cyclone (Type C-II) that is blocked by the Apennines, while a new surface cyclone is generated over the Adriatic Sea. The results reveal that the greatest number of cyclones that occur over the Adriatic are initiated in the lee sides of mountain ranges in the western Mediterranean (the Alps, the Atlas, the Pyrenees and the Apennines) and associated with an upper-level trough traversing the mountain range.

The influence of the upper-level trough on the lifecycle of a Mediterranean cyclone initiated to the lee of the Alps (12-15 Nov 2004) was investigated through a numerical analysis with the use of factor separation and piecewise PV inversion methods. The analyzed cyclone was initiated in the early hours of 12 Nov 2004, and advected towards the Mediterranean Sea. The analysis identified that the upper-level trough was the crucial ingredient of the phenomenon, and that in the absence of upper-level dynamical factors a much weaker cyclone does not form in the lee side of the Atlas mountain, but rather further to the east. Furthermore, the numerical analysis indicated that the Atlas orography is responsible for the deepening in the first phase of the event, while the upper-level trough was the main ingredient of the second phase of the event. Though neither deepening rates were comparable, nor synoptic setting and thermal anomaly creation processes were alike compared with typical cases of Alpine lee cyclogenesis, the existence of the two stages of cyclone deepening seems to imply a dynamical resemblance of cyclone generation process in both regions. In addition to the cyclone deepening, upper-level dynamical factors showed responsible for faster advection of the system towards the Mediterranean Sea, while orographic influence was to keep the cyclone closer to the mountain lee. Considerable differences of cyclone paths in simulations with variable intensity of upper-level PV anomaly indicated that upper-level dynamical factors have a potential to control the tracks of cyclones initiated in the Atlas lee on their way towards the Mediterranean.

The influence of the mesoscale modifications was further investigated through the creation of a number of sensitivity simulations with the arbitrary mesoscale modifications in the incident upper-level trough structure. The two isolated cores of the strongest mesoscale circulations accounted for 75% of the cyclone intensity in the quasi-adiabatic baroclinic stage of cyclone development over the land. Over the Mediterranean a spread of 15 hPa was recorded, mainly due to different speeds of advection towards the Mediterranean. The spread of cyclone tracks was the greatest just prior the cyclone entered over the Mediterranean sea and become confluent over the Ionian Sea in the dissipation phase of the cyclone lifecycle, seemingly aided by the orientation of the Atlas mountains, Sicily, southern parts of the Apennine and Balkan peninsulas. The strong influence of the mesoscale modifications in the initial conditions suggests that a considerable part of the upper-level control of lee cyclogenesis is played by mesoscale upper-level circulations.

A statistics of the initial-analysis upper-level potential vorticity (PV) errors was evaluated based on the difference between the ECMWF and National Centers for Environmental Prediction (NCEP) global analysis, addressing both intensity and displacement errors of the individual mesoscale upper-level circulations. The results of the error statistics, calculated at each model level, were used to create an ensemble of sensitivity simulations of the MAP IOP 15 event (Mesoscale Alpine Programme; Intensive Observing Period), which was a typical case of a deep Genoa cyclogenesis taking place during 06-09 Nov 1999. Thus, the introduced PV modifications in the initial conditions reflected the realistic estimate of the initial-analysis errors. The choice made was to use the 90th percentile of both displacement and intensity errors in order to estimate possibly the highest level of realistic uncertainty in the specification of the upper-level trough dynamics.

The analysis reveals that the numerical forecast of the Genoa cyclone intensity and path strongly depends on the initial-analysis uncertainties in the upper-level dynamical factors. The spread of cyclone intensities increased through the initial phase of cyclone development and reached its maximal values (18 hPa which equaled 50% of the cyclone intensity) during the end of the first and beginning of the second phase of deepening (18 UTC 06 Nov 1999 – 12 UTC 07 Nov 1999). During this time period the cyclone was moving southeastward along the northern and middle part of the Apennine peninsula. Subsequently, in the mature and towards the dissipation stage of cyclone development i.e. before the onset of pronounced cyclolysis, the spread of cyclone intensities decreased, indicating that the upper-level dynamical factors were not the main contributor to the cyclone maintenance in these stages of the lifecycle.

The location of the very initiation of the MAP IOP 15 cyclone was not substantially changed due to the initial modifications in the upper-levels, indicating that southwestern part of the Alpine lee is a strong predictor of this event. However, soon after the initiation, cyclone tracks diverged with cyclone positions ranging from the Gulf of Genoa to the northern Adriatic. This is shown to be due to variability in the flow linearity over the SW part of the Alpine range, which influenced the position of the cyclone initiation. For example, the reduced non-linearity in the simulation with increased intensity of the upper-level trough enabled the Mistral front to extend further to the east and move the low-level thermal anomaly and developing frontal system towards the northern Adriatic. After this initial increase (of approx 200 km), the spread of tracks remained constant until the mature phase of cyclone development and dissipation phase of the upper-level streamer. In this phase, the spread of cyclone centre positions strongly increased up to 750 km towards the final period of the analysis (12 UTC 08 Nov 1999 – 00 UTC 09 Nov 1999). The analysis revealed that this increase resulted from different upper-level cut-off and rollup dynamics throughout the ensemble. It appears that the above consequences from differing interactions between the upper-level streamer and the Alpine orography, primarily due to changed position of the trough and variability of subsequently induced synoptic critical levels over the Alps.

Bora in the northern Adriatic showed highly sensitive to the initial-analysis uncertainties in the upper-level dynamics, due to the propagation of initial uncertainties to (1) Genoa cyclone intensity and track and (2) background flow (associated with blocking on the Alps and formation of the eastern branch of the flow surrounding the Alps). The latter is associated with the (non)existence of synoptic critical levels, their differing altitudes and span of the integral background Froude number over several flow regimes throughout the ensemble. As a result, the propagation of initial-analysis uncertainties resulted in a spread of Bora intensity of ±30% of the wind speed in the control run, present permanently during the whole event.

Therefore, the uncertainties in the initial-analysis of the macroscale dynamics propagate to smaller-scales in a chain of dynamically related mesoscale events, with a strong potential to decrease the accuracy of mesoscale numerical weather prediction in the area. Since the high sensitivity of the numerical weather forecast to the initial conditions often yields a deterministic forecast of a limited quality, it is very likely that the significant improvement of the accuracy of mesoscale numerical weather prediction in the region could be reached through the establishment of the limited area model ensemble prediction system.

8. References

Aebischer, U., and C. Schär, 1998: Low-Level Potential Vorticity and Cyclogenesis to the Lee of the Alps. *J. Atmos. Sci.*, **55**, 186-207.

Alpert, P., M. Tsidulko, S. Krichak, and U. Stein, 1996: A multi-stage evolution of an ALPEX cyclone, *Tellus*, **48A**, 209-220.

Bajić, A., 1989: Severe bora on the northern Adriatic. Part I: Statistical analysis. *Rasprave-Papers*, **24**, 1-9.

Belušić, D., M. Pasarić, and M. Orlić, 2004: Quasi-periodic bora gusts related to the structure of the troposphere. *Quart. J. Roy. Meteor. Soc.*, **130**, 1103-1121.

Bender, M.A., R.E. Tuleya, and Y. Kurihara, 1987: A numerical study of the effect of island terrain on tropical cyclones. *Mon. Wea. Rev.*, **115**, 130-155.

Betts, A. K., and M. J. Miller, 1993: The Betts-Miller scheme. – In: The representation of cumulus convection in numerical models. K. A. Emanuel and D. J. Raymond, (Eds.), Amer. Meteor. Soc., 246p.

Blackadar A. K., 1979: High resolution models of the planetary boundary layer. *Adv. Environ. Sci. and Eng.*, Vol. **1**, J. Pfafflin and E. Ziegler, (Eds.), Gordon and Breach, 50-85.

Bleck, R., and C. Mattocks, 1984: A preliminary analysis of the role of potential vorticity in Alpine lee cyclogenesis. *Beitr. Phys. Atmos.*, **57**, 357-368.

Bluestein, H. B., 1992: Synoptic-Dynamic Meteorology in Midlatitudes, Volume I - Principles of Kinematics and Dynamics. Oxford University Press, 431pp.

Bougeault, P., P. Binder, A. Buzzi, R. Dirks, R. Houze, J. Kuettner, R. B. Smith, R. Steinacker, and H. Volkert, 2001: The MAP Special Observing Period. *Bull. Am. Meteor. Soc.*, **82**, 433–462.

Bretherton, F. P., 1966: Baroclinic instability and the short wavelength cut-off in terms of potential vorticity. *Quart. J. Roy. Meteor. Soc.*, **92**, 335-345.

Buzzi A., and S. Tibaldi, 1978: Cyclogenesis in the lee of Alps: A case study. *Quart. J. Roy.*

Meteor. Soc., **104**, 271-287.

Buzzi A., D'Isidoro, M., and S. Davolio, 2003: A case-study of an orographic cyclone south of the Alps during the MAP SOP. *Quart. J. Roy. Meteor. Soc.*, **129 B**, 1795–1818.

Cavaleri L., L. Bertotti, and H. Schmidt, 1999: A Critical Analysis of the Wind Climatology of the Adriatic Sea from Different Sources. *Theor. Appl. Climatol.*, **62**, 187-197.

Charney J. G. 1947: The dynamics of long waves in a baroclinic westerly current. *J. Meteorol.*, **4**, 135–163.

Charney, J. G., 1955: The use of primitive equations of motion in numerical prediction. *Tellus*, **7**, 22-26.

Davies, H. C., and H. Wernli, 2003: Quasi-geostrophic theory. *Encyclopedia of the Atmospheric Sciences*, J. Holton, J. Pyle, and J. Curry (Eds.), Cambridge University Press, 1787-1794.

Davis C. A., and K. Emanuel, 1991: Potential vorticity diagnostics of cyclogenesis. *Mon. Wea. Rev.*, **119**, 1929-1953.

Davis, C.A., 1992: Piecewise Potential Vorticity Inversion. *J. Atmos. Sci.*, **49**, 1397–1411.

Dell'osso, L., and DJ. Radinović, 1984: A case study of cyclone development in the lee of Alps on 18 March 1982. *Beitr. Phys. Atmos.*, **57**, 369-379.

Dudhia, J., 1993: A nonhydrostatic version of the Penn State/NCAR mesoscale model: Validation tests and simulation of an Atlantic cyclone and cold front. *Mon. Wea. Rev.*, **121**, 1493-1513.

Dudhia, J., 1996: A multi-layer soil temperature model for MM5. Preprints, The 6th PSU/NCAR Mesoscale Model Users' Workshop, 22-24 July 1996, Boulder, Colorado, 49-50.

Durran, D. R., 1990: Mountain waves and downslope winds. *Atmospheric Processes over Complex Terrain*, Meteor. Monogr., No. **45**, Amer. Meteor. Soc., 59-81.

Eady T. E., 1949: Long waves and cyclone waves. *Tellus*, **1**, 33–52.

Egger J., 1988: Alpine lee cyclogenesis—Verification of theories. *J. Atmos. Sci.*, **45**, 2187–2203.

Egger J., P. Alpert, A. Tafferner, and B. Ziv, 1995: Numerical experiments on the genesis of Sharav cyclones: Idealized simulations. *Tellus*, **47A**, 162-174.

Enger, L., and B. Grisogono, 1998: The response of bora-type flow to sea surface temperature. *Quart. J. Roy. Meteor. Soc.*, **124**, 1227-1244.

Epifanio, C. C., 2003: Lee vortices. *Encyclopedia of the Atmospheric Sciences*, J. Holton, J. Pyle, and J. Curry (Eds.), Cambridge University Press, 1150-1160.

Ertel, H., 1942: Ein neuer hydrodinamischer Wirbelsatz. *Met. Z.,* **59**, 271-281.

Fantini, M., and S. Davolio, 2001: Instability of neutral Eady waves and Orography. *J. Atmos. Sci.,* **58**, 1146-1154.

Gill, A. E., 1982: Atmosphere-Ocean Dynamics. International Geophysics Series, Vol. **30**, Academic Press, 662pp.

Göhm, A., and G. J. Mayr, 2005: Numerical and observational case-study of a deep Adriatic bora. *Quart. J. Roy. Meteor. Soc.*, **131**, 1363-1392.

Göhm, A., G. J. Mayr, A. Fix, and A. Giez, 2008: On the onset of bora and the formation of rotors and jumps near a mountain gap. *Quart. J. Roy. Meteor. Soc.*, **134**, 21-46.

Grell, G. A., J. Dudhia, and D.R. Stauffer, 1994: A description of the fifth-generation Penn State/NCAR mesoscale mode (MM5). NCAR Techincal Note, NCAR/TN-398+STR, 117 pp.

Grubišić, V., 2004: Bora-driven potential vorticity banners over the Adriatic. *Quart. J. Roy. Meteor. Soc.*, **130**, 2571-2603.

Hoinka K. P., Richard, E., Poberaj, G., Busen, R., Caccia, J.-L., Fix, A., and H. Mannstein, 2003: Analysis of a potential-vorticity streamer crossing the Alps during MAP IOP 15 on 6 November 1999. *Quart. J. Roy. Meteor. Soc.*, **129 B**, 609-632.

Holton J. R., 1972: An introduction to dynamic meteorology. International Geophysics Series, Vol. **16**, Academic Press, 320pp.

Hong, S.-Y., and H.-L. Pan, 1996: Nonlocal boundary layer vertical diffusion in a medium-range forecast model. *Mon. Wea. Rev.*, **124**, 2322-2339.

Horvath, K., Ll. Fita, R. Romero, and B. Ivančan-Picek, 2006: A numerical study of the first phase of a deep Mediterranean cyclone: Cyclogenesis in the lee of Atlas Mountains. *Meteorol. Z.*, **15**, 133-146.

Horvath K., and Ivančan-Picek, B., 2008: A numerical analysis of a deep Mediterranean lee cyclone: sensitivity to mesoscale potential vorticity anomalies. *Meteorol. Atmos. Phys.*, in press.

Horvath, K., Y.-L. Lin, and B. Ivančan-Picek, 2008a: Classification of Cyclone Tracks over Apennines and the Adriatic Sea. *Mon. Wea. Rev.*, **136**, 2210–2227.

Horvath, K., Ivatek-Šahdan, S., Ivančan-Picek, B., and V. Grubišić, 2008b: Evolution and structure of severe cyclonic bora: contrasts between the northern and the southern Adriatic. Submitted to *Wea. Forecasting*.

Hoskins, B. J., M. E. McIntyre, A. W. Robertson, 1985: On the use and significance of isentropic potential vorticity maps. *Quart. J. Roy. Meteor. Soc.*, **111**, 877-946.

Hunt, J. C. R., H. Olafsson, and P. Bougeault, 2001: Coriolis effect on orographic and mesoscale flows. *Quart. J. Roy. Meteor. Soc.*, **127**, 601-633.

Ivančan-Picek, B., and V. Tutiš, 1996: A case study of a severe Adriatic Bora on 28 December 1992. *Tellus*, **48A**, 357-367.

Ivančan-Picek, B., Glasnović, D. and Jurčec, V., 2003: Analysis and Aladin prediction of a heavy precipitation event on the Eastern side of the Alps during Map IOP 5. *Meteorol. Z.*, **12**, 103-112.

Ivatek-Šahdan, S., and B. Ivančan-Picek, 2006: Effects of different initial and boundary conditions in ALADIN/HR simulations during MAP IOPs. *Meteorol. Z.*, **15**, 187-197.

Jurčec, V., 1989: Severe Adriatic bora storms in relation to synoptic developments. *Papers of Meteorological Society of Croatia*, **24**, 11–20.

Jurčec, V., B., Ivančan-Picek, V. Tutiš, and V. Vukičević, 1996: Severe Adriatic Jugo wind. *Meteorol. Z.*, **5**, 67-75.

Kain, J. S., and J. M. Fritsch, 1993: Convective parametrization for mesoscale models: the Kain-Fritsch scheme. The representation of cumulus convection in numerical models. K. A. Emanuel and D. J. Raymond, Eds., Amer. Meteor. Soc., 246 pp.

Kain, J. S., 2002: The Kain-Fritsch convective parametrization: An update. *J. Appl. Meteor.*, **43**, 170–181.

Kleinschmidt, E., 1950: Über Aufbau und Entstehung von Zyklonen (1. Teil), *Met. Runds.*, **3**, 1-6.

Klemp J. B., and D. R. Durran, 1987: Numerical modelling of bora winds. *Meteorol. Atmos. Phys.*, **36**, 215-227.

Kuettner, J. P., 1986: The aim and conduct of ALPEX (Alpine Experiment (ALPEX)). *WMO Proceedings of the Conference on the Scientific Results of the Alpine Experiment (ALPEX), ICSU-WMO, GARP Publ. Ser.,* **27**, 3-13.

Kuo, Y.-H., J. R. Gyakum, and Z. Guo, 1995: A case of rapid continental mesoscale cyclogenesis. Part I: Model sensitivity experiments. *Mon. Wea. Rev.*, **123**, 970-997.

Lagouvardos, K., and V. Kotroni, 2000: Use of the METEOSAT water vapor images for the diagnosis of a vigorous stratospheric intrusion over central Mediterranean. *Meteorol. Appl.*, **7**, 205-210.

Lin, Y.-L., 2007: *Mesoscale dynamics*. Cambridge University Press, New York, 630 pp.

Mansfield, D., 2001: Project III.1: IPV analysis in relation to satellite images. In *Improvement of nowcasting techniques*, Lagouvardos, K., Liljas, E., Conway, B., and J. Sunde, (Eds.):, COST Action 78**,** Final Report. European Commission, 189-201.

Massacand, A. C., H. Wernli, and H. C. Davies, 1998: Heavy precipitation on the Alpine southside: An upper-level precursor. *Geophys. Res. Lett.*, **25**, 1435-1438.

Mattocks, C., and R. Bleck, 1986: Jet streak dynamics and geostrophic adjustment process during the initial stages of lee cyclogenesis. *Mon. Wea. Rev.*, **114**, 2033-2056.

McGinley, J., 1982: A Diagnosis of Alpine Lee Cyclogenesis. *Mon. Wea. Rev.*, **110**, 1271-1287.

Pedgley, D., 1972: Desert depression over north-east Africa. *Met. Mag.*, **101**, 228-243.

Pandžić K., and T. Likso, 2005: Eastern Adriatic typical wind field patterns and large-scale atmospheric conditions. *Int. J. Climatol.,* **25**, 81-98.

Pettersen, S., 1956: *Weather analysis and forecasting*. Vol. **1**, New York, McGraw-Hill, 428 pp.

Pettersen S., and S. J. Smebye, 1979: On the development of extratropical cyclones. *Quart. J. Roy. Meteor. Soc.*, **97**, 457-482.

Pichler, H., and R. Steinacker, 1987: On the synoptics and dynamics of orographically induced cyclones in the Mediterranean. *Meteorol. Atmos. Phys.*, **36**, 108-117.

Pierrehumbert, R. T., 1985: A theoretical model of orographically modified cyclogenesis. *J. Atmos. Sci.,* **42**, 1244-1258.

Radinović, D., 1965: Cyclonic activity in Yugoslavia and surrounding areas. *Arch. Met. Goeph. Biokl.*, **A 14**, 392-408.

Radinović, D., 1987: *Mediterranean Cyclones and Their Influence on the Weather and Climate*, WMO, PSMP Rep. Ser. 24, 131 pp.

Reisner, J., R. J. Rasmussen, and R. T. Bruintjes, 1998: Explicit forecasting of supercooled liquid water in winter storms using the MM5 mesoscale model. *Quart. J. Roy. Meteor. Soc.*, **124B**, 1071-1107.

Romero, R., 2008: A method for quantifying the impacts and interactions of potential vorticity anomalies in extratropical cyclones. *Quart. J. R. Meteor. Soc.*, **134**, 385-402.

Rossby, C. G., 1939: Relation between variations in the intensity of the zonal circulation of the atmosphere and the displacements of the semi-permanent centers of action. *J. Marine Res.,* **2**, 28-55.

Rossby, C. G., 1940: Planetary flow patterns in the atmosphere. *Quart. J. Roy. Meteor. Soc.*, **66**, 68-87.

Saffman, P. G., and G. R. Baker, 1979: Vortex interactions. *Ann. Rev. Fluid Mech.*, **106**, 95-122.

Scorer, R.S., 1949: Theory of waves in the lee of mountains. *Quart. J. Roy. Meteor. Soc.*, **75**, 41-56.

Shapiro, M. A., and A. J. Thorpe, 2004: THORPEX: a global atmospheric research programme for the beginning of the 21st century. *WMO Bull.*, **53**, 222-226.

Smith, R. B., 1984: A theory of lee cyclogenesis. *J. Atmos. Sci.*, **41**, 1159-1168.

Smith, R. B., 1987: Aerial observations of the Yugoslavian bora. *J. Atmos. Sci.*, **44**, 269-297.

Speranza, A., A. Buzzi, A. Trevisan, and P. Malguzzi, 1985: A theory of deep cyclogenesis in the lee of the Alps: Part I, Modification of baroclinic instability by localized topography. *J. Atmos. Sci.*, **42**, 1521-1535.

Stein, U., and P. Alpert, 1993: Factor separation in numerical simulations, *J. Atmos. Sci.*, **50**, 2107-2115.

Steinacker R., and H. Volkert, 2001: The MAP Special Observing Period. *Bull. Am. Meteor. Soc.*, **82**, 433–462.

Thorpe, A. J., 1985: Diagnosis of a balanced vortex structure using potential vorticity. *J. Atmos. Sci.*, **42**, 397-406.

Tibaldi, S., A. Buzzi, and A. Speranza, 1990: Orographic cyclogenesis. In *Extratropical Cyclones*, C. Newton and E. O. Holopainen (Eds.), Amer. Meteor. Soc., 107-128.

Trigo I. F., D. Trevor, H. C. Davies, and G. R. Bigg, 1999: Objective Climatology of Cyclones in the Mediterranean Region. *J. Climate*, **12**, 1685–1696.

Tsidulko, M., and P. Alpert, 2001: Synergism of upper-level potential vorticity and mountains in Genoa lee cyclogenesis – A numerical study, *Meteorol. Atmos. Phys.*, **78**, 261-285.

Van Bebber, W., 1891: Die Zugstrassen des Barometrische Minima. *Meteorol. Z.*, **8**, 361–366.

Večenaj, Ž., 2005: Procesi makrorazmjera kod olujnog vjetra u Dalmaciji (Macroscale processes and severe winds in Dalmatia). BSc Thesis, University of Zagreb, pp59.

Zhang, D. L., and R. A. Anthes, 1982: A high-resolution model of the planetary boundary layer. Sensitivity tests and comparison with SESAME-79 data. *J. Appl. Meteor.*, **21**, 1594-1609.

Zhang, D. L., and J. M. Fritsch, 1986: Numerical simulation of the meso-β scale structure and evolution of the 1977 Johnstown flood. Part I: Model description and verification. *J. Atmos. Sci.*, **43**, 1913-1943.

9. Abstract

Cyclones that appear in the Adriatic Sea basin strongly influence the climate and weather conditions in the area. A classification various types of cyclone tracks on the meso-β scale was performed based on the analysis of four years (2002 – 2005) of operational ECMWF T511 dataset. The analysis indicates that four types of cyclones over the Adriatic Sea can be identified: (1) Type A: Genoa cyclones, with subcategories (I) continuous track and (II) discontinuous track. (2) Type B: cyclones developed in situ over the Adriatic Sea without any connections with other pre-existing cyclones in the surrounding area, with subcategories (I) northern Adriatic cyclones and (II) middle Adriatic cyclones. (3) Type AB: two cyclones co-exist and stride over the Apennines ("twin" or "eyeglass" cyclones). (4) Type C: cyclones moving from the Mediterranean Sea, but not from the Gulf of Genoa (non-Genoa cyclones), with subcategories (I) continuous track and (II) discontinuous track. The results reveal that the greatest number of cyclones that appear in the Adriatic are initiated in the lee sides of mountain ranges in the western Mediterranean (such as the Alps, the Atlas, the Pyrenees and the Apennines), associated with an upper-level trough traversing over the mountain range.

The influence of the upper-level trough on the lifecycle of the typical Mediterranean cyclone initiated to the lee of the Alps (12-15 Nov 2004) is investigated through a numerical analysis with the use of factor separation and piecewise potential vorticity inversion methods. The upper-level trough is shown to be the necessary ingredient of the event and primary deepening factor in the mature stage of cyclone development. However, the Atlas orography is the main contributor to the deepening in the first phase of deepening. Therefore, despite the differences in synoptic setting, creation of thermal anomaly and deepening rates through the generation phase, the existence of two phases of the deepening results suggest the dynamical resemblance of the cyclogenesis to the lee of the Atlas and the Alps. In addition, the analysis of the ensemble of simulations with macroscale and mesoscale perturbations to the upper-level potential vorticity anomaly suggests that cyclone track and intensity are controlled the

most by the strongest mesoscale upper-level potential vorticity anomaly cores (local maximums of potential vorticity) embedded in the trough.

The sensitivity of the MAP IOP 15 Genoa lee cyclogenesis event (06-09 Nov 1999) to the initial-analysis uncertainties in the upper-level precursor is numerically analyzed though the ensemble of sensitivity simulations. Modifications in the initial conditions are created with the use of 90th percentile of derived potential vorticity global model analysis error statistics, reflecting uncertainty in both intensity and position of the upper-level trough. The maximal spread of intensities in the ensemble reaches almost 50% of the cyclone intensity in the control run, and occurs during the most rapid deepening phase of the cyclone. In contrast, the strongest spread of cyclone centre positions is present in the late mature and dissipation phases, reaching up to 750 km, due to different upper-level cut-off dynamics, modified by the Alpine orography. The Bora strength is strongly sensitive to the cyclone intensity and position, but also to the properties of the background flow, with a resulting spread of wind speeds of ±30% compared to the Bora intensity in the control run. The variability of the background flow throughout the ensemble of simulations is evidenced through the (non)existence of synoptic critical levels and their varying altitudes as well as a span of the integral background Froude number over several flow regimes. Therefore, the initial-analysis uncertainties in the macroscale dynamics propagate to a range of smaller-scale phenomena in a chain of dynamically related mesoscale events, having a strong potential to decrease the mesoscale numerical forecast accuracy in the region. This suggests that the considerable improvement of the quality of the mesoscale numerical weather prediction in the area is very likely to be reached through a limited area model ensemble prediction system.

10. Prošireni sažetak[1]

Sažetak

Ciklone koje se nalaze nad Jadranskim morem snažno utječu na klimu i vrijeme u našim krajevima. U ovom radu, na osnovu operativnih ECMWF analiza kroz razdoblje 2002-2005, napravljana je mezo-β klasifikacija tipova i putanja ciklona koje se javljaju nad Jadranskim morem. Analiza ukazuje na postojanje četiri osnovna tipa ciklona nad Jadranom: (1) Tip A: Genovska ciklona, sa podkategorijama (I) kontinuirana ciklona i (II) diskontinuirana ciklona. (2) Tip B: ciklone nastale „*in situ*" nad Jadranom bez vidljive povezanosti sa drugim postojećim ciklonama u regiji, sa podkategorijama (I) ciklone nastale nad sjevernim Jadranom i (II) ciklone nastale nad srednjim Jadranom. (3) Tip AB: ciklona blizanka u kojoj dvije ciklone postoje istovremeno. (3) Tip C: ciklone koje dolaze iz Sredozemlja, ali ne iz Genovskog zaljeva, sa podkategorijama (I) kontinuirana ciklona i (II) diskontinuirana ciklona. Rezultati pokazuju da je većina ciklona koje se pojavljuju nad Jadranom nastala u zavjetrini planinskih lanaca u zapadnom Sredozemlju (Alpe, Atlas, Pireneji i Apenini), uz advekciju visinske doline koja prelazi preko planinskog lanca.

Utjecaj visinske doline na životni ciklus tipične sredozemne ciklone nastale u zavjetrini planine Atlas (12-15. studeni 2004), numerički je analiziran upotrebom metoda separacije faktora („*factor separation*") i inverzije potencijalne vrtložnosti („*potential vorticity inversion*"). Rezultati identificiraju visinsku dolinu kao ključan čimbenik razvoja ciklone, koji daje glavni doprinos produbljivanju ciklone u zreloj fazi njezina razvoja. Međutim, u početnoj fazi najveći doprinos jačanju ciklone ima orografija planinskog lanca Atlas. Tako unatoč razlikama u sinoptičkoj situaciji, procesu nastanka termalne anomalije i intenzitetu

[1] Prošireni sažetak (i.e. Extended abstract, written in Croatian) napisan je na zahtjev Vijeća Fizičkog odsjeka PMF-a. U ovoj disertaciji zamišljen je kao kratki sažetak cijelog rada i pregled svakog pojedinačnog poglavlja sa zaključcima za to poglavlje. Čitatelj/ica se zbog kompletnosti upućuje na tekst radnje napisan na engleskom jeziku.

produbljivanja u početnoj fazi životnog ciklusa, postojanje dvije faze razvoja sugerira dinamičku sličnost ciklogeneze u zavjetrini Atlasa i Alpa. Također, analiza ansambla testova osjetljivosti sa makroskalnim i mezoskalnim modifikacijama u intenzitetu anomalije potencijalne vrtložnosti sugeriraju da su putanja i intenzitet ciklone najsnažnije vezani za najjače mezoskalne jezgre visinske potencijalne vrtložnosti (lokalne maksimume potencijalne vrtložnosti) unutar same doline.

Analiza osjetljivosti MAP IOP 15 genovske ciklone (06-09. studeni 1999) na početne nesigurnosti u visinskoj dinamici numerički je analizirana putem ansambla testova osjetljivosti. Modifikacije u početnih uvjetima određene su 90-im percentilom izračunate statistike pogreške globalnih modela u polju potencijalne vrtložnosti, kako za intenzitet tako i za položaj visinske doline. Najveći rasap intenziteta dostiže skoro 50% intenziteta ciklone tijekom perioda produbljivanja ciklone. Suprotno, najveći rasap putanja od 750 km zabilježen je u kasnoj zreloj i disipativnoj fazi životnog ciklusa ciklone zbog različite dinamike visinske ciklone promijenjene interakcijom sa alpskom orografijom. Jakost bure značajno je ovisna o intenzitetu i položaju ciklone, ali i o karakteristikama pozadinskog strujanja („*background flow*“), rezultirajući rasapom intenziteta bure od ±30% u odnosu na brzinu vjetra u kontrolnoj simulaciji. Promjenjivost pozadinskog strujanja u ansamblu testova osjetljivosti pokazana je kroz (ne)postojanje sinoptičkih kritičnih nivoa i varijabilnost njihove visine te raspon integralnog Froudeovog broja kroz više režima strujanja. Dakle, nesigurnosti u makroskalnoj dinamici se prenose na procese manje skale u lancu dinamički povezanih mezoskalnih procesa, što ima snažan potencijal za smanjenje točnosti mezoskalne numeričke prognoze vremena u našem području. Taj zaključak sugerira da se značajno poboljšanje točnosti mezoskalne numeričke vremenske prognoze u našim krajevima može postići uspostavom mezoskalnog ansambl prognostičkog sustava.

10.1 Uvod

Ciklone koje se pojavljuju nad širim područjem Jadranskog mora jako utječu na klimu i vrijeme u regiji. Unatoč uobičajeno blagoj klimi, ciklonalna aktivnost nad Jadranom i centralnim Sredozemljem ima dominantan utjecaj na hidrološki utjecaj te na aktivaciju cijelog niza ekstremnih vremenskih uvjeta u regiji, kao što su bura i jaka orografska oborina.

Zavjetrinske ciklone su najčešći tip ciklone nad Jadranom (Poglavlje 2), a kako je unatoč razvoju sofisticiranih numeričkih modela, šire područje zavjetrine Alpa upravo područje smanjene točnosti numeričkih prognoza vremena, neophodno je potpuno razumijevanje procesa nastanka zavjetrinske ciklogeneze i nesigurnosti vezanih uz rezultate prognostičkih modela. S obzirom da su dinamički procesi u visinskoj troposferi glavni prediktori zavjetrinske ciklogeneze, numerička analiza njihovog utjecaja kao i studija osjetljivosti zavjetrinske ciklogeneze na početne nesigurnosti u opisu visinske dinamike je od trajne važnosti za povećanje kvalitete operativne (numeričke) prognoze vremena u našem području.

U Poglavlju 1 (10.2) prikazan je pregled dosadašnjih pristupa u istraživanju zavjetrinske ciklogeneze. Meso-β klasifikacija ciklonalne aktivnosti nad Jadranom dana je u Poglavlju 2 (10.3), dok se metode separacije faktora i inverzije potencijalne vrtložnosti (PV), korištene u numeričkoj analizi, opisuju u Poglavlju 3 (10.4). U Poglavlju 4 (10.5), numerički se istražuje utjecaj makroskalnih i mezoskalnih dinamičkih cirkulacija u visinskoj troposferi na nastanak i životni ciklus ciklone nastale u zavjetrini planinskog lanca Atlas, te se procesi njezina nastanka uspoređuju sa procesima geneze tipične alpske zavjetrinske ciklone. U Poglavlju 5 (10.6) dani su rezultati statistike pogreške analize globalnih modela u polju potencijalne vrtložnosti (PV). Konačno, u Poglavlju 6 (10.7) istražuje se osjetljivost MAP IOP 15 genovske zavjetrinske ciklone na pogreške u početnim dinamičkim uvjetima u gornjoj troposferi, kroz ansambl numeričkih testova osjetljivosti određenih izračunatom statistikom pogreške globalnih modela. Ovaj pristup omogućuje kvalitativnu i kvantitativnu procjenu utjecaja nesigurnosti u početnim dinamičkim uvjetima u gornjoj troposferi na numeričku prognozu intenziteta i putanje analizirane genovske ciklone, kao i jakosti bure na sjevernom Jadranu.

10.2 Fenomenologija i teorije zavjetrinske ciklogeneze

Područje Genovskog zaljeva je poznato kao područje vrlo učestale ciklogeneze. Važnost ovog fenomena rezultirala je i nizom eksperimenata, kao što su „Alpine Experiment“, 1982 (ALPEX; vidi Kuettner 1986) i „Mesoscale Alpine Programme“, 1999 (MAP; npr. Bougeault i sur. 2001).

Slijedeći rezultate istraživanja i mjerenja, osnovna obilježja Alpske zavjetrinske ciklogeneze su:

(a) zavjetrinska ciklogeneza vezana je za postojanje visinske doline i ciklone „majke“ sjeverno od Alpa;

(b) produbljivanje ciklone događa se u dvije faze: u prvoj fazi prizemna ciklona se intenzivno produbljuje zbog frontalne retardacije i separacije toka („*flow splitting*“), dok se u drugoj fazi ciklona produbljuje manje intenzivno u procesu koji nalikuje baroklinoj interackiji, protežući se kroz cijelu troposferu;

(c) razvoj zavjetrinske ciklone počinje prije nego baroklina zona zbog frontalne retardacije nastane u zavjetrini;

(d) skala duboke zavjetrinske ciklone je veličine internog Rossbyjevog radijusa deformacije (NL_z / f , gdje je L_z vertikalna skala gibanja). Utjecaj orografije je stvaranje „*high-low*“ dipola.

Prema uvjetima u visinskoj atmosferi postoje dva tipa zavjetrinske ciklogeneze (Pichler i Steinacker 1987): češći jugozapadni tip („*Vorderseiten*“, Slika 1.1a) i rjeđi sjeverozapadni tip („*Überströmungs*“, Slika 1.1b).

Za strujanje preko mezoskalnih planina (Alpe, Stjenjak) s Rossbyjevim eksternim brojem (R_o=U/fL) oko 1, utjecaj Zemljine rotacije ne može biti zanemaren, no također je prevelik da bi bio aproksimiran kvazi-geostrofičkom teorijom. Do danas, postoje dvije konzistentne teorije zavjetrinske ciklogeneze:

(1) teorija stvaranja baroklinog vala (Smith 1984);

(2) orografska modifikacija barokline nestabilnosti tj. teorija normalnog moda zavjetrinske ciklogeneze (Speranza i sur. 1985).

Ove teorije opisane su u Poglavljima 1.2.1 i 1.2.2. Verifikacija ovih teorija (Poglavlje 1.2.3) pokazala je da niti jedna od ovih teorija ne može adekvatno opisati nelinearni razvoj zavjetrinske ciklone tijekom prve faze njezina razvoja.

Kako je zavjetrinska ciklogeneza inherentno vezana za postojanje visinske doline, odnosno povećane vrijednosti visinske PV, sljedeći aspekti koncepta „*PV thinking*“ (vidi Hoskins i sur. 1985) se mogu primijeniti na razumijevanje promatranog fenomena:

(1) PV je očuvana na izentropskoj površini u adijabatskoj atmosferi bez sudjelovanja trenja;
(2) princip invertibilnosti, koji je primjenjiv bez obzira na prisutnost dijabatskih efekata ili prisustva trenja.

Tako se konceptualna veza između prve faze (koja nije u ravnoteži) i druge faze ciklogeneze (koja jest u ravnoteži) može tražiti putem principa invertibilnosti, iz kojega slijedi da orografska perturbacija u prvoj fazi mora biti vezana za (i) termalnu anomaliju ili (ii) prizemnu PV anomaliju. Dok je (i) vezano za frontalnu retardaciju, (II) je vezano za prizemni primarni „*PV banner*“ koji se stvara na jugozapadnom dijelu Alpa, čijim postojanjem se također pokušala obrazložiti veća učestalost ciklogeneze u Genovskom zaljevu nego u zavjetrini istočnih Alpa (Aebischer i Schär 1998).

Mattocks and Bleck (1986) prvi su numerički primijenili princip invertibilnosti (sa kvazi-geostrofičkom formulacijom) na problem zavjetrinske ciklogeneze. Kasnije, postupak inverzije PV višeg reda razvijen je uz pomoć nelinearnih jednadžbi ravnoteže i razvoje „*piecewise*“ formulacije inverzije PV (Davis i Emanuel 1991; Davis 1992, vidi Poglavlje 3.2). Potonji je pristup korišten u ovom radu, omogućujući numeričke eksperimente koji analiziraju utjecaj i makroskalnih i mezoskalnih modifikacija u intenzitetu i položaju anomalije visinske PV na interakciju gornje i prizemne troposfere u procesu zavjetrinske ciklogeneze.

10.3 Ciklonalna aktivnost u Jadranu

Da bi se upotpunila dosadašnja slika o ciklonalnoj aktivnosti u našem području, mezo-β klasifikacija tipova i putanja ciklona koje se pojavljuju u Jadranu napravljena je korištenjem operativne „*long cut-off*“ T511 analize Europskog centra za srednjeročnu prognozu vremena

(ECMWF) horizontalne rezolucije ~40 km kroz razdoblje 2002-2005. Objektivni kriteriji manualne detekcije i praćenja ciklone uključili su tlak reduciran na standardni nivo i cirkulaciju (za metodologiju vidi Poglavlje 2.1) da bi se identificirale ciklone na skali relevantnoj za Jadran i razdvojile termalne depresije od ciklona. Provedena analiza identificirala je četiri osnovna tipa ciklona nad Jadranom:

(1) A – Genovska ciklona (Genovski zaljev i sjeverna Italija)
   a. A-I – kontinuirana genovska ciklona
   b. A-II – diskontinuirana genovska ciklona
(2) B – Jadranska ciklona
   a. B-I – sjeverojadranska ciklona
   b. B-II – srednjejadranska ciklona
(3) AB – Ciklona blizanka („*twin*“, „*eyeglass*“)
(4) C – Ciklona koje nema izvorište niti u Jadranu ni u Genovskom zaljevu
   a. C-I – kontinuirana ciklona
   b. C-II – diskontinuirana ciklona

Prvi i najčešći tip ciklone nad Jadranom (Tip A) je genovska ciklona (35%, Tabela 2.1), koja se najčešće javlja zimi. Nađene su dvije podkategorije: (I) kontinuirana genovske ciklona (Tip A-I) i (II) diskontinuirana genovska ciklona (Tip A-II). Kontinuirani tip ciklone uobičajeno prelazi nad Jadran preko sjevernih Apenina i dolinom rijeke Po, bez značajne perturbacije prizemne cirkulacije (Slika 2.1a). Nakon dolaska nad sjeverni Jadran većina ciklona Tipa A-I se giba duž jadranskog bazena, dok manji dio prelazi u kontinentalnu Hrvatsku. Međutim, manji dio genovskih ciklona se giba prema Jadranu nešto južnije, u području srednjih Apenina, zbog čije visine (2912 m) dio tih ciklona postaje blokiran na planini (Slika 2.1b), pri čemu se nova prizemna ciklona stvara nad Jadranom (Tip A-II).

Drugi tip ciklone (Tip B) je ciklona nastala „*in situ*“ nad Jadranom bez vidljive povezanosti sa postojećim ciklonama u regiji. Ove ciklone su najmanjih horizontalnih dimenzija nad Jadranom, naizgled određene širinom jadranskog bazena (~ 200 km) i čine oko 26 % svih ciklona (Tabela 2.1). Identificirana su dva područja nastajanja ovih ciklona (Slika 2.2): (I) sjeverni Jadran (Tip B-I) i (II) srednji Jadran (Tip B-II). Dok ciklona Tipa B-I fenomenološki sliči na genovsku ciklonu, ciklona Tipa B-II je obično plića (nad Jadranom gdje najčešće i disipira) i kraćeg trajanja, te su češća u toplije doba godine.

Najrjeđi tip ciklone nad Jadranom (Tip AB) je ciklona blizanka (eng. „*twin*“, „*eyeglass*“), koji se javlja u 6 % slučajeva (Slika 2.3, Tabela 2.1). Ovaj tip ciklone obilježava istovremena prisutnost i evolucija dva ciklonalna centra, jednog nad Jadranom, a drugog nad Genovskim zaljevom, koji se najčešće istovremeno gibaju duž Apenina prema jugoistoku.

Četvrti tip ciklone (Tip C) je ciklona koja dolazi nad Jadran iz Sredozemlja, ali ne iz Genovskog zaljeva. Pronađene su dvije podkategorije: (I) kontinuirana ciklona (Tip C-I) koja prelazi preko Apenina nad Jadran (Slika 2.4a) i (II) diskontinuirana ciklona (Tip C-II) koja je blokirana nad Apeninima, dok se nova prizemna ciklona stvara nad Jadranom (Slika 2.4b). Tip C ciklone najčešće se javlja zimi, dok ljeti gotovo da i ne dolazi do Jadrana. Naime, u toplije doba godine područje najčešće ciklogeneze u Sredozemlju je Iberijski poluotok. Pritom mehanizam stvaranja nije vezan za visinsku dolinu, što rezultira smanjenom mogućnošću advekcije ovih ciklona prema Jadranu (Poglavlje 2).

Klimatološka klasifikacija je pokazala da je većina ciklona koje se pojavljuju nad Jadranom nastala u zavjetrini planinskih lanaca u zapadnom Sredozemlju (Alpe, Atlas, Pireneji i Apenini), uz advekciju visinske doline koja prelazi preko planinskog lanca. Kako su planine i uvjeti u visinskoj troposferi najjači prediktori zavjetrinske ciklogeneze, studija utjecaja visinske doline na stvaranje zavjetrinskih ciklona, kao i njihova prediktabilnost u ovisnosti o nesigurnostima u analizi visinskih cirkulacija je od velike važnosti za operativnu vremensku prognozu u našim područjima.

10.4 Metode i opis modela

Dvije su osnovne metode korištene u ovom radu: separacija faktora („*factor separation*“) opisana u Poglavlju 3.1 i inverzija potencijalne vrtložnosti („*potential vorticity inversion*“) opisana u Poglavlju 3.2. Numerička analiza napravljena je mezoskalnim nehidrostatičkim modelom MM5, pri čemu su parametri modela i detalji numeričkih simulacija dani u Poglavlju 3.3.

10.5 Osjetljivost ciklogeneze u zavjetrini planina Atlas na dinamičke uvjete u visinskoj troposferi

Da bi se ocijenila sličnost cikogeneze u zavjetrini Alpa s procesom ciklogeneze u zavjetrini planina Atlas, kao područja česte geneze sredozemnih ciklona, te utjecaj visinske vrtložnosti na nastanak i razvoj ciklonalnog sustava, numerički je analiziran slučaj duboke ciklone nastale u zavjetrini planine Atlas (12-15. studeni 2004. godine, Slika 4.2). Nakon advekcije visinske doline preko Atlasa (Slika 4.3), te potom i gibanja prizemne ciklone prema Sredozemlju, ovaj ciklonalni sustav se približio Jadranu, uzrokujući iznimno jaku i dugotrajnu buru na Jadranu sa udarima do 60 ms^{-1}.

Numerička analiza ovog tipičnog slučaja ciklogeneze u zavjetrini planine Atlas istražila je utjecaj dinamičkih uvjeta u visinskoj troposferi na stvaranje ciklone. Dodatno, zbog usporedbe sa Alpskom ciklogenezom, numerički je određen i utjecaj orografije planinskog lanca Atlas i prizemnog toka senzibilne topline. Visinski uvjeti u gornjoj troposferi, tj. visinska dolina bila je osnovni čimbenik koji je utjecao na stvaranje ciklone u zavjetrini planine Atlas. Naime, u testu osjetljivosti sa uklonjenom visinskom dolinom, znatno slabija ciklona koja se formirala nije nastala u zavjetrini planinskog lanca, već znatno istočnije. Stoga su se u metodi separacije faktora koristili testovi osjetljivosti sa 50% intenziteta doline uklonjenih iz početnih uvjeta (Slika 5.6), da bi se zadržala sličnost numeričkih rješenja sa stvarnom dinamikom ovog procesa.

Nadalje, analiza je ukazala na postojanje dvije faze razvoja analizirane ciklone: u prvoj je glavni doprinos produbljenju ciklone imala orografija, dok je u drugoj dominantan bio utjecaj visinske dinamike (Slika 4.7). Unatoč razlikama u sinoptičkoj situaciji, procesu stvaranja termalne anomalije i kvantitativnim iznosima intenziteta produbljivanja u usporedbi sa dokumentiranim slučajevima Alpske ciklogeneze, postojanje dvije faze razvoja ukazuje na dinamičku sličnost ciklogeneze u zavjetrini Atlasa i Alpa. Također, visinski procesi su znatno utjecali na putanju ciklone i njezinu bržu advekciju prema Sredozemlju (Slika 4.8), dok je utjecaj orografije bio zadržavanje ciklone bliže zavjetrini planine. Značajne razlike u položajima ciklone u simulacijama sa različitim intenzitetom anomalije potencijalne vrtložnosti sugerira da dinamički uvjeti u gornjoj troposferi imaju ključan utjecaj na klimatološke putanje ciklona nastalih u zavjetrini planine Atlas u gibanju prema Sredozemlju.

Utjecaj mezoskalnih jezgri visinske PV proučavan je putem ansambla testova osjetljivosti s proizvoljno modificiranim intenzitetima mezoskalnih cirkulacija unutar visinske doline u gornjoj troposferi (Slika 4.9). Rezultati pokazuju da je stvaranje i produbljivanje ciklone bilo najviše određeno utjecajem lokalnih mezoskalnih visinskih cirkulacija tj. jezgri povišenih vrijednosti PV, kao dominantnih čimbenika koji su utjecali na razvoj promatrane zavjetrinske ciklone. Tako su najjače jezgre mezoskalne cirkulacije (Slika 4.10) bile odgovorne za do 75% intenziteta ciklone u njezinom razvoju nad sjevernoafričkim kopnom. Apsolutne razlike rasapa intenziteta su se ulaskom ciklone nad Sredozemlje povećale (15 hPa), djelomično zbog različite brzine advekcije ciklone prema moru, gdje je vjerojatno glavni doprinos produbljivanju bio vezan za utjecaj vlage iz mora i dijabatskih procesa. Rasap putanja ciklona bio je najveći u trenutku prije advekcije nad Sredozemlje (Slika 4.11), u drugoj fazi razvoja ciklone primarno određenoj interakcijom visinske i prizemne atmosfere. Po ulasku nad Sredozemlje, putanje ciklona su konvergirale, posebno prema disipativnoj fazi životnog ciklusa ciklone, što je naizgled bilo potpomognuto orijentacijom planina Atlas, Sicilije, južne Italije i Balkanskog poluotoka. Značajan utjecaj najintenzivnijih mezoskalnih modifikacija na razvoj i putanju ciklone ukazuje da su intenzivne mezoskalne jezgre anomalija visinske PV odgovorne za značajan dio visinskog dinamičkog utjecaja na prizemnu atmosferu, odnosno visinsku kontrolu ciklogeneze u zavjetrini planinskog lanca Atlas.

10.6 Statistika pogreške analize potencijalne vrtložnosti

U prethodnim poglavljima vidjeli smo da su visinski dinamički uvjeti u gornjoj troposferi osnovni generator kako Alpske, tako i Atlaske ciklogeneze i da su zavjetrinske ciklone vrlo osjetljive na proizvoljne modifikacije visinske PV. Međutim, prediktabilnost takvih sustava nemoguće je ocijeniti putem proizvoljnih modifikacija u početnim uvjetima, već je neophodno osigurati realnost testova osjetljivosti, bar u statističkom smislu.

Da bi se ocijenila nesigurnost u početnim uvjetima s obzirom na visinske procese u gornjoj troposferi, proučene su razlike u analizama dvaju globalnih centara: Europskog centra za srednjoročne prognoze vremena („*European Centre for Medium-Range Weather Forecast“,* ECMWF) i Nacionalnih centara za prognozu okoliša („*National Centers for Environmental Prediction“*, NCEP). Za izračun statistike koristila se baza dubokih ciklona u Sredozemlju, napravljena kroz projekt „*Mediterranean experiment*“ (MEDEX). Detalji postupka koji omogućuje izračun vertikalne strukture pogreške u visinkoj PV i njezinu podjelu na pogrešku u amplitudi (intenzitetu) i pogrešku u fazi (položaju) su prikazani u Poglavlju 5. Rezultati na 300 hPa pokazuju da su pogreške u položaju gotovo simetrične obzirom na smjer i u prosjeku iznose oko 50 km, dok ekstremne pogreške (određene 90-im percentilom) iznose oko 150 km (Slika 5.1). S druge strane, pogreška u intenzitetu je ovisna o intenzitetu PV i u prosjeku iznosi od 21% za vrijednost PV=1 PVU do 9% za PV=7 PVU, odnosno za slučaj 90-og percentila od 40% do 15% (Slika 5.2).

10.7 Osjetljivost genovske ciklone na nesigurnosti u analizi dinamičkih uvjeta u gornjoj troposferi

U prethodnim poglavljima vidjeli smo da numerička prognoza intenziteta i putanje zavjetrinskih ciklona u zapadnom Sredozemlju značajno ovisi o makroskalnim i mezoskalnim obilježjima visinske doline. S tim saznanjem postavlja se pitanje: koja je osjetljivost zavjetrinskih ciklona u regiji početne nesigurnosti vezane za intenzitet i položaj visinskih dinamičkih uvjeta?

Rezultati statistike pogreške u polju PV iskoristili su se u nizu testova osjetljivosti tipičnog slučaja duboke genovske ciklone MAP IOP 15 („*Mesoscale Alpine Programme*“; „*Intensive Observing Period*“) u razdoblju 06-09. studeni 1999. Uz brzu advekciju visinske vrtložnosti preko Alpa i pojavu duboke zavjetrinske ciklone (Slike 6.1, 6.2), vrijeme je u našim krajevima obilježila bura, čija je srednja brzina na Masleničkom mostu (vidi Slike 6.9 i 6.10) bila i veća od 25 ms^{-1} (sa udarima preko 40 ms^{-1}). Pri stvaranju ansambla testova osjetljivosti za modifikaciju početnih uvjeta (Slika 6.4) koristile su se vrijednosti 90-og percentila statistike pogreške PV, vertikalno usrednjene po nivoima 500-100 hPa za vrijednosti veće od 1 PVU. Tako su modifikacije potencijalne vrtložnosti u početnim uvjetima bile odraz najvećih mogućih realnih nesigurnosti vezanih za numerički opis stanja visinske doline, omogućavajući analizu osjetljivosti i prediktabilnosti zavjetrinskih ciklona na pogreške u početnim uvjetima isključivo u položaju i intenzitetu visinske doline.

Analiza otkriva da je numerička prognoza intenziteta i putanje genovske ciklone značajno ovisna o nesigurnostima u visinskim dinamičkim početnim uvjetima. Rasap intenziteta ciklone u njezinu centru povećavao se tijekom početne faze razvoja i dosegao 18 hPa (oko 50% intenziteta ciklone u kontrolnoj simulaciji) krajem prve faze i u početku druge faze razvoja (18 UTC 06. studeni 1999. – 12 UTC 07. studeni 1999., Slika 6.5). Tijekom tog razdoblja ciklona se gibala prema jugoistoku duž sjevernog i srednjeg dijela Apeninskog poluotoka. Međutim, u zreloj i disipativnoj fazi razvoja ciklone rasap intenziteta ciklone se smanjio, ukazujući na slab utjecaj početnih nesigurnosti na intenzitet ciklone u ovim fazama njezina životnog ciklusa.

Položaj samog nastanka MAP IOP 15 ciklone nije bio značajnije promijenjen modifikacijama u početnim uvjetima, ukazujući da je jugozapadni dio zavjetrine Alpa bio jak prediktor položaja nastanka ove zavjetrinske ciklone (Slika 6.6). Međutim, ubrzo nakon nastanka, putanje ciklona su divergirale pokrivajući područje od Genovskog zaljeva do sjevernog Jadrana. Taj je rasap putanja uzrokovan promjenjivošću (ne)linearnosti strujanja preko jugozapadnog dijela Alpa, koji je odredio položaj nastanka prizemne ciklone. Tako je, na primjer, smanjena nelinearnost prizemnog strujanja u simulaciji sa povećanim intenzitetom visinske potencijalne vrtložnosti omogućila širenje fronte mistrala prema istoku, što je efektivno pomaknulo centar termalne anomalije i nastajućeg frontalnog sustava prema sjevernom Jadranu (Slika 6.7). Nakon ovog početnog povećanja (gdje su centri bili međusobno udaljeni do ~ 200 km), rasap putanja je ostao značajnije nepromijenjen do zrele faze razvoja ciklone i disipativne faze životnog ciklusa visinske doline. U tom razdoblju, rasap putanja ciklone se izrazito povećao i dostigao 750 km u zadnjem dijelu prognostičkog razdoblja (12 UTC 08. studeni 1999 – 00 UTC 09. studeni 1999). Analiza je pokazala da je to povećanje vezano za različitu nelinearnu dinamiku visinske ciklone („*cut-off*“ i „*rollup*“ procesa, Slika 6.8). Izgledno je da su te razlike nastale zbog različitog intenziteta interakcije visinske doline sa alpskom orografijom, do čega je došlo zbog početnih promjena u položaju visinske doline i potom nastalih sinoptičkih kritičnih nivoa iznad Alpa.

Bura se u sjevernom Jadranu pokazala vrlo osjetljivom na početne nesigurnosti u dinamičkim uvjetima u gornjoj troposferi, uslijed njihova prenošenja na nesigurnosti u: (1) intenzitetu ciklone i njezine putanje (Slika 6.11) i (2) pozadinskom („*background*“) strujanju (koje je povezano sa blokingom na Alpama i nastankom istočne grane strujanja oko Alpa). Potonje je pokazano kroz (ne)postojanje sinoptičkih kritičnih nivoa u dijelu simulacija i rasap njihovih visina (Slika 6.12) te raspon integralnog pozadinskog Froudeovog broja kroz više režima strujanja (Slika 6.13). Kao rezultat, propagacija početnih nesigurnosti uzrokovala je rasap intenziteta bure od ±30% u usporedbi sa kontrolnom simulacijom tijekom trajanja gotovo cijele epizode.

Dakle, početne nesigurnosti u makroskalnoj dinamici se prenose na procese manje skale u lancu dinamički povezanih mezoskalnih procesa, što ima snažan potencijal za smanjenje točnosti mezoskalne numeričke prognoze vremena u našem području. Kako velika osjetljivost numeričke prognoze vremena na početne uvjete često vodi determinističkoj prognozi ograničene točnosti, vrlo je vjerojatno da se značajno poboljšanje točnosti mezosklane numeričke prognoze vremena u našim krajevima može postići uspostavom mezoskalnog ansambl prognostičkog sustava.

11. Curriculum vitae

Name: **Kristian Horvath**

Personal data

Birth date	25 April 1977.
Place of birth	Zagreb, Croatia
Father's name	László Horváth
Mother's name	Šefka Kurbegović-Horvat
Address	Bijenička cesta 35a, Zagreb
E-mail	horvath@cirus.dhz.hr

Education

2002	Graduate physics degree (field: Physics of the atmosphere and the sea) on the Faculty of Science, University of Zagreb, Croatia
2003	Enrolment of the postgraduate studies at the Geophysics Department of the Faculty of Science, University of Zagreb
2004	Teaching assistance at the Geophysics Department during the obligatory civil service
2006	Enrolment of doctoral studies

Employment

2003- Graduate Research Assistant on the project "Storms and natural disasters in Croatia", funded by Ministry of Science, Technology and Sports of the Republic of Croatia; Project Leader: Dr. Sc. Branka Ivančan-Picek

Meteorological and Hydrological Service, Grič 3, Zagreb, Croatia
Department for research and modelling of atmospheric processes

Tel	+385–01–4565 752
Fax	+385–01–4565 630
E-mail	horvath@cirus.dhz.hr
Www	http://www.dhmz.htnet.hr/index.php
Personal	http://radar.dhz.hr/~horvath

Scholarships and research stays

08.2003	Hungarian Meteorological Service, funded by RC LACE (Regional Cooperation for Limited Area modelling in Central Europe) topic: Mesoscale data assimilation
09-10.2004	Hungarian Meteorological Service, funded by RC LACE (Regional Cooperation for Limited Area modelling in Central Europe) topic: Mesoscale data assimilation
11-12.2004	University of Balearic Islands, funded by Ministry of Environment of Republic of Spain topic: Numerical modelling of deep Mediterranean cyclogenesis and extreme Bora along the Adriatic
04-05.2005	Hungarian Meteorological Service, funded by Ministry of Education and Culture of Republic of Hungary topic: Mesoscale data assimilation
10-11.2005	Hungarian Meteorological Service, funded by RC LACE (Regional Cooperation for Limited Area modelling in Central Europe) topic: Mesoscale data assimilation
02-04.2006	North Carolina State University, Mesolab (Prof. Yuh-Lang Lin), funded by Ministry of Science, Education and Sports of Republic of Croatia and NSF Grant ATM-0344237 topic: Climatology and Numerical analysis of Adriatic cyclones
05-06.2007	University of Balearic Islands, funded by Ministry of Science, Education and Sports of Republic of Croatia topic: Predictability of orographical cyclogenesis in the Mediterranean

Awards, invited talks

2005	"Young scientist award" (European Geosciences Union) for the best oral presentation and the most innovative research work, 7th Plinius Conference on Mediterranean Storms, 5.10.-7.10. 2005., Crete, Greece
05.2007	"Cyclonic activity in the Adriatic, generation factors and effects on Bora", 15.05., Phys. Dept., University of Balearic Islands, Spain
06.2007	European Meteorological Society "Young scientist travel award" for the poster "Classification of cyclone tracks over Apennines and the Adriatic Sea", 29th International conference on Alpine meteorology, Chambery, France

Foreign languages

English:	active knowledge
Hungarian:	active knowledge
German:	passive knowledge

Conferences/Workshops/Summer schools

2003|1	Observational Database Training, 14.4.-18.4., Budapest, Hungary
2	Data Assimilation Workshop, 20.10.-22.10, Budapest, Hungary
3	13th ALADIN Workshop, 23.11.-27.11., Praha, Czech Republic
4	C programming course, 15.-19.12., Zagreb, Croatia
2004|5	Mediterranean school on Mesoscale Meteorology, 7.6.-11.6., Alghero, Italy
6	11th Conference on Mountain Meteorology and MAP Meeting, 21.6.-25.6, Mount Washington Valley, USA
7	High Resolution Data Assimilation towards 1-4 km Resolution, 15.11.-17.11., Exeter, UK
2005|8	International Conference on Alpine Meteorology and MAP Final Conference, 22.5.-29.5., Zadar, Croatia
9	15th ALADIN Workshop, 6.6.-10.6., Bratislava, Slovakia
10	From Micro to Meso, 26.9.-30.9., Castro Marina, Italy
11	7th Plinius Conference on Mediterranean Storms, 5.10.-7.10., Crete, Greece
12	ALADIN-HIRLAM Workshop on Code Maintenance and Data Assimilation, 14.11.-18.11., Budapest, Hungary
2006|13	European Wind Energy Conference (EWEC), 27.2.-2.3., Athens, Greece
14	Renewable energy sources in Republic of Croatia, 29.5.-31.5., Šibenik, Croatia
15	Mediterranean School on Mesoscale Meteorology, 2nd edition, 4.6.-9.6., Alghero, Italy
16	12th Conference on Mountain Meteorology, 28.8.-1.9., Santa Fe, USA
2007|17	Numerical methods and adiabatic formulation of models, Meteorological Training Course, 19.03.-29.03., European Centre for Medium-Range Weather Forecast, Reading, UK
18	29th International Conference on Alpine Meteorology, 04.06.-08.06, Chambery, France
19	9th Plinius Conference on Mediterranean Storms, 10.9.-13.9., Varenna, Italy
20	29th EWGLAM and 14th SRNWP Meetings, 08.10.-11.10., Dubrovnik, Croatia
2008|21	AMS/COMET/MSC Mountain Weather Workshop: Bridging the Gap Between Research and Forecasting
22	13th Conference on Mountain Meteorology, 11.8.-15.8., Whistler, Canada
23	10th Plinius Conference on Mediterranean Storms, 22.9.-24.9., Nicosia, Cyprus

12. List of publications

No.	Publication
1	Horvath, K., S. Ivatek-Šahdan, B. Ivančan-Picek, and V. Grubišić, 2008 : Evolution and structure of severe cyclonic Bora : contrast between the northern and southern Adriatic. Submitted to *Wea. Forecasting.*
2	Horvath, K., and B. Ivančan-Picek, 2008: A numerical analysis of a deep Mediterranean lee cyclone: sensitivity to mesoscale potential vorticity anomalies. *Meteorol. Atmos. Phys.* In press (available on http://www.springerlink.com/content/2h73358434q505m8/).
3	Horvath, K., Y.-L. Lin, B. Ivančan-Picek, 2008: Classification of the Cyclone Tracks over Apennines and the Adriatic Sea. *Mon. Wea. Rev.*, **136**, 2210-2227.
4	Horvath, K., Ll. Fita, R. Romero, B. Ivančan-Picek, 2006: A numerical study of the first phase of a deep Mediterranean cyclone: Cyclogenesis in the lee of Atlas Mountains. *Meteorol. Z.*, **15**, No. 2; 133-146.
5	Horvath, K., Ll. Fita, R. Romero, B. Ivančan-Picek, I. Stiperski, 2006: Cyclogenesis in the lee of the Atlas Mountains: A Factor Separation numerical study. *Adv. Geosci.*, **7**, 327-331.
6	Horvath, K., Ll. Fita, R. Romero, B. Ivančan-Picek, 2005: The influence of orography during deep Mediterranean cyclogenesis 11-15 November 2004. *Croatian Meteorological Journal*, **40**, 373-376.
7	Kos I., D. Belušić, A. Jeričević, K. Horvath, D. Koračin, M. Telišman-Prtenjak, 2004: Education and research: Initial development of the Atmospheric Lagrangien Particle Stochastic (ALPS) Dispersion Model. *Geofizika*, **21**, 37-52.
8	Horvath, K., B. Ivančan-Picek, 2003: Evaluation of the ALADIN/LACE mesoscale model during the MAP SOP experiment. *Croatian Meteorological Journal*, **38**, 11-20.